Geochemické studium procesů, relevantních pro hodnocení bezpečnosti hlubinného úložiště radioaktivních odpadů:

Formy uranu a scénáře jeho retence v prostředí sedimentárních hornin na lokalitě přírodního analogu Ruprechtov

Geochemical study of processes, relevant to safety assessment of deep geological repositories:

Uranium forms and enrichment scenario in a sedimentary system at the Ruprechtov natural analogue site

RNDr. Václava Havlová

Dizertační práce/Doctoral Thesis

Školitel/Supervisor: Doc. RNDr. Emil Jelínek, CSc.

Externí školitel/External supervisor: Dr.Ulrich Noseck (GRS)

Praha 2011

Univerzita Karlova,
Přírodovědecká fakulta,
Ústav geochemie, mineralogie a nerostných zdrojů.
Praha, 2011

Ústav jaderného výzkumu Řež a.s., ÚJV No. 13760, 2011.

Prohlášení:

Prohlašuji, že jsem závěrečnou práci zpracovala samostatně a že jsem uvedla všechny použité informační zdroje a literaturu. Tato práce ani její podstatná část nebyla předložena k získání jiného akademického titulu.

Announcement:

Thereby I declare that I wrote the Thesis independently and that I quoted all the information and references used. Neither the Thesis presented nor their substantial part has not been submitted for obtaining of other or the same academic degree respectively.

V Praze, 15.04.2011

RNDr. Václava Havlová

Abstract

U migration was studied in order to better understand to processes of safety relevant elements, particularly U. The rock sequence on the site can be analogous to a potential rock overburden of deep geology repositories.

A multidisciplinary approach was undertaken in order to identify and characterise U mobilisation/immobilisation processes within sedimentary clayey rocks with organic matter enriched interlayers. Both conventional methods and modern sophisticated spectroscopic methods were combined. Sequential extraction, wet chemical method and even spectroscopic methods proved that U prevailed in the U(IV) form in low-oxidised samples. It moved towards more easily releasable fractions with sample ageing (oxidation).

The combination of SE, μ-XRF and μ-XAFS results proved U to be unexpectedly associated with As and P, leading to the presumption that U(VI) from groundwater was reduced to U(IV) on As pyrite.

The evaluation of the hydrogeochemical conditions and isotope analyses then brought the results into broader context: Sedimentary organic matter within the sedimentary layers was microbially oxidised, releasing dissolved organic matter and providing H^+ in order to dissolve sedimentary inorganic carbonates. SO_4^{2-} could be reduced under reducing groundwater conditions, thus causing FeS_2 formation. As got also reduced and precipitates on FeS_2 surfaces. U was reduced on As covered pyrite surfaces to U(IV) and reacted with phosphates (PO_4^{3-}), produced by microbial organic matter oxidation. U phosphates (ningyoite) were thus formed. The $^{234}U/^{238}U$ activity ratio determination proved the fact that U(IV) phases had been stabile for more than 1 Ma. This fact strongly supports potential barrier function of similar rock systems (clayey sedimentary rock with organic matter content). On the other hand, it is necessary to stress important role of CO_2 in increased mobility of U(VI) in reducing groundwater conditions.

Abstrakt

Studium migrace U v přírodním prostředí představuje významný příspěvek pro poznání procesů významných pro hodnocení bezpečnosti hlubinného úložiště jaderného odpadu. V případě přírodního analogu Ruprechtov lze sedimentární horniny považovat za analogii pokryvných útvarů nad hostitelskými masivy hlubinného úložiště.

K identifikaci a charakterizaci procesů mobilizace a imobilizace U v prostředí jílových hornin s obsahem organické hmoty byl využit multidisciplinární přístup.

Sekvenční extrakce, chemická analýza na mokré cestě i spektroskopické metody prokázaly, že v málo oxidovaných vzorcích se U vyskytuje převážně ve formě U(IV). Při oxidaci vzorku s časem se U přesunuje směrem ke snáze uvolnitelným formám. Současně metody prokázaly asociaci U s As a P. Tento výsledek vedl k teorii, že se U(VI) z podzemní vody redukoval na U(IV) na povrchu pyritu pokrytém precipitovaným As.

Analýza hydrogeologických, hydrogeochemických dat a analýzy stabilních izotopů pomohly zařadit výše uvedené výsledky do obecného konceptu imobilizace U: Oxidace organické hmoty probíhá za mikrobiální katalýzy a vytváří redukční prostředí v blízkosti vrstev bohatých oganickou hmotou. Oxidovatelné látky (např. SO_4^{2-}) v podzemní vodě jsou redukovány, čímž je umožněn vznik pyritu FeS_2. Na jeho povrchu se sráží povlak As, na jehož povrchu je U(VI) redukován na U(IV). Ten reaguje s PO_4^{3-}, uvolněným mikrobiální oxidací organické hmoty, za vzniku fosfátu U(IV), ningyoitu. Formy U(IV) jsou dlouhodobě stabilní (1Ma). Díky tomuto závěru je možno deklarovat potenciální bariérovou funkci hornin obdobného typu (jílové sedimenty-organická hmota), jež mohou tvořit pokryvné vrstvy hostitelského masivu hlubinného úložiště. Naopak je nutno zdůraznit vliv CO_2 na zvýšenou mobilitu U(VI) i v redukčním prostředí podzemních vod.

Publication list

The core of the Thesis consists of following 6 publications (included in Appendix):

[I.] HAVLOVA, V., LACIOK, A., VOPALKA, D., ANDRLIK, L. (2006): Geochemical study of uranium mobility in Tertiary argillaceous system at Ruprechtov site, Czech Republic. Czechoslovak Journal of Physics, Vol. 56 (2006), Suppl. D, D1-D6.

[II.] DENECKE, M. AND HAVLOVA, V. (2007): Elemental correlations observed in Ruprechtov Tertiary sediment: micro-focus fluorescence mapping and sequential extraction. S&T publication. In Buckau G. and Kienzler B., Duro L., Montoya V. (eds.): 2rd annual workshop proceedings of 6th EC FP FUNMIG IP, Stockholm, November 21-23, 2006, 315-320. SKB Technical Report, TR-07-05.

[III.] NOSECK U., SUKSI, J. , HAVLOVA, V., BRASSER, T. (2007): Uranium enrichment at Ruprechtov site – Uranium disequilibrium series and geological development. S&T publication. In: Buckau G. and Kienzler B., Duro L., Montoya V., Delos A. (eds.) 3rd annual workshop proceedings of 6th EC FP FUNMIG IP, Edinborough, GB, Nov. 25 – 29, 2007**,** 317-325. Report NDA 2007.

[IV.] HAVLOVÁ, V., BRASSER, TH., CERVINKA, R., NOSECK, U., LACIOK, A., HERCIK, M., DENECKE, M., SUKSI, J., DULINSKI, M., ROZANSKI, K. (2007): Ruprechtov Site (CZ): Geological Evolution, Uranium Forms, Role of Organic Matter and Suitability as a Natural Analogue for RN Transport and Retention in Lignitic Clay. Proc. of Reposafe Conference, Braunschweig Nov. 6 – 9, 2007, 203-212, GRS-S-49.

[V.] NOSECK, U., BRASSER, TH., SUKSI, J., HAVLOVA, V., HERCIK, M., DENECKE, M.A., FÖRSTER, H.J. (2008): Identification of uranium enrichment scenarios by multi-method characterisation of immobile uranium phases. J. Phys. Chem. Earth, Vol. 33, Issue 14-16, 961-977.

[VI.] NOSECK, U., ROZANSKI, K., DULINSKI, M., HAVLOVA, V., SRACEK, O., BRASSER, TH., HERCIK, M., BUCKAU, G. (2009). Carbon chemistry and groundwater dynamics at natural analogue site Ruprechtov, Czech Republic: Insights from environmental isotopes. Applied Geochemistry, Volume 24, Issue 9, 1765-1776.

Further important publications worth reading are:

- NOSECK, U. & BRASSER, TH. (2006): Radionuclide transport and retention in natural rock formations – Ruprechtov site. GRS-218, 157 S. + CD, Köln, 2006.
- HAVLOVA, V., NOSECK, U., CERVINKA, R., BRASSER, T, DENECKE, M. HERCIK, M. (2007): Uranium enrichment at Ruprechtov site - Characterisation of key processes. S+T presentation. 3rd annual meeting of IP FUNMIG, Edinborough, GB, Nov. 25 – 29, 2007. NDA report.
  http://www.nda.gov.uk/documents/upload/3rd-Annual-Workshop-Proceedings-of-the-Integrated-Project-Fundamental-Processes-of-Radionuclide-Migration-6th-EC-FP-IP-FUNMIG.pdf.
- NOSECK, U., SUKSI, J., HAVLOVA, V., ČERVINKA, R.. (2008): Uranium geochemistry at Ruprechtov site. S&T publication. In: Buckau G. and Kienzler B., Duro L., Montoya V., Delos A. (eds.) 4th annual workshop proceedings of 6th EC FP FUNMIG IP, Karlsruhe November 24– 27, 2008. 383-390. Report FZK-INE, FZKA 7461.
- VOPÁLKA, D., HAVLOVÁ, V. AND ANDRLÍK, M. (2008): Characterisation of U(VI) behaviour in the Ruprechtov site (CZ). Ïn Merkel B. J. And Hasche-Berger (2008): Uranium mininng and hydrogeology. Springer-Verlag, Berlin, Heidelberg, 2008.
- HAVLOVÁ, V., ČERVINKA, R., HAVEL, J. (2009): Interrelation of mobile organic matter and sedimentary organic matter at the Ruprechtov site. Buckau G. and Kienzler B., Duro L., Montoya V., Delos A. (eds.) 4th annual workshop proceedings of 6th EC FP FUNMIG IP, Karlsruhe November 24– 27, 2008. 383-390. Report FZK-INE, FZKA 7461.
- CERVINKA R., STAMBERG K., HAVLOVA V., NOSECK U. (2010): Humic substances extraction, characterization and interaction with U(VI) at Ruprechtov site (CZ). Radiochim. Acta 99, 1–12 (2011) / DOI 10.1524/ract.2011.1806.

Scientific reports can be obtained from the author.

Preface

The Thesis explains how the study of processes in a natural system can be used to demonstrate issues important for the safety assessment of a deep geological repository (DGR) of spent nuclear fuel and high level waste. Such a system with processes relevant for the task mentioned is called “natural analogue” (www.natural-analogues.com). The work was focused on processes - namely mobilisation/retention processes - that uranium, an important DGR inventory element, can undergo within rocks with clay and organic constituents. Moreover, uranium forms and phases were studied in detail, accompanied by groundwater sampling and analyses, natural isotope analyses in both solid and groundwater samples, study of organic matter components, etc.

The activities followed a scheme that can be assigned as “a puzzle system” proceeding from investigation of “single puzzle pieces” (e.g. characterisation of the natural system geology and hydrogeology, organic matter constituents and behaviour, characterisation of the U mobile/immobile phases, etc.) to a more integral investigation and characterisation of a complex natural system, integrating results e.g. from “single piece” investigations. Finally a complete “puzzle picture” was assembled, i.e. the geochemical evolution of the system and in particular the uranium enrichment scenario at the site were outlined.

The study comprised both laboratory and in-situ work at the Ruprechtov natural analogue site (Czech Republic) under close cooperation with a broad international scientific team. The core of the Thesis is formed by papers and publications No. **[I.]-[VI.],** that can be potentially supplemented by the publications Noseck and Brasser (2006), Havlová et al. (2007 and 2009), Noseck et al. (2009), Vopálka et al. (2008).

The activities, as the input for the Thesis, basically performed at Nuclear Research Institute Rez plc., (NRI Rez), included namely rock and groundwater sampling and monitoring, rock characterisation, sequential extraction, organic matter characterisation and groundwater geochemistry evaluation. The original results that the Thesis presented is based on, are namely focused on sequential extraction (uranium form definition), groundwater chemistry evaluation and definition of uranium mobilisation/immobilisation conditions. All the activities were performed in inseparable and close cooperation with GRS Braunschweig, Helsinki University, FZK-INE Karlsruhe and University Krakow.

The persons I am mostly grateful are the key members of “Ruprechtov crew”: Dr. U. Noseck, Dr. Thomas Brasser, M. Hercík, R. Červinka and J. Suksi who should definitely be named as co-authors of the Thesis presented.

More of all, I would like to thanks to Dr. Ulrich Noseck (GRS Braunschweig), being undoubtedly the most powerful engine for all the research on Ruprechtov site. He was the force that brought all of us forward from analyses results to conclusions. Ulrich, thanks for years of fruitful cooperation and friendship. And also thanks for reviewing and commenting the Thesis.

I thank also to Thomas Brasser (GRS) and Mirek Hercík (NRI Rez plc.), the field geology guys, as without their ideas, experience and skills in practical field geology the research cannot be realized at all. A special tribute to Mirek who passed away unexpectedly in June 2010 and will be missed by all the people around.

Many thanks to Juhani Suksi for his inventory, concerning U(IV)/U(VI) wet chemical separation and U isotope activity ratios, and many fruitful discussions. Then, I would like to thank Radek Červinka, who, made a nice

piece of work concerning organic matter characterisation on the site and slowly took over the Project. Moreover, many thanks for all the help with the graphics (the cover) and corrections.

Melissa Denecke (FZK-INE) is acknowledged for her work on micro X-ray fluorescence (μ-XRF) and micro X-ray absorption fine structure (μ-XAFS). Kazimierz Rozanski and Marek Dulinski (Krakow University) for carbon and oxygen isotope analyses.

Many thanks to Jana Palágyiová and Věnka Paluková for their work in the lab.

I wish to express my sincere thanks to Doc. Emil Jelínek, CSc. for his steady effort to push me to finish my doctoral studies. I am also thankful to NRI Rez plc. and the head of Waste Disposal department Ing. Antonín Vokál, CSc.

Finally, I wish to express my dearest thanks to my family - Mirek, Madlenka and Vojta, and to my Mum for all their support.

Acknowledgement

The research on the Ruprechtov natural analogue site was funded by RAWRA (CZ), Ministry of Trade and Industry (CZ, POKROK 1-H-PK/25; TIP FR-TI1/362), by the European Commission (EURATOM FP 6, FUNMIG, Contract No. 516514) and by the German Federal Ministry of Economics (BMWi) under contract no's 02 E 9551 and 02 E 9995.

Contact: Ústav jaderného výzkumu Řež a.s., Odd. Ukládání odpadů
Nuclear Research Institute Rez plc., Waste disposal department
Husinec-Řež 130, 240 68 Řež
hvl@ujv.cz

Content

List of tables

List of figures

Abbreviations

AR	activity ratio $^{234}U/^{238}U$
D	deuterium, ^{2}H
DGR	deep geological repository
DIC	dissolved inorganic carbon (content in µg/L)
DOC	dissolved organic carbon (content in µg/L)
DOM	dissolved organic matter
FZK-INE	Forschungzentrum Karlsruhe Institut für Nukleare Entsorgung, Germany
GRS	Gesellschaft für Anlagen-und Reaktorsicherheit (GRS) mbH
MALDI TOF	Matrix Assisted Laser Desorption/Ionization - Time Of Flight Mass spectrometry
MOM	mobile organic matter
NA	natural analogue
NDA	Nuclear Decommissioning Authority
RAWRA	Radioactive waste repository authority
SA	safety analyses
SE	sequential extraction
SF	spontaneous fission
SIC	sedimentary inorganic carbon (content in mg/L)
SKB	Svensk Kärnabränlehanterin AB, Sweden
SNF	spent nuclear fuel
HLW	high level waste
SOC	sedimentary organic carbon (in mg/L)
SOM	sedimentary organic matter
TOC	total organic carbon (content in mg/L)
µ-XAFS	micro X-ray absorption fine structure
µ-XRF	X-ray fluorescence

1. INTRODUCTION

1.1. Deep geological repository safety and the natural analogue concept

The basic concept of deep geological disposal of spent nuclear fuel (SNF) and high-level radioactive waste (HLW) is to isolate the waste from the human environment for the long term. To assess the long-term safety of a deep geological repository (DGR) for radioactive waste, it is necessary to look at the barrier function of the surrounding geological environment, i.e. the host rock and adjacent/overlying rock formations (e.g. sedimentary rocks). A typical DGR disposal system, providing complex safety functions based on engineered and natural barriers is presented on Fig. 1.

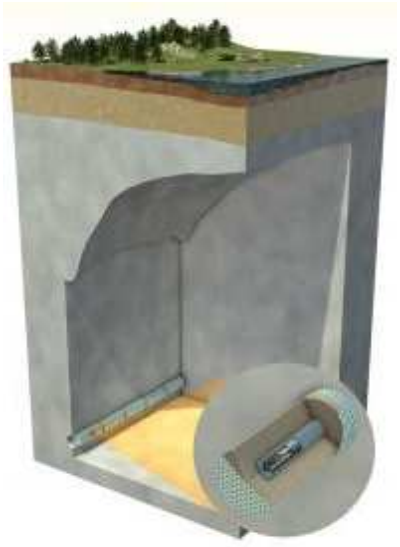

Fig. 1 Deep geological repository disposal concept, accepted in Czech Republic: spent fuel is disposed of directly in steel containers into the granitic host rock. The disposal boreholes and tunnels are sealed with bentonite buffer and bentonite/granite backfill (www.rawra.cz).

The possible future development of the disposal system and the relevant processes can be simulated with the help of long-term safety analyses, which in turn are based on assumptions that have to be verified. '**Natural**

analogues' are a particularly suitable instrument for such verification purposes as they usually represent naturally occurring systems, where physical, chemical, and/or microbiological processes that can be expected in repository systems (or parts thereof) are developing (or have developed) over geological time periods.

The very first definition of the term 'natural analogue' (Côme & Chapman, 1986) was presented as *"...an occurrence of materials or processes which resemble those expected in a proposed geological waste repository*." The definition has subsequently been refined by the addition (McKinley, 1989): "*The essence of a natural analogue is the aspect of testing of models - whether conceptual or mathematical - and not a particular attribute of the system itself*", and by an IAEA review group which noted that; *"Natural analogues are defined more by the methodology used to study and asses them than by any intrinsic physic-chemical properties they may possess"* (IAEA, 1989).

Basically, natural analogue studies use information from the closest possible approximations, or direct analogies, of the long-term behaviour of materials and processes found in, or caused by, a repository to develop and test models appropriate to performance assessment (www.natural-analogues.com). Natural analogues enable the study of repository-like systems which have evolved over geological time scales, more closer to DGR safety assessment in contrary to short-term laboratory experiments The disadvantage is that the boundary conditions and the source term are often unknown or poorly defined. Well known natural analogues are for example Oklo, Cigar Lake (Fig. 2), Pocos de Caldas, Oman (e.g. Chapman et al, 1990; Alexander, 1992; Cramer and Smellie, 1993; Liu, 1995; Smellie, 1996, 1998; Gurban et al., 1998; Linklater, 1998; Zetterström, 2000; Bruno et al., 2001, etc.). Natural analogues focused on crystalline rock and being relevant to CZ disposal

concept are for example Palmottu (Blomqvist et al., 1998, 2000; Suksi et al., 2006 ad.) or El Berrocal (Gomez et al., 1992; Montoto et al., 1996, Bruno et al., 1998, Miller et al., 2000 etc.).

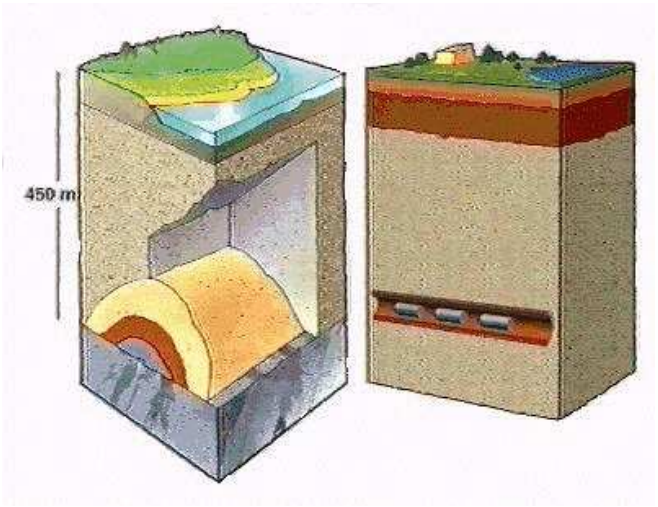

Fig. 2 Cigar lake natural analogue (left) , that can be used for the demonstration of the DGR concept (right): U deposit, surrounded by a clay halo without any trace of U at the surface (www.natural-analogues.com).

The Ruprechtov site in the north-western part of the Czech Republic, has been investigated in order to follow the mentioned approach. Due to its unique geological structure (see further) it can be considered as an analogue for potential migration processes of relevant elements (particularly uranium) in DGR overburden sedimentary rocks, containing increased contents of organic matter. The natural system is then used for studying the influence of system constituents, including organic matter, on uranium mobilisation/immobilisation processes. The activities have been performed for 15 years (since 1996). Extensive geological, hydrogeological, geochemical, isotope investigations, accompanied by geochemical and transport modelling has taken place and will be finalised by a bilateral project (GRS-NRI, 2009-2012), being focused on redox processes within the system.

1.2. Uranium importance for the safety assessment of deep geological repositories

There is a long line of elements/radionuclides of importance for a DGR long-term safety analysis, considering their potential impact on human according to different scenarios. One of the most important elements is uranium, originating from burn-out fuel rod material (spent fuel rods) or vitrified reprocessed waste (high level waste).

Several uranium isotopes will be present in the initial repository radionuclide inventory – see an example in Tab. 1 (data from Carbol and Enkvist, 1997 and SKB, 1999). All of the nuclides are long-lived (see minimum half-life for ^{233}U). An example of activities and possible inventory of individual uranium nuclides in spent fuel after 40 years from discharge from the reactor, i.e. before fuel disposal (calculations from SKB, 1999) is also included to demonstrate activities that are considered for safety assessment calculations.

Tab. 1 Uranium isotopes of relevance for safety assessment. Potential oxidation state in the environment, half-life and nuclide inventory in spent fuel (initial activity 40 years after discharge from reactor) are listed. (after Carbol and Enkvist, 1997; SKB, 1999).

Isotope	Oxidation state in environment	Half-life (years)	Activity (Bq/t U) 40 years after discharge from reactor
^{233}U	U(IV,V,VI)	1.592×10^{5}	3.1×10^{6}
^{234}U	U(IV,V,VI)	2.454×10^{5}	4.5×10^{8}
^{235}U	U(IV,V,VI)	7.037×10^{8}	4.5×10^{8}
^{236}U	U(IV,V,VI)	2.342×10^{7}	1.0×10^{10}
^{238}U	U(IV,V,VI)	4.468×10^{9}	1.2×10^{10}

Therefore, all the processes that uranium can potentially undergo on the way from DGR into the surrounding environment have to be considered and must be understood in order to estimate the potential risk arising for human and

biota. Typical assessment time frames to be considered are several 100 000 to 1 Million years.

For uranium retardation, i.e. process slowing down its migration velocity towards the surface, sorption and complexation are the most important processes. Precipitation and co-precipitation play a role in reducing the concentration of uranium. The interaction with colloids and /or organic matter might impact the sorption and precipitation behaviour.

As uranium and all his radioisotopes are known to be highly redox sensitive, environment redox conditions have to be evaluated (e.g. Philippi et al., 2007; Langmuir, 1978, 1997; Ervanen, 2004; etc.), taking into account both rock and groundwater chemistry with stress on redox influencing compounds (O_2 access, organic matter, sulphide mineral presence, microbial activity etc.).

The main oxidation states of uranium in nature are (IV) and (VI); oxidation state (V) occurs only rarely. U(IV) is essentially insoluble in mildly acidic to alkaline groundwaters and its solubility is commonly controlled by uraninite or coffinite, while U(VI) is potentially more mobile due to the much higher solubility of U(VI) phases (Philippi et al., 2007; Langmuir, 1998; Murakami et al., 1997; Lieser, 1995; Ivanovich and Harmon, 1982 etc.). Reduction of the soluble, oxidised form of uranium U(VI) is an important mechanism for the U immobilisation. This process used to be generally regarded as abiological, however increasing trend of proofs brings on focus microbial life involment, speeding up the potential course of the reaction (Lovley et al., 1991, Lovley and Phillips, 1992; Gorby and Lovley, 1992; Pedersen, 2000 etc.).

2. The Ruprechtov natural analogue site

2.1. Geographical and geological settings

The Ruprechtov site is situated in the NW part of the Czech Republic in Hroznětín part of the Sokolov Basin (see Fig. 3). The basin is filled with Oligocene and Miocene sediments, represented mainly by an argillised pyroclastical complex with a thickness of 0 – 100 m. The basal Staré-Sedlo Formation (or equivalent rocks) fills depressions on the basement top and is overlain by the so-called volcano-detritic formation, which is intercalated by lignite seams, also in association with more sandy material (see Fig. 4).

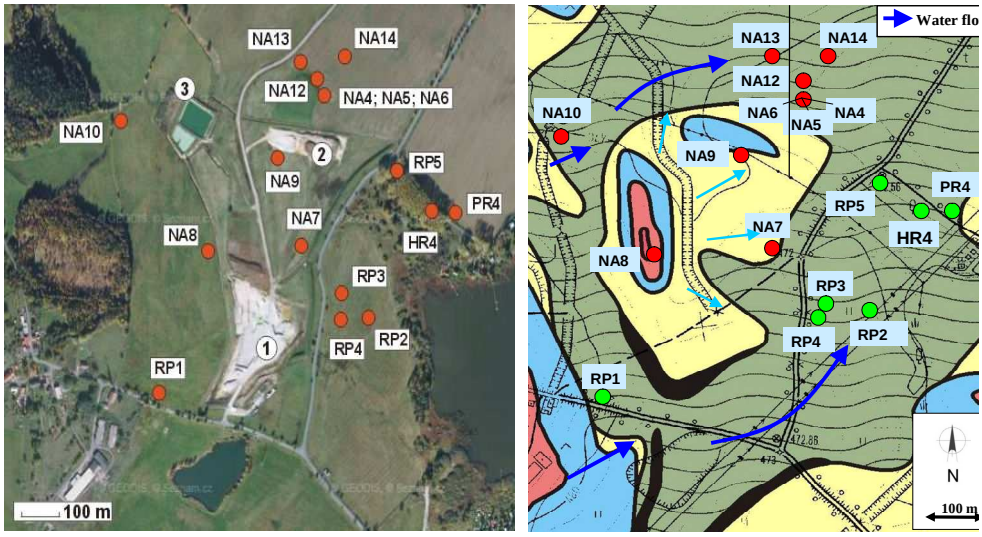

Fig. 3: Left: Aerial view of the Ruprechtov site with borehole localisation and 1) kaoline pit; 2) kaoline deposition place ; 3) sludge pond (© Červinka, 2008).

Right: Sketch of the same area with geological settings shown. Yellow: kaolin, pink, red and blue: granite, green: Tertiary pyroclastic sediments - see publication No. [VI.].

Therefore, the rock sequence defined above is denoted as the *clay/lignite horizon.* Uranium enrichment (up to several hundred ppm) can be usually found within the lower part of the clay/lignite horizon, below the lignite

seams. Sediment cores and groundwater were sampled from a system of boreholes, drilled and maintained on the site since 1996. For localisation of the boreholes see the simplified geological profile presented in Fig. 3.

Granitic rocks, belonging to the Karlovy Vary Massif, underlie the sedimentary sequence. The granites underwent intensive weathering in Mesozoic ages, causing kaolinization. Two rock types can be distinguished (Kominek et al., 1994): older Horský granite (325–310 Ma; low U content 3.4–13.4 ppm) and younger Krušnohorský granite (< 305 Ma; U content up to 28 ppm). The crystalline rock is considered as a potential uranium source. A detailed geological description can be found in publication No. **[I.]** and **[IV.]**, including a model describing the geological development at Ruprechtov site in publication No. **[IV.]**.

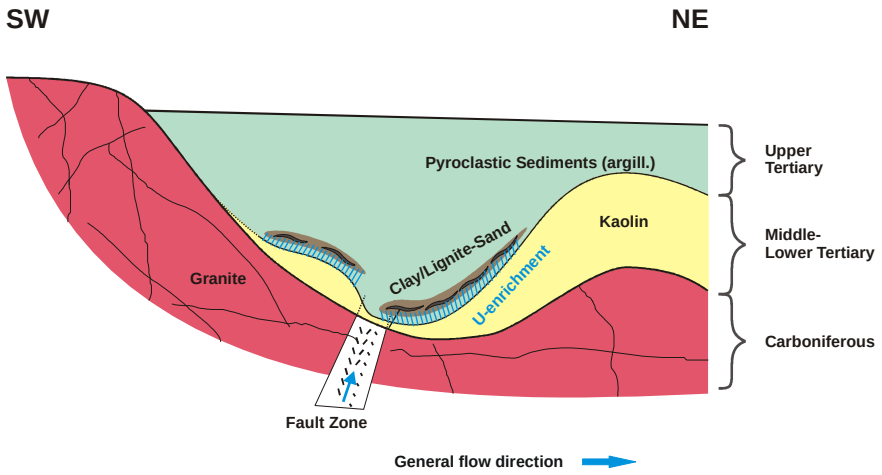

Fig. 4: Simplified geological cross section of the Tertiary basin at the Ruprechtov site (Noseck and Brasser, 2006).

Generally, two types of rock sequences were studied: the so called clay/lignite horizon, i.e. a sequence of Tertiary sedimentary montmorillonitic clays with organic-rich layers, partly with high uranium accumulations; and the underlaying granite where the clay sequence is either thin or not fully developed.

2.1. Hydrogeochemistry and hydrogeology of the site

Low mineralized waters characterize the chemical conditions at the site, with ionic strengths in the range from 0.003 mol/L to 0.02 mol/L. All DOC values are in a range between 1 mg/L and 5 mg/L. Uranium concentration in groundwater did not exceed 12 µg/l and is higher in the more oxidising granitic waters than in the waters from the clay/lignite horizon (see below). The groundwater composition is shown in Tab. 2 and 3, altogether with allocation of layers of groundwater sampling.

The pH-values vary in the range from 6.2 to 8 and the Eh-values from 435 mV to -280 mV. More oxidising conditions with lower pH-values are found in the near-surface granite waters of the infiltration area. In the clay/lignite horizon the conditions are more reducing with Eh-values as low as -280 mV. For further information see publication No. **[VI.]** and Noseck et al. (2008).

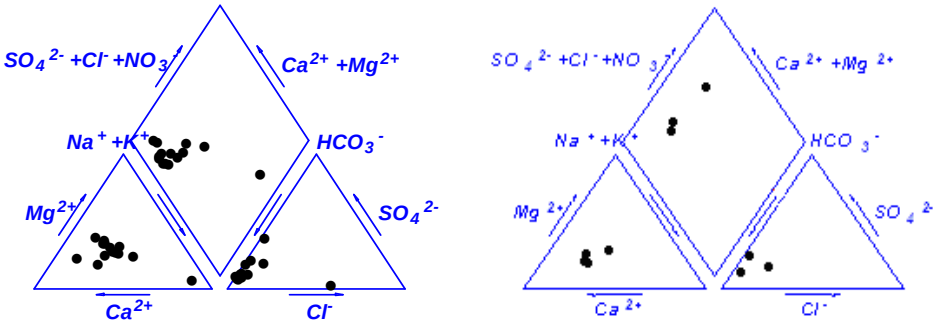

Fig. 5: Piper diagrams of groundwater chemical composition from clay/lignite horizon (left) and granite (right). Noseck and Brasser (2006).

A detailed investigation of hydrogeology at the site, supported by natural isotope analyses (D, ^{3}H, ^{13}C, ^{14}C, ^{18}O, ^{34}S), was performed, resulting in a groundwater flow model of the site. Infiltration areas of the site are located

into the outcropping granites in the western and southern parts (see Fig. 6). Preferential water flows do not represent a continuous aquifer, but rather distinct areas of increased permeability. In general, active water flow is presumed to be confined to the Tertiary formation and the underlying granite. Both flow systems are separated by a kaolin layer of variable thickness. However, there are strong indications for local connections of the flow systems in the underlying granite and in the Tertiary sediments in the northern part, where the kaolin thickness is very small and the existence of fault zones was confirmed (Noseck U. in publication No. **[IV.]**). For a detailed description of the methodology, the results, and conceptual model of flow pattern see publication No. **[VI.].**

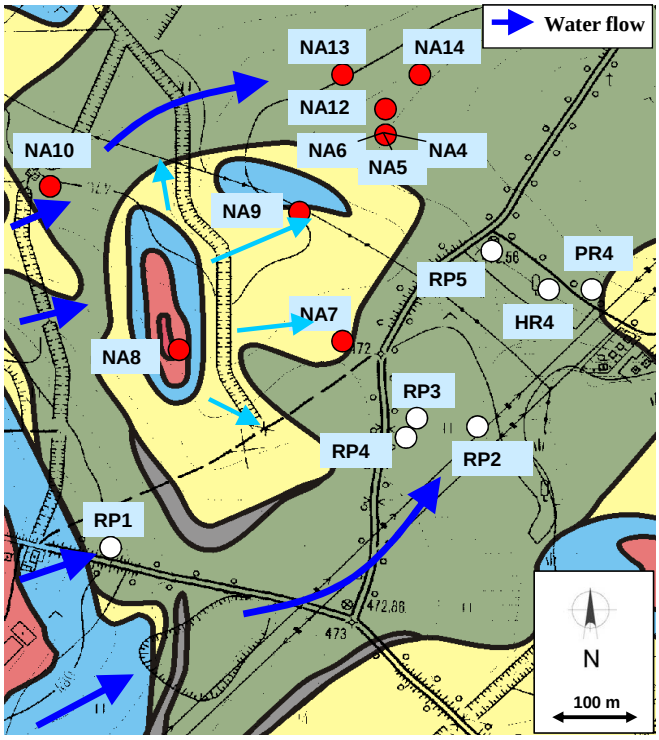

Fig. 6 Conceptual model of the groundwater flow pattern in the studied Ruprechtov aquifer system (Noseck U. in publication No. [IV.]).

Tab. 2 Physical and chemical parameters of Ruprechtov groundwaters studied (2004). Concentrations in mg/L. Eh-values are expressed in mV. Data were adopted from publication No. [IV]; for Uranium from Hercik et al. (2008).**

	T [°C]	pH1	pH2	pH3	Eh1	Eh2	Al	Fe	Ca	Na	Mg	K	Si	Cl	SO_4	PO_4^{2}	NO_3	CO_2	HCO_3	CH_4	U**
NA4	9.6	n.a.	6.7	6.7	n.a.	6	0.20	1.87	51.00	23.30	23.60	13.10	10.30	3.90	19.80	0.19	0.80	40.71	330.5	0.63	0.0004
NA5	9.0	n.a.	7.1	7.0	n.a.	-10	0.26	0.99	68.90	45.25	29.35	12.30	7.80	8.80	31.50	0.47	0.40	43.60	469.3	0.1	0.0009
NA6	9.8	8.0[1)]	7.8[1)]	7.6	-280[2)]	-115[1)]	0.22	0.73	48.00	37.20	18.60	12.05	7.40	3.60	49.50	0.2	1.20	6.70	291.8	0.07	0.0013
NA7	9.1	8.0[1)]	7.1[1)]	7.5	-35[1)]	-107[1)]	0.33	0.13	86.85	16.40	17.90	6.50	4.40	6.60	28.20	0.72	1.10	9.60	332.1	0.01	0.0013
NA8	9.0	6.2[1)]	6.5[1)]	6.2	48[1)]	143[1)]	0.10	1.32	26.24	10.90	4.00	1.40	15.05	4.30	59.10	0.3	1.70	31.70	44.20	n.a.	0.0032
NA9	7.3	7.2[1)]	6.8[1)]	7.0	324[1)]	355[1)]	0.15	0.91	28.03	14.10	5.30	2.70	18.70	0.60	11.80	0.08	1.10	8.60	163.5	n.a.	0.0008
NA10	8.4	7.4	6.9	6.7	240	485	n.a.	0.37	40.40	15.50	8.40	8.40	13.00	5.90	40.80	0.16	7.20	24.50	159.4	0.003	0.0091
NA11	9.80	6.9	7.0	7.1	-91	65	n.a.	5.45	65.60	91.20	28.90	18.90	7.70	10.40	178.6	0.30	1.40	40.60	379.0	0.01	0.0009
NA12	9.1	6.6	6.7	6.7	-160[2)]	15	n.a.	2.27	44.70	20.10	19.80	9.70	15.90	4.30	22.90	0.04	0.30	63.00	269.2	0.03	0.0002
NA13	9.9	7.6	7.4	7.7	-252[2)]	25	n.a.	0.83	54.60	35.80	21.70	16.50	8.00	10.10	22.90	0.14	1.00	10.50	349.0	0.04	0.0027
NA14	9.2	6.8	7.0	6.9	-59	120	n.a.	0.10	48.70	39.50	20.80	14.60	12.60	13.60	30.80	0.21	2.30	32.80	316.6	0.02	0.0006
NA15	9.4	7.3	7.1	6.7	58	245	n.a.	0.31	31.60	25.30	12.50	10.80	11.60	4.00	40.10	0.10	3.50	13.80	186.7	0.004	0.001
RP1	9.7	6.81[1)]	6.7[1)]	6.4	149[1)]	363[1)]	0.14	0.34	31.00	13.40	8.80	2.90	16.80	20.70	19.80	0.35	3.20	44.40	117.0	n.a.	0.015
RP2	9.6	7.7[1)]	7.3[1)]	7.7	-3.8[1)]	25[1)]	0.21	2.89	47.10	41.80	23.80	10.30	3.30	26.40	55.00	0.11	2.50	1.00	277.0	n.a.	0.0011
RP5	9.1	7.0[1)]	6.9[1)]	6.9	133[1)]	160[1)]	0.25	1.16	43.70	19.20	21.40	11.20	9.90	5.54	14.80	0.15	2.20	20.50	279.0	n.a.	0.0007

pH1: measured in-situ; pH2: measured on-site; pH3: measured in laboratory (T=20°C); Eh1: measured in-situ, Eh2: measured on-site
[1)] sampling campaign from May 2003, [2)] long-term value

Tab. 3 Content of DIC, DOC, SO_4^{2-} (mg/L) and natural isotopes (‰ and pmc) in Ruprechtov groundwaters. Data were adopted from publication No. [IV.].

Borehole No.			NA4	NA5	NA6	NA7/1	NA7/2	NA8	NA9	NA10	NA11	NA12	NA13	NA14	NA15	RP1	RP2	RP3	RP5	HR4	PR4
Screened horizon		[m]	34.5 – 36.5	19.3 - 21.3	33.4 - 37.4	15.5 - 19.5	10.5 - 11	8.5 - 24	4.4 - 10	19.5 - 27.5	33.2 - 39	36.5 - 39.3	42.2 - 48	67.6 - 77.6	28.8 - 31.6	5 - 18	25 - 43	25 - 48	30 - 58	46.5 - 95	5 - 32
Lithology			C/L, U	C/L, U	C/L, U	K	C/L, U	GR	K	GR	C/L, U	C/L, U	C/L, U	GR	GR	GR	C/L, U	C/L, U	C/L, U	GR	C/L, U
DIC		[mg/L]	74.2	90.8	60	61.7	60.8	14.5	37.1	33.8	82.4	67	68.8	69.1	39.4	33.4	52.4	59.7	58.1	n.a.	n.a.
DOC		[mg/L]	4.22	n.a.	3.27	3.88	n.a.	3.01	n.a.	1.99	n.a.	3.69	2.32	n.a.	n.a.	1.36	1.83	n.a.	n.a.	n.a.	n.a.
SO_4^{2-}		[mg/L]	19.8	31.5	49.5	28.2	12.3	59.1	11.8	40.8	178.6	22.9	22.9	30.8	40.1	19.8	55.0	24.6	14.8	n.a.	n.a.
$\delta^{18}O$		[‰]	-9.78	-8.98	-9.27	-8.96	-9.00	-9.22	-8.95	-8.89	-9.00	-8.87	-9.24	-9.33	-9.88	-9.52	-9.81	-9.60	-9.75	-9.31	-9.00
^{14}C	DIC	[pmc]	3.2	5.3	13.1	n.a.	39.4	71.9	72.1	54.6	7.8	26.5	n.a.	9.8	11.8	21.0	16.8	13.3	6.4	29.9	n.a.
	DOC	[pmc]	40.0	n.a.	n.a.	n.a.	n.a.	64.6	n.a.	n.a.	n.a.	70.0	44.3	n.a.	n.a.	n.a.	n.a.	n.a.	n.a.	n.a.	n.a.
$\delta^{13}C$	DIC	[‰]	-11.0	-10.9	-12.4	n.a.	-16.1	-21.9	-20.5	-16.2	-9.6	-16.0	n.a.	-12.8	-13.7	-16.8	-13.2	-15.3	-11.7	-14.5	n.a.
	DOC	[‰]	-26.6	-25	-26.8	n.a.	-27.3	-27.8	-27.1	-26.4	n.a.	-25.6	-27.2	n.a.	n.a.	n.a.	-26.6	-26.6	n.a.	-26.2	n.a.
$\delta^{34}S$	SO_4^{2-}	[‰]	24.63	n.a.	23.5	n.a.	20.4	-8.5	n.a.		n.a.	20.11	n.a.	16.43	n.a.	3.48	n.a.	n.a.	n.a.	n.a.	n.a.

C/L, U = clay/lignite, uranium; K = kaoline; GR = granite

2.2. Uranium occurrence

Uranium enrichment within the sedimentary rocks showed a heterogeneous distribution, however it was usually detected in the vicinity of organic enriched layers (e.g. publication No. **[I.]** Noseck and Brasser, 2006). Original detritic (monazite, rhabdophane, xenotime, zircon) and newly formed uranium (IV) minerals (uraninite (UO_2), ningyoite (U, Ca, $Ce)_2(PO4)_{2.1}$-$2H_2O$, tristamite (Ca, U, Fe)(PO_4, SO_4).$2H_2O$) were identified using both, thin section microscopy and electron probe spectrometry (for example see Fig. 7; Sulovský, 2005). In one case, U(VI) sulphate was presumably distinguished – see Fig. 8., further, publication No. **[I.]**, and Noseck and Brasser (2006).

As only mineral grains up to 1 μm were accessible by electron spectroscopy and carefully studied, it was presumed, that a part of the U content is bound in different indefinable forms within the sedimentary rock (Sulovský, 2005), sorbed on organic matter, Fe minerals or dispersed etc.

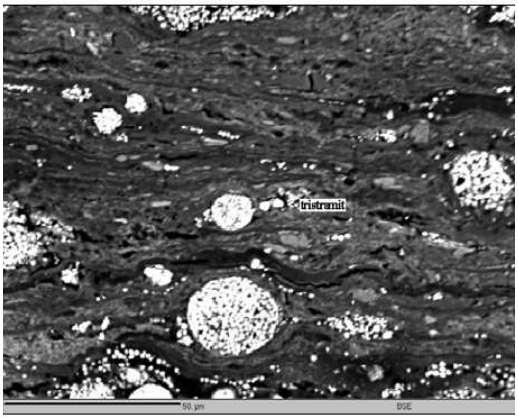

Fig. 7 Thin section area from a sample from borehole RP 5 with 2 grains of tristamite (in circle; Sulovský, 2005).

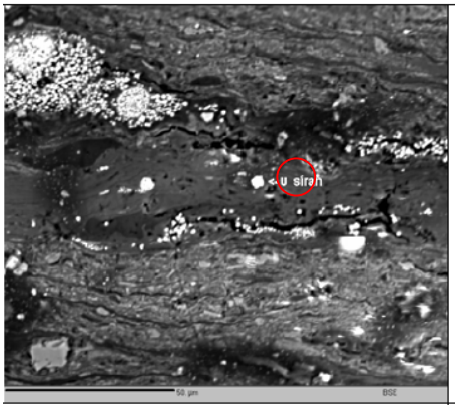

Fig. 8 Uranyl suphate grain in a sample from borehole RP5 (in red circle, Sulovský, 2005).

However, U sorption on organic matter was not confirmed: uranium was not found to be directly bound on organic matter (no correlation of U content with SOC content; lignite seams, see publication No. **[I.]**). The highest concentration was usually found below the coal layers in more sandy horizons (identified by visual and gamma activity examination during drilling campaigns). Following this conclusion uranium occurrence within the sedimentary rock was presumed to be of more complex character. Thus more sophisticated and detailed activities had to be employed.

3. Uranium form determination

3.1. Methodology

As stated above, the identification of U forms, both in sediments and groundwater was found to be more complex than expected. Therefore, several sophisticated methods were used in order to determine

- forms of U bound in the sediment and their correspondence with other constituents of the system,
- redox state for different U forms in the sediments and groundwater,
- U isotope ratios in different forms as tracer of the long-term stability/instability of the system.

The following methods were used:

- **Sequential extraction** (SE, for methodology see publications No. **[I.]**, **[II.]**, **[IV]**, **[V.]**) as conventional method using consequent leaching of rock material in order to identify different trace metal forms (modified after Tessier et al,. 1979, and Percival, 1990). Uranium forms are identified as

  1. **easily exchangeable**,

  2. **bound on alumosilicates/carbonate complexes**; in older publications referred as U bound in carbonates (see below),

  3. **bound on Fe/Mn oxides**,

  4**. reduced U(IV)**; in older publications referred as U bound on organic matter/in reduced state or U in reduced form/bound on organics (see further),

  5. **in residuum**.

  A statistical evaluation of the interrelation of U with other elements (Na, K, Fe, S, Al, As, P) was used in order to identify mutual interrelations

between system phases. (see publication No. **[II.]**). Moreover, the real phases dissolving in each step of extraction were evaluated on the basis of released elements.

- **Micro X-ray fluorescence (μ-XRF) and micro X-ray absorption fine structure (μ-XAFS) –** modern material surface analytical methods (FZK-INE; for methodology see Denecke et al., 2005 and publication No. **[II.]**).
- **$^{234}U/^{238}U$ activity ratio (AR) measurements in sequential extraction leachates and groundwater** (in cooperation with Helsinki University, for methodology see publication No. **[III.]** and Suksi et al., 2006).
- **U(IV) and U(VI) state using wet chemical method in sediments and groundwater** (Helsinki University, for methodology see publication No. **[III.]**).

The samples used originated from different boreholes and horizons, Information about the sediment samples studied and the methods used are summarized in Tab. 4. For the localisation of each borehole see Fig. 3.

Tab. 4 Sediment samples used and methods conducted within the research.

Method applied/ Borehole	**NA4**	**NA5**	**NA6**	**NA10**	**NA11**	**NA12**	**NA13**	**NA14**	**NA15**
Horizon type	Clay /lignite (Tc)	Clay /lignite (Tc)	Clay /lignite (Tc)	Granite	Clay /lignite (Tc)	Clay /lignite (Tc)	Clay /lignite (Tc)	Clay /lignite (Tc)	Granite
$^{234}U/^{238}U$-AR			**x**		**X**	**x**	**x**	**x**	**x**
U(IV)/U(VI)-separation			**x**		**x**	**x**	**x**	**x**	**x**
Sequential extraction			**x**	**x**	**x**	**x**	**x**	**x**	**x**
μ-XRF, μ-XAFS	**x**		**x**						

*AR denotes the activity ratio (see text), Tc – Tertiary; **x** denotes method used on the given sample*

Moreover, ageing study for 2 samples, NA13 and NA14, was performed (granularity under 300 μm and 300-600 μm). **Sequential extraction** according to the methodology, defined in publication No**. [I.]**, was performed periodically since 2006 to 2009 year in order to see trace metal form changes due to oxidation/alteration effects during storage under oxic atmosphere. AR and U(IV)/U(VI) were analysed in the leachates.

3.2. Results

Results of U sequential extraction are presented on Fig. 9. Their evaluation is included in publications No. **[I.], [II.], [III.] and [IV.].**

Concerning, that association of U with organic matter was not proved, the 4th sequential extraction step can be re-assigned as U in reduced form. Similarly, as carbonates were not found in the sediments in larger extent and K is excessively leached in SE step 2 probably as result of alumosilicate dissolution, the 2nd sequential extraction step would be further assigned as U bound on alumosilicate and/or in carbonate complexes (see publications No. **[I.]** and **[II.]).**

Uranium in the samples was namely presented in three dominant forms: U bound on alumosilicates and/or carbonate complexes, U in reduced form and in residuum. It is important to notice that with increasing depth and in the presence of a clay/organic rich environment the distribution of U changes in prospect of U in reduced form. In sample NA10 (17,15 m). Uranium is present namely in the residual form (i.e. in detritic minerals from the rock).

The **sequential extraction** distribution pattern of U forms in fresh samples (shortly after sampling) is illustrated in Fig. 12 (NA13 2006; NA14A 2006). Both NA13 and NA 14A samples stem from lower parts of the clay/lignite and show remarkable similarities. The leachates from the first three SE steps contain less than 25% of the total U. (see publ. No. **[V.]**). These results are

valid also for other samples from the clay/lignite horizon from higher depth (see Fig. 9 and publication **No. [II.]**).

Study on sediment ageing and sensitivity of U content in different forms is presented further (3.2.1)

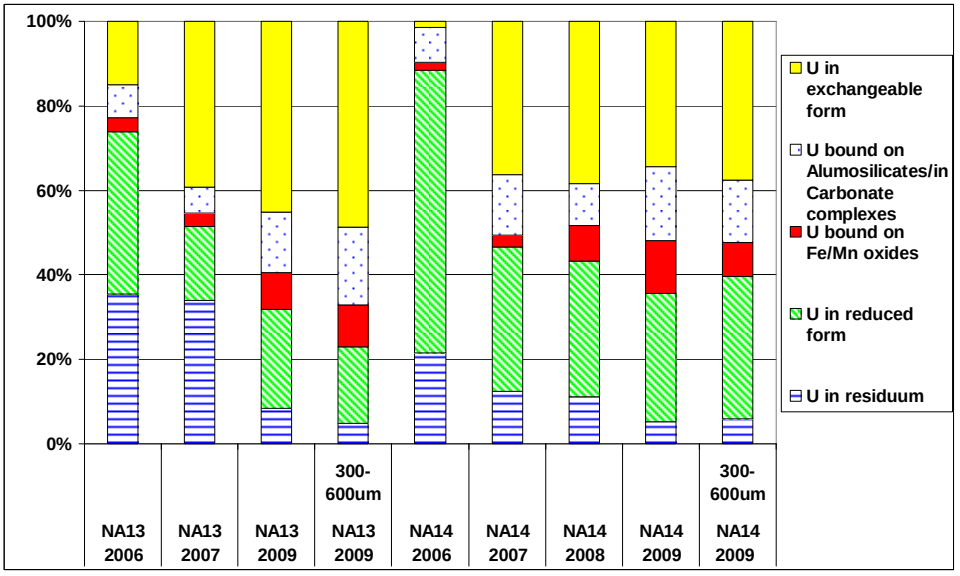

Fig. 9 Fractions (in %) of U in the sediment samples (SE results). NA10&NA15A origin from kaolinized granite layers, the rest of the samples from the clay/lignite horizon (see publication No. [II.]).

However, the sequential extraction method cannot be used as a solitaire and all-to-prove method, as without additional methods one cannot precisely define phases being dissolved during each SE step. One possibility is the combination with modern surface analytical methods. In this case, both **micro-focus fluorescence mapping** (publication No. **[II.])** and sequential extraction of Ruprechtov clay samples proved that U accumulation in the sediment cannot be correlated with Fe and S, but U can be found in association with As. **µ-X**AFS analysis revealed presence of U-phosphate phases in the sediment in the vicinity of arsenopyrite nodules. This result was corroborated by the cluster analysis of SE leachates (using PAST software,

Hammer and Ryan, 2001) for all elements of importance (U, K, Na, Ca, S, Fe, As, P- see Fig. 10). The analyses showed a clear correlation between U and P in SE leachates from different sediment samples. Moreover, a cluster analysis showed that there was no direct interrelation between U on the one hand and Fe and S on the other hand. Interrelation was also not proved between organic matter (represented as total organic carbon content, TOC) and U content. For details see references No. **[II].** and **[V].**

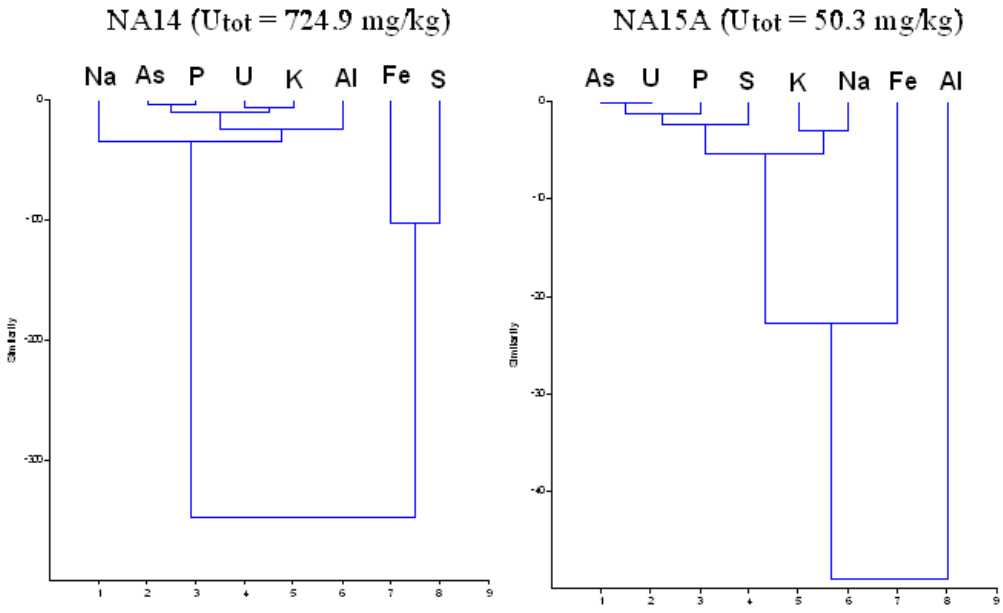

Fig. 10 Cluster analyses (using the code PAST, Hammer and Ryan P.D., 2001) for the element content in each sequential extraction leachate for 2 Tertiary clay samples from the Ruprechtov site. NA14 sample - Tertiary clay, rich in organic matter, high U content; NA15 - Tertiary clay, low organic matter and U content – see publ. [II.] and [V.].

In order to better understand the uranium enrichment and distinguish between different immobile phases, a separation method for U(IV) and U(VI) (Ervannen et al. 1996) has been modified and applied to solid samples from the clay/lignite layers from the different boreholes NA6, NA11, NA12, NA13 and NA14 (Helsinki University, namely publication No. **[III.]**). Moreover,

$^{234}U/^{238}U$ activity ration (AR) measurement was applied not only for U(IV) and U(VI) separate phases, but also for SE leachates to test the correlation of U forms, released by the different methods.

For detailed results of U(IV)/U(VI) separation for solid samples see publication No. **[III.].** The AR differs significantly in the U(IV) and U(VI) phases, with ratios <1 in the U(IV) phase and ratios >1 in the U(VI) phase in nearly all samples.

AR values significantly below unity are caused by the preferential release of ^{234}U, which is facilitated by α-recoil process and subsequent ^{234}U oxidation (Suksi J. in publication No. **[III.]**, see also e.g., Suksi et al. 2006).

In general, the AR for SE leachates for clay/lignite horizon samples correlate well with the U(IV)/U(VI)-separation results, since both methods observed the major part of uranium from the clay/lignite horizon to be associated with the U(IV) phase. This form is expected to be present predominantly in SE step 4 and 5 (U in reduced form and in residuum).

In order to confirm that uranium in SE steps 4 and 5 is really in the tetravalent state, AR analyses in the different SE leachates from sample NA13 were performed. Results are shown in Fig. 11. The analyses were limited to the leachates from SE step 1, 2, 4 and 5, since the uranium content in SE step 3 is always very low, < 3 % of total uranium. For details see publ. No. **[III.]** and **[V.].**

AR in SE steps 1 and 2 reaches values above 1.75. Comparing this value with results from U(IV)/U(VI)-separation it can be stated that uranium extracted in these first two SE steps was U(VI). In contrast, ARs in the leachates from SE steps 4 and 5 are around 0.5 to 0.6, which matches well the values observed in the U(IV) and U(res) fractions from U(IV)/U(VI)-separation (Suksi in publication No. **[III.],** for basis see Suksi et al. 2006).

The results confirmed that uranium in SE steps 4 and 5 was in U(IV) state.

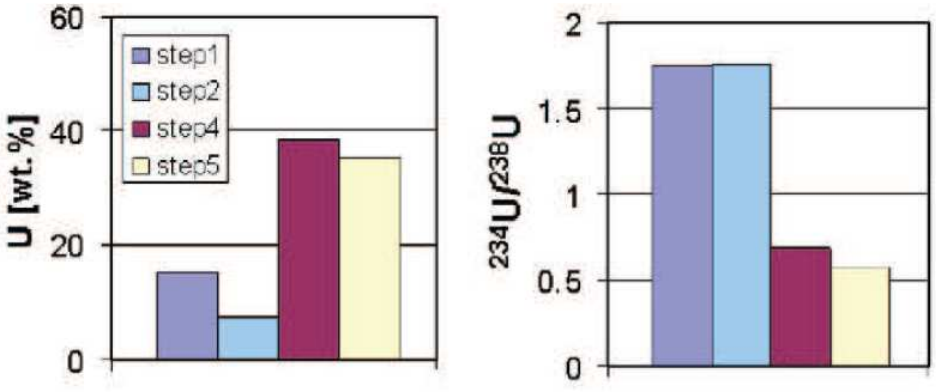

Fig. 11 U content (%) and activity ratios (AR) in sequential extraction leachates for sample NA13 (2007; cf Fig. 7 in publication No. [V.]).

As mentioned above, AR values significantly below unity are caused by the preferential release of ^{234}U. In order to attain low AR values of approx. 0.2 in the U(IV) phase, U in the sample must have been stable for a sufficiently long time, i.e. no significant release of bulk uranium has occurred during the last million years. This is in agreement with the hypothesis that the major uranium input into the clay/lignite horizon occurred during Tertiary, more than 10 My ago (Noseck et al. 2006), and is a strong indicator for the long-term chemical stability of the reduced U(IV) form(s) – see publication No. **[III.]**.

3.1.1. Study of the influence of ageing on U forms in the sediment

The rock material from NA13 borehole (depth 54,87 m) and NA 14 (60,69 m) was left for 3 years under oxic conditions and every year the sequential extraction was repeated in the same procedure (1 g of grain size fraction below 300 μm; in 2009 also the fraction 300 – 600 μm; procedure after publication No. [1]).

The results for U distribution between the different fractions are summed up in Tab. 5 and in Fig. 12. The analyses showed a trend in shifting uranium in the direction to more easy releasable forms (1.- 3. SE step), i.e. decrease of U in reduced form mainly towards the exchangeable form (see Fig. 12 and Tab. 6). The pattern for both samples can be described as rapid decrease of U in reduced form fraction in the first year after sampling (2006-2007), followed bya slow reduction of the residual U content and increase of exchangeable uranium and other more accessible uranium forms. The overall mass transfer in U forms is shown in Tab. 6.

Tab. 5 Uranium content (mg/g) in sequential extraction step fractions. Samples NA13 (depth 54,87 m) and NA 14 (60,69 m) were used in the size fraction under 300 μm (1 g for each analyses), except specified fractions. Year of analyses is specified.

	NA13 2006	NA13 2007	NA13 2009	NA13 2009 300-600μm	NA14 2006	NA14 2007	NA14 2008	NA14 2009	NA14 2009 300-600μm
Exchangeable	36.2	90.0	120.0	133.0	1.5	6.9	180.0	175.0	200.0
Alumosilicates/ Carbonate complexes	18.5	14.0	38.0	50.0	8.3	39.6	47.5	89.5	79.5
Fe/Mn oxides	8.1	7.5	23.0	27.0	1.9	8.9	39.5	63.5	42.5
U in reduced form	92.3	40.0	62.0	49.0	66.8	317.1	150.0	155.0	180.0
Residuum	84.9	77.8	22.5	13.5	21.6	102.4	53.0	26.5	32.0

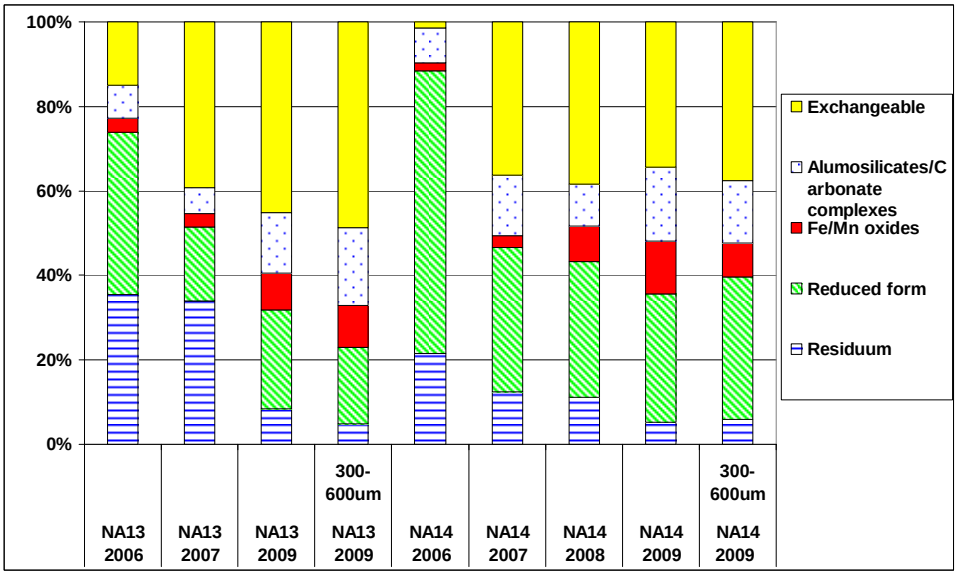

Fig. 12 Uranium forms in samples from NA 13 (54.87 m) and NA 14 (60.69 m) within 4 years of exploration. The samples were left under normal atmosphere and SE was repeated in the same way every year with the same material (all the samples: fractions under 300 μm; samples marked also fraction between 300 and 600 μm) – non-published results.

Tab. 6 Mass transfer of uranium (in %) within U forms, analysed by SE, between 2006 and 2009 (size fraction under 300 μm). Positive number - increase of U content, negative number – decrease of U content.

	NA13 change in %	NA14 change in %
Exchangeable	+ 33.7	+ 32.9
Alumosilicates/Carbonate complexes	+ 10.7	+ 9.2
Fe/Mn oxides	+ 6.5	+10.6
U in reduced form	- 20.5	- 36.3
Residuum	- 30.4	- 16.4

A notable increase of the U content can be spotted in the easily releasable uranium forms: exchangeable U and U bound in alumosilicates/ as carbonate complexes. The increase in the U content in the exchangeable form reached notable similar numbers for both samples: + 33.7% for sample NA 13 and + 32.8% for NA14 respectively. The similar trend can be visible also for U

bound on alumosilicate/as carbonate complexes: + 10.7% for NA13 and + 9.2% for NA14 respectively.

The decrease can be observed for U in less accessible forms: meanwhile the decrease of the uranium content in the residual fraction is more substantial for sample NA13 (-30,4%) compared to NA14 (-16,4%) due to a lower content of U in reduced form (see Fig. 9); the more remarkable shift from reduced form towards easily releasable fractions is spotted in sample NA14 (-36,3%) in comparison with NA13 (-20,5%).

The results showed a notable sensitivity of the clay/organic rich samples to atmosphere exposure that caused a U redistribution within the rock samples towards more easily removable forms. The results laid the baseline for further research on the Ruprechtov site, focused on the study of redox sensitive processes and its influence on the U distribution in clay/organic rich sediments (project RAWRA/NRI/GRS/University of Helsinki; 2009 - 2013).

Activity ratio ^{234}U/^{238}U determination in SE leachate samples, as mentioned in 3.2 and in publication No. **[III.],** was also performed for "aged" samples, NA13 and NA14. ARs were measured for SE leachates obtained during from 2006 and 2009 (according to the methodology in publication No. **[III.]**). The results are presented in Tab. 7 and Tab. 8 and in Fig. 13 and Fig. 14. In 2008 and 2009 2 samples of each SE step solution were analysed in order to cross-check the analytical procedure (samples assigned as B). Missing AR data, especially for the 3rd SE step, were caused by a low U content in the solution and inconsistent output of the measurement.

Considering the AR results, a clear difference can be spotted between the isotope content in each U form, leached in the individual SE steps, in the year 2006, and the other years, respectively. The significant decrease of the AR in fractions from SE step 1 and 2 from values between 1.7/1.8 to values around 1.4 in NA13 and to values around 1.2/1.3 for NA14 would be expected if low

accessible U with ARs below unity is altered into an accessible U form, thereby lowering the AR in the accessible fractions. AR for residual U showed only a small change during the years, not exceeding 10% of the original AR in year 2006 (cf Tab. 8). The AR data did not change significantly in the years 2008 and 2009.

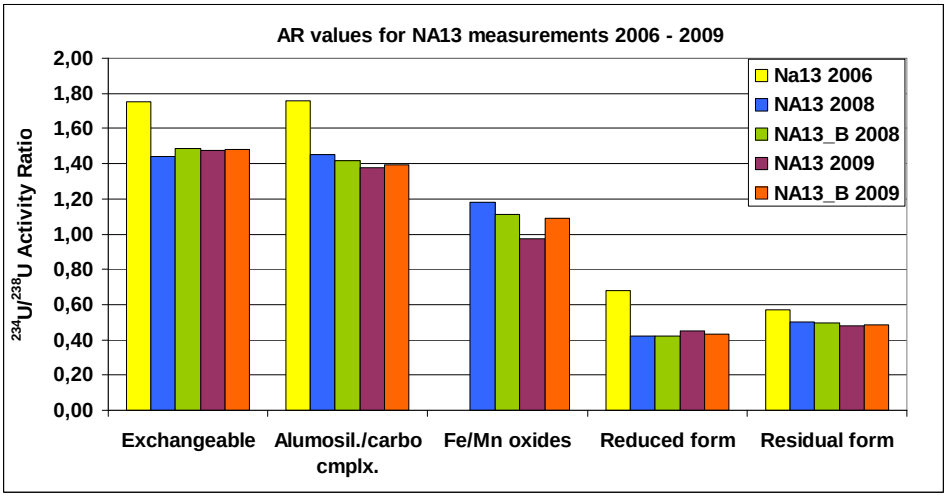

Fig. 13 Activity ratios in sequential extraction leachates for sample NA13 in the period 2006 to 2009. The samples were left under normal atmosphere for 3 years (see above).

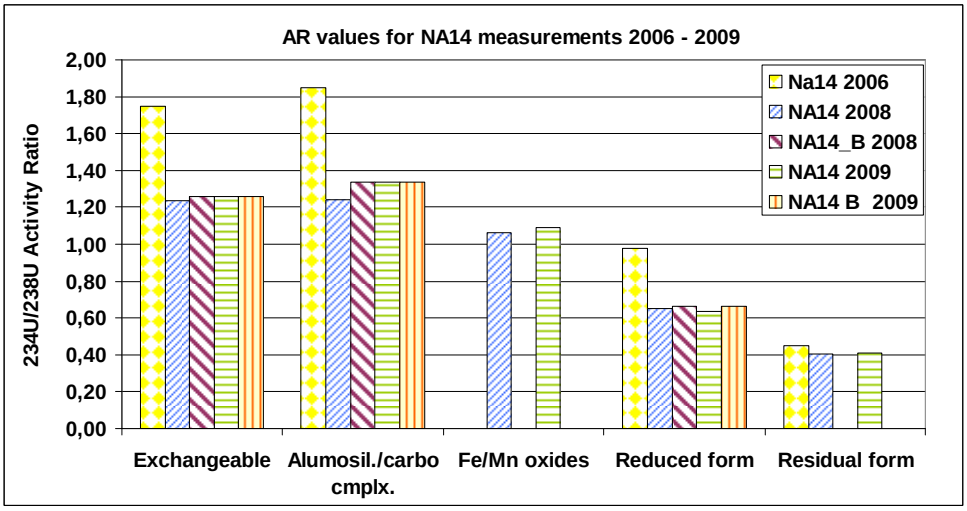

Fig. 14 Activity ratios in sequential extraction leachates for sample NA14 in the period 2006 to 2009. The samples were left under normal atmosphere for 3 years (see above).

Tab. 7 Values of activity ratios $^{234}U/^{238}U$ (AR) for SE leachates, representing specified U forms, during the period 2006-2009.

	NA13 2006	NA13 2008	NA13_B 2008	NA13 2009	NA13_B 2009
Exchangeable	1.75	1.44	1.49	1.47	1.48
Alumosil./carbo cmplx.	1.76	1.45	1.42	1.38	1.40
Fe/Mn oxides		1.18	1.11	0.97	1.09
U in reduced form	0.68	0.42	0.42	0.45	0.43
Residual form	0.57	0.50	0.49	0.48	0.48
	NA14 2006	**NA14 2008**	**NA14_B 2008**	**NA14 2009**	**NA14_B 2009**
Exchangeable	1.75	1.24	1.26	1.26	1.26
Alumosil./carbo cmplx.	1.85	1.24	1.34	1.34	1.34
Fe/Mn oxides		1.06		1.09	
U in reduced form	0.98	0.65	0.67	0.63	0.67
Residual form	0.45	0.40		0.41	

Tab. 8 Change of activity ratio (∆AR) for every year of sample ageing, compared to initial AR value in 2006 year.

	NA13 2006	NA13 2008	NA13_B 2008	NA13 2009	NA13_B 2009
Exchangeable		-0.31	-0.26	-0.28	-0.27
Alumosil./carbo cmplx.		-0.31	-0.34	-0.38	-0.36
Fe/Mn oxides					
U in reduced form		-0.26	-0.26	-0.23	-0.25
Residual form		-0.07	-0.08	-0.09	-0.09
	NA14 2006	**NA14 2008**	**NA14_B 2008**	**NA14 2009**	**NA14_B 2009**
Exchangeable		-0.51	-0.49	-0.49	-0.49
Alumosil./carbo cmplx.		-0.61	-0.51	-0.51	-0.51
Fe/Mn oxides					
U in reduced form		-0.33	-0.31	-0.35	-0.31
Residual form		-0.05		-0.04	

Generally, the ARs detected are in good agreement with SE results: Easily accessible forms of U are generally dominated by AR values well above 1, i.e. by the U(VI) form, in comparison with low AR values (0.6 max.) for SE step 4 and 5 in sample NA 13. The only exception is AR value 0.98 for reduced U form of NA14 sample (2006; see Fig. 14) that is higher than AR values that had been measured for U reduced forms (around 0,6). The reason for increased value has not been explained so far. As similar results were obtain during the very recent recearch on the site (2009-2010), general theory of AR values for different U phases will be further under development and evaluation.

Concluding, it can be stated that uranium within the clay/lignite horizon was found namely in the reduced state as U(IV) in correlation with As minerals (arsenopyrite). The U(IV) phase remained stable over geological times under the reducing conditions in the clay/lignite horizon, being represented by low U(IV) AR values (in some cases below 0.5), which only form, when for a sufficient long time (million years) no significant release of bulk U occurs. (see publ. No. **[III.]** and **[V.])**.

The results presented became a key step for the development of the conceptual model for the $^{234}U/^{238}U$ activity ratios in the U-groundwater-sediment-system in the clay/lignite horizon (Noseck U., in publ. No. **[V.]**) and the model of potential uranium mobilisation/immobilisation within a reducing sedimentary environment (see publications No. **[IV.]**, **[V.]**, and **[VI.]**).

4. Sedimentary organic matter behaviour

As it was stated above, U-enriched seams were identified on the site in the vicinity of lignite-rich layers with carbon (C) concentrations up to 400 ppm. (Noseck et al., 2004). Even though organic matter is usually presumed to be an efficient U sorbent, here uranium was not directly accumulated within the organic layers. A further striking inconsistency found on the site was the discrepancy between the high content of sedimentary organic matter (SOM, up to 40 % of SOC content) and its low content in the groundwater (max. 5 mg/L of dissolved organic carbon, DOC, see Tab. 3), accompanied also with a low content of colloids (cf. Noseck and Brasser, 2006; Hauser et al., 2006).

Therefore, the further step towards a conceptual model of U mobilisation and immobilisation was the determination of organic matter behaviour and its potential influence on U migration at the site. Publications No. **[IV.]-[VI.]** were namely dedicated to this approach.

4.1. Methodology

Identification of potential processes involving all system components, i.e. the clay/lignite horizon, the underlying granite, the groundwater, the organic matter (either SOM or DOM) and uranium included:

- **Uranium form evaluation** - see above
- **Ground water analyses** – for details see publication No. **[IV.]**, **[VI.],** Tab. 2 and Tab. 3
- **Stable isotope analyses** in groundwater – for details see publications No. **[IV.]**, and **[VI.]**

  The natural isotopes are often used for tracing natural geochemical processes. The ratios $^{2}H/^{1}H$, $^{18}O/^{16}O$, $^{13}C/^{12}C$ and $^{34}S/^{32}S$ can be presented, referring to the internationally accepted standards (VSMOW,

VPDB, VCDT respectively), as per mil. deviations (δ^2H and δ^{18}O, δ^{13}C and δ^{34}S), as in example Eq. (1) – Ivanovich and Harmon (1982). For more details of isotope use for Ruprechtov natural analogue site investigation see publication No. **[VI]**:

$$\delta^{34}S = \left(\frac{(\frac{^{34}S}{^{32}S})_{sample}}{(\frac{^{34}S}{^{32}S})_{standard}} - 1 \right) * 1000 \qquad (1)$$

- **Sedimentary, dissolved and mobile organic matter analyses** – for details see publication No. **[IV.]**

4.2. Results

Despite the high sedimentary organic matter (SOM) content in the clay/lignite-sand horizon (up to 40 wt.%), the concentration of dissolved organic matter (DOM) in Ruprechtov groundwater), referred to as dissolved organic carbon (DOC) in mg/L, was generally low (app. 5 mg/L). Comparing the system with conditions at the sediment/groundwater system in Gorleben with similar geological features (Buckau et al., 2000), a striking difference was evident: The highest DOC concentrations at Gorleben groundwater reached up to 200 mg/L, being formed mainly by humic acids. However, considering the Ruprechtov case, only a small fraction of SOM, 2.8 %, was found to be releasable as mobile organic matter (MOM) into solution. The substances leached out artificially from SOM have the same MALDI TOF fingerprint as natural DOM in the groundwater from Ruprechtov site. Therefore, humic acid extracted from SOM can be considered as representative for mobile organic matter (MOM, Havlova et al., 2009). However, a thorough research (Cervinka, 2007; Cervinka et al., 2010) showed that MOM in groundwater has only a minor influence on U complexation.

SOM that is present in the rock sequence can potentially play a more important role in processes of U migration. It might act as natural sorbent and usually can have a strong impact on the environmental conditions. However, in case of Ruprechtov site, uranium enrichment was never found directly within organic rich layers. The uranium rich sequences were usually found in sandy horizons with increased permeability in close vicinity of the organic rich layers (Noseck and Brasser, 2006).

Concerning that, the interest was then focused onto natural processes that SOM can potentially undergo. One of them is the degradation (mineralisation/oxidation) process. The evidence for SOM and its influence on the groundwater composition and subsequently on the uranium migration was searched for namely in the groundwater composition from Ruprechtov boreholes (Tab. 2 and Tab. 3).

The conceptual model of SOM decomposition was described e.g. in Buckau et al. (2000; see Fig. 15).

Preliminary results indicated that microbial SOM degradation probably takes place at Ruprechtov site (Noseck and Brasser, 2006), e.g. the presence of framboidal pyrites as a typical sign of microbial processes (see Fig. 16).

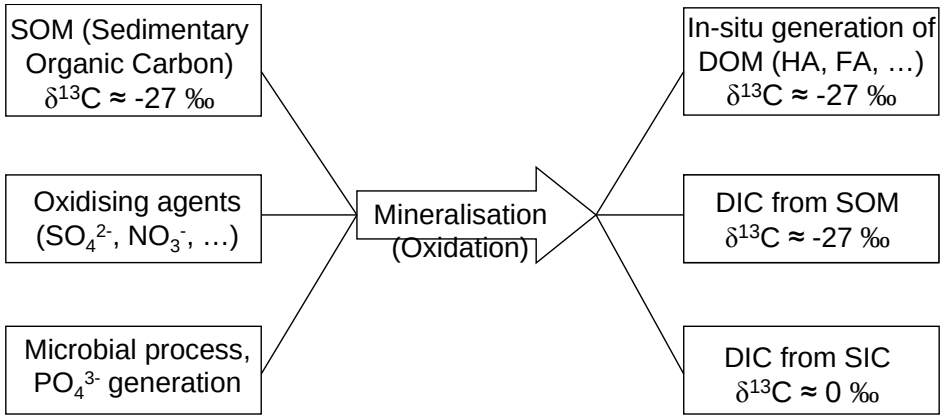

Fig. 15 Conceptual model of sedimentary organic matter mineralisation (oxidation; after Buckau et al., 2000), including characteristic $\delta^{13}C$ values.

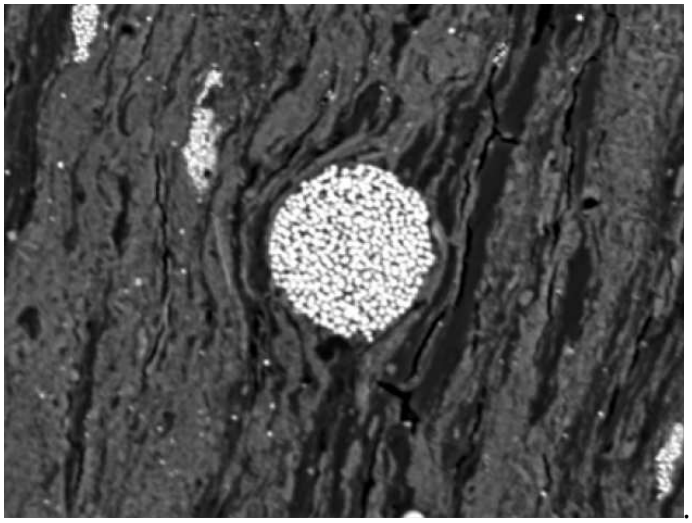

Fig. 16 Fromboidal pyrite in sample NA14 (from 61m depth) – Sulovský. (2005).

Several microbial processes can lead to oxidation of SOM and reduction of oxidising agents, like SO_4^{2-} or NO_3^-, if present in the groundwater of the sedimentary system. SOM can thus partly be oxidised to inorganic CO_2/carbonate, but another part can be also released as DOM. In the next stage of the degradation process more of the inorganic carbon is released, followed by increasing DOM oxidation. Carbonic acid releases one proton and dissolves as HCO_3^-. In contact with carbonate in the sediments (referred as sedimentary inorganic carbon, SIC) this process results in its dissolution and additional input of DIC of sedimentary origin.

These processes are indicated at Ruprechtov site, by a positive correlation of the DOC content in groundwater with the DIC content (see Fig. 17). An increase of the DIC concentration, particularly in the clay/lignite horizon, is generally followed by an increased DOC release – for details see Havlová et al. (2007) and publ. No. **[IV.]** - as a potential result of microbial SOM degradation.

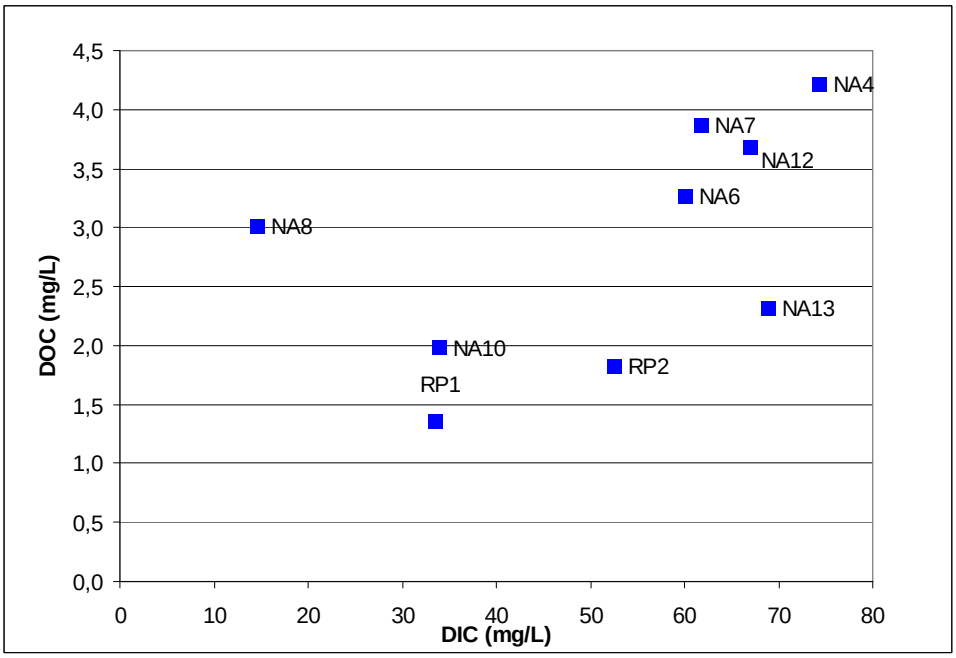

Fig. 17 Dissolved inorganic carbon (DIC, mg/L) vs. dissolved inorganic carbon (DOC, mg/L, as a measure of dissolved organic matter DOM content) in Ruprechtov groundwater wells. From publication No. [IV.].

In order to clearly understand the involvement of organic matter into processes within the sedimentary rock environment, the carbon isotope evolution must be also involved into the explanation (for details see Havlova et al., 2008 and publication No. **[IV.]**).

As mentioned above, degradation of organic matter can follow the scheme in Fig. 15. Microbial processes lead to oxidation of SOM. SOM is then partly oxidised and released into the groundwater (mg/L DIC), with $\delta^{13}C$ values of about –27 ‰, and partly released as DOM, represented as DOC content in mg/L, with $\delta\ ^{13}C$ value also about –27‰. Formation of carbonic acid results in additional release of DIC of sedimentary origin with $\delta^{13}C$-values of app. 0 ‰. The isotopic signature of DIC in different boreholes leads then to value of $\delta^{13}C$ approx. -13.5 ‰ (equimolar mixing line, see Buckau et al., 2000).

Here, on Ruprechtov site the process was clearly spotted, resulting in two different patterns of cabon isotope signature development (see Fig. 18):

- boreholes from granitic environment: dissolution of SOM without major influence of microbial oxidation processes ($\delta^{13}C$ values of about –27 ‰),
- boreholes from clay/lignite horizon: dissolution with microbial oxidation contribution ($\delta^{13}C$ values of about -13.5 ‰).

The last value mentioned can be thus considered as an indication of mixing of both processes: organic matter oxidation and sedimentary inorganic carbon dissolution. For details see Havlova et al. (2008), publications No. [**IV]** and namely No. **[VI]**.

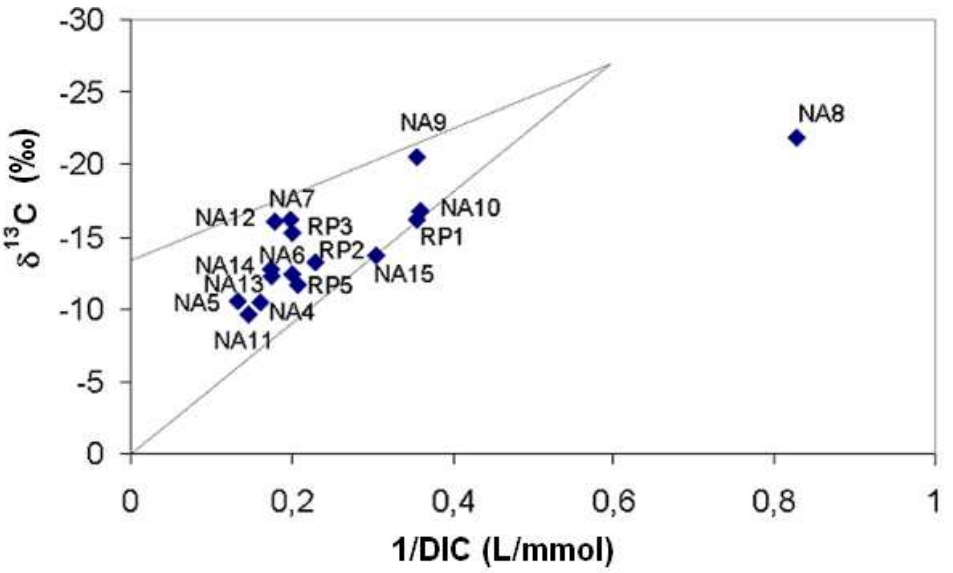

Fig. 18 Comparison of 1/DIC (L/mmol) vs. $\delta^{13}C$ (‰) in different wells from Ruprechtov site (Havlova et al., 2007).

The sulphur ^{34}S isotope content of the groundwater and sediment samples can also add a significant proof for microbial SOM degradation processes.

Complete oxidation of organic matter accompanied by sulphate (as electron acceptor) reduction can be written as:

$$SO_4^{2-} + 2\ CH_2O = H_2S + 2\ HCO_3^-$$

In presence of iron the reaction product can be fixed as iron mono-sulphide and afterwards be transformed into pyrite. Moreover, the microbial sulphate reduction is accompanied by isotope fractionation. The lighter isotope ^{32}S is preferentially metabolised by microbes and therefore residual sulphate SO_4^{2-} molecules in groundwater become enriched in the isotope ^{34}S, whereas $\delta^{34}S$ values in forming solid sulphides S^{2-} decrease.

The pattern mentioned can be spotted also within the Ruprechtov system: The groundwater from the clay/lignite-sand layer show increased $\delta^{34}S$-values in the range of 16.43 to 24.63 ‰, which is a clear indication of microbial sulphate reduction. The results of the $\delta^{34}S$ trend in groundwater samples are shown in Fig. 19, in dependence of $\delta^{13}C$.

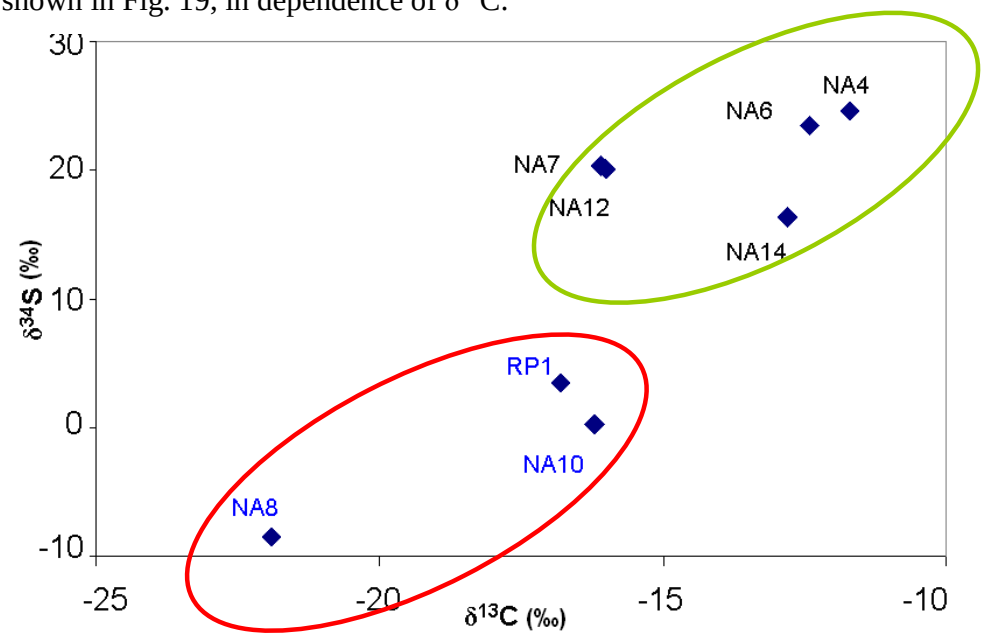

Fig. 19 Isotopic composition of Ruprechtov groundwater samples ($\delta^{13}C$, ‰ vers. $\delta^{34}S$, ‰) in samples from infiltration boreholes (granite, red circle) and from clay/lignite layers.

Moreover, the mineralisation (oxidation) of SOM can be accompanied by the reduction of oxidising agents (SO_4^{2-} and NO_3^-), i.e. a decrease of oxidising agent concentrations with progress of the oxidation process and thus with increase of the DOC content. The trend is traceable for SO_4^{2-} concentration analyses in the Ruprechtov groundwater (see Fig. 20). NO_3^- species does not show a direct trend with DOC, however the NO_3^- content can be tricky due to potential anthropogenic contamination. Therefore two sets of data are included to demonstrate the potential influence of extreme data: the first data set includes an extraordinary high NO_3^- value for NA10, the second one excludes this extreme value that might be caused by anthropogenic contamination. Then, a slightly decreasing trend can be visible within the second data set (NO3_rev., see Fig. 21).

On the other hand, a general reverse trend can be spotted for phosphates (PO_4^{3-}) – see Fig. 20. Those are supposed to be produced by microbial mediated SOM metabolism, causing reduction of sulphates and nitrates and release of originally SOM-bound phosphates into the solution.

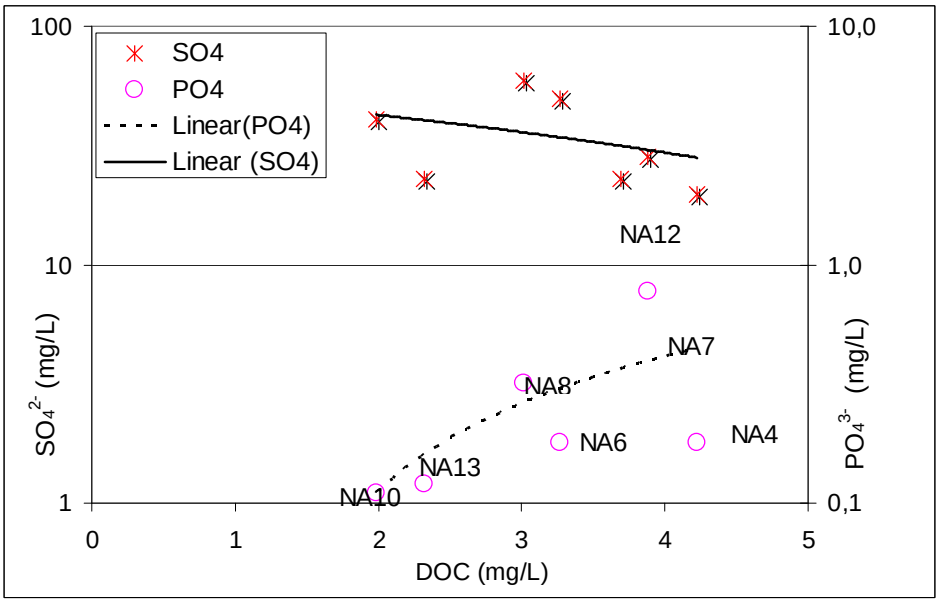

Fig. 20 Concentration of sulphates and phosphates (in mg/L) in Ruprechtov groundwaters vs. dissolved organic carbon content (DOC, mg/L).

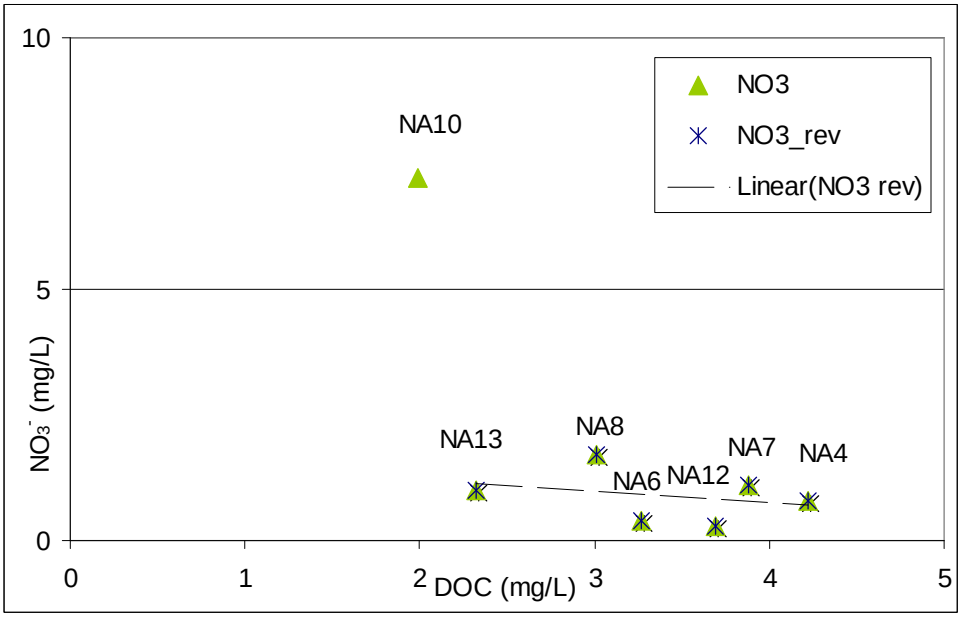

Fig. 21 Concentration of nitrates (mg/L) in Ruprechtov groundwaters vs. dissolved organic carbon (DOC, mg/L). NO_3^- – complete data set; trend line NO3_rev: NA10 value excluded.

Considering all the mentioned processes above, two patterns in the natural isotope composition at the site can be spotted (see publications **[IV]** and **[VI.]** for details):

- samples from granitic recharge area (red circle), where microbial SOM oxidation takes place to a limited extent, resulting in low $\delta^{34}S$ values ($\delta^{34}S$ ranging from -8.5 to 3 ‰). Moreover, contribution to SIC dissolution is low, thus $\delta^{13}C$ values reach up to ~ -22 ‰, originating mainly from SOM source.
- samples from clay/lignite horizon (green circle) where increased $\delta^{34}S$-values in the groundwater indicates significant microbial reduction of sulphate to sulphide ($\delta^{34}S$ in the range of 16.43 to 24.63 ‰), accompanied with increased $\delta^{13}C$ values as indication of mixing of DIC from the SOM source (-26 ‰) and DIC from dissolved SIC (~ 0 ‰). Contribution of mantle CO_2 source is also presumed (-2.7 ‰.) – see the model by U. Noseck in publication No. **[VI]**.

.

5. Uranium mobilisation/immobilisation scenario at the Ruprechtov site

In the first level of the project the single-task scientific topics were dealt with, e.g. sedimentary organic matter (SOM) behaviour or uranium immobilisation as smallest puzzle pieces. Organic matter on the site was found having no significant influence neither on U complexation and/or mobilization by dissolved organic species in groundwater, nor on U direct sorption on organic SOM (publication No **[I.]**.

The application of macroscopic and microscopic methods provided a detailed insight into the U enrichment processes at the Ruprechtov site. Confocal µ-XRF and µ-XAFS identified U in the sediment as U(IV), being associated with As(V) on arsenopyrite layers and forming ningyoite (U phosphate) and uraninite (U oxide) minerals (publication No. **[II.]**). In order to separate U(IV) and U(VI), a wet chemical method was also applied for the first time to Ruprechtov samples, confirming that the major fraction of immobile uranium occurs in the tetravalent state (publication No. **[III.]**) and that mobile U in groundwater is predominantly in U(VI) form, even under reducing conditions. Moreover, the $^{234}U/^{238}U$ activity ratio method proved the long-term stability of U in the system, showing no evidence for a U mobilisation during the last million years.

In the second step previous single scientific task results, were combined together with results from characterisation of organic matter and isotope analyses in the system, enabling insight into the role of microbial activity and organic matter in the uranium immobilization process. (publications No. **[IV.], [V.], [VI.])**.

The indication for the geological development and the proposed uranium immobilisation at the Ruprechtov site can be summarised as (details see in publication No. **[IV.], [V.], [VI.]**):

- Granite intrusion with increased content of U in Mezozoic.
- Granite kaolinisation.
- Activation of the system due to volcanic activity (volcanic ash deposition, increased CO_2 influx, etc.)
- Uranium U(VI) release from the underlying granite into the groundwater. U(VI) probably formed U carbonate complexes, and was transported into more permeable zones. Due to a high partial pressure of carbonate U(VI) carbonate complexes can be present under reducing conditions in the groundwater.
- Generally, organic matter degradation is presumed to be a microbially mediated process contributing to U(VI) reduction and U(IV) immobilisation into solid phases.
- SOM within clay/lignite layers was microbially oxidised, releasing DOM and providing protons to dissolve SIC, altogether forming reducing conditions. Phosphates (PO_4^{3-}) were also released.
- Oxidation agents (e.g. SO_4^{2-}) in groundwater were simultaneously reduced as electron donors.
- Subsequently, reduction of sulphate from the groundwater led to FeS_2 formation. Furthermore, dissolved As in groundwater got sorbed onto FeS_2, forming FeAsS precipitates.
- U(VI) in groundwater (probably in the form of carbonate complexes) were reduced to U(IV) on FeAsS surfaces.
- U(IV) reacted with phosphates PO_4^{3-}, released by organic matter degradation, and uranium phosphates (e.g. ningyoite) were thus

formed. The process took place under reducing conditions in the vicinity of organic matter.

- Uraninite might have formed at later stages of the geological history at conditions where phosphate concentration might have decreased.
- Uranium became then stable and immobile in the long term time sequence.
- Any major uranium mobilization has not been spotted in the system for the last million years indicated by the low $^{234}U/^{238}U$ activity ratio values.

6. Conclusions

uranium immobilisation processes were studied within a sedimentary rock sequence at the Ruprechtov natural analogue site. The research used the natural system in order to better understand processes of the safety relevant element (uranium) within a rock sequence, analogous to a potential host-rock overburden of a deep geological repository for spent nuclear fuel and high level waste.

A multi-disciplinary approach was undertaken in order to study uranium mobilisation/immobilisation processes within a sedimentary clayey rock with organic matter enriched interlayers.

Sequential extraction is a widely used tool that can be applied for identification of trace metal forms within the sediment. However, it cannot be used without further supporting analyses, namely identifying which substances dissolve within each step. In the case of Ruprechtov samples, it was found by detailed analysis of trace metals in the different SE fractions that due to the absence of carbonates and no direct correlation of U with organic matter, the uranium leached in the 2nd SE step has to be termed as „uranium bound on alumosilicates and/or carbonate complexes“ and within the 4^{th} SE step as „uranium in reduced form U(IV) respectively“.

Sequential extraction of uranium from sedimentary samples from the Tertiary clay/lignite horizon proved that U mainly prevailed in the U(IV) form in low-oxidised samples. With sample ageing (oxidation) it moves towards more easily accessible fractions that enable its easier mobilisation and release.

The combination of SE results with results from modern spectroscopic methods (μ-XRF, μ-XAFS) laid the key stone to the uranium mobilisation/immobilisation model:

Uranium was proved to be associated with As and P, instead of Fe and S as expected, leading to the presumption that U(VI) from groundwater was

reduced on arsenopyrite surfaces that had been formed due to reducing conditions within the clay /organic rich sediment.

The hydrogeochemical evaluation and isotope analyses then brought this result into a broader context of the site: Organic matter degradation was a microbial mediated process contributing indirectly to U(VI) immobilisation into secondary U(IV) phases. SOM within the sedimentary layers was microbially oxidised, releasing DOC and providing protons to dissolve SIC. The oxidation agents (SO_4^{2-} and NO_3^-) were reduced. Reduction of sulphate caused FeS_2 formation. Dissolved As got sorbed onto FeS_2, forming thin FeAsS precipitates. U(VI), released from the underlying granite, was reduced to U(IV) on FeAsS surfaces and reacted with phosphates (PO_4^{3-}), produced by microbial SOM oxidation. Uranium phosphates (ningyoite) were thus formed. Uranium exists predominantly in the U(IV) state, stable and immobile. It was proved that U(IV) mineral phases stayed stable for more than million years. On the other hand, the presence of U(VI) in reducing groundwaters was possible only due to complexation into carbonate complexes.

The results mentioned above are the most important contribution to the potential use in a deep geological repository Safety Case: Sedimentary rock can provide under certain circumstance a strong barrier function for radionuclides, in this case for uranium, potentially decreasing its activity and reducing its potential impact to the environment.

The key parameter is the presence of organic matter that contributed to maintaining reducing conditions in the clay/lignite layers. The presence of organic rich horizons does not naturally mean increased mobilization of radionuclide due to organic ligand complexation or organic colloid formation as there is no indication for significant uranium release during the last million

years within reducing conditions of clay/lignite layers. A potential influence of the natural CO_2 flux and its role in radionuclide complexation and migration in this case must be stressed.

7. References

ALEXANDER, W.R. (Ed.; 1992): A natural analogue study of cement-buffered hyperalkaline groundwaters and their interaction with a sedimentary host rock - I: Source-term description and geochemical code database validation. NAGRA Technical Report Series (NTB 91-10), Nagra, Wettingen, Switzerland.

BLOMQVIST, R., KAIJA, J. , LAMPINEN, P., PAANANEN, M., RUSKEENIEMI, T., KORKEALAAKSO, J., PITKÄNEN, P., LUDVIGSON, J.-E., SMELLIE, J., KOSKINEN, L., FLORÍA, E., TURRERO, M., GALARZA, G., JAKOBSSON, K., LAAKSOHARJU, M., CASANOVA, J., GRUNDFELT, B., HERNAN, P. (1998): The Palmottu natural analogue project. Phase I: Hydrogeological evaluation of the site. European comission report EUR 18202 EN.

BLOMQVIST, R., RUSKEENIEMI, T., KAIJA, J., AHONEN, L., PAANANEN, M., SMELLIE, J., GRUNDFELT, B., PEDERSEN, K., BRUNO, J., PÉREZ DEL VILLAR, L., CERA, E., RASILAINEN, K., PITKÄNEN, P., SUKSI, J., CASANOVA, J., READ, D., FRAPE, S. (2000): The Palmottu natural analogue project. Phase II: Transport of radionuclides in a natural flow system at Palmottu. European comission report EUR 19611 EN.

BRUNO J., DURO L, DE PABLO, L., CASAS, I., AYORA, L., DELGADO, J., GIMENO, J., PEÑA, J., LINKLATER, C., PÉREZ DEL VILLAR, L., GÓMEZ, P. (1998): Estimation of the concentrations of trace metals in natural systems: The application of codissolution and coprecipitation approaches to El Berrocal (Spain) and Poços de Caldas (Brazil). Chemical Geology, Vol. 151, Iss. 1-4, 277-291.

BRUNO, J., DURO, L., GRIVÉ, M. (2001): The applicability and limitations of the geochemical models and tools used in simulating radionuclide behaviour in natural waters. Lessons learned from the Blind Predictive Modelling exercises performed in conjunction with Natural Analoque studies. SKB Technical Report TR 01-20.

BUCKAU, G., ARTINGER, R., GEYER, S., WOLF, M., FRITZ, P., KIM, J.I. (2000): Groundwater in-situ generation of aquatic humic and fulvic acids and the mineralization of sedimentary organic carbon.- Applied Geochemistry, 15, pp. 819-832.

CARBOL P. AND ENQUIST (2007): Compilation of sorption data for performance assessment. SKB Report R-97-13.

CERVINKA R. (2007): Report on uranium complexation by isolated humic substances from the Ruprechtov site. PID 2.2.20**.** Project Internal Deliverable. FUNMIG IP project.

CERVINKA R., STAMBERG K., HAVLOVA V., NOSECK U. (2010): Humic substances extraction, characterization and interaction with U(VI) at Ruprechtov site (CZ). Radiochim. Acta 99, 1–12 (2011) / DOI 10.1524/ract.2011.1806.

CHAPMAN, N., MCKINLEY, I. G., SHEA, M., SMELLIE, J. A. T. (1990): The Pocos de Caldas project: Summary and implications for radioactive waste management. SKB Technical Report TR 90-24; NAGRA Technical Report 90-33; UK DOE Report WR90-055.

CÔME, B. & CHAPMAN, N.A. (eds) (1986): Natural analogue working group; first meeting, Brussels, Novenber 1985. CEC Nuclear Science and Technology Report, EUR 10315, Commision of the European Communitoes, Luxembourg.

CRAMER, J. , SMELLIE, J.A.T. (1993): The AECL/SKB Cigar Lake Analog Study: Some implications for performance assessment. In: Fifth CEC Natural Analogue Working Group meeting and Alligator Rivers Analogue Project (ARAP) final workshop. Proceedings of an international workshop held in Toledo, Spain, 5-9 October 1992 (EUR 15176 EN), pp. 137-155.

DENECKE, M.A., JANSSENS, K., PROOST, K., ROTHE, J., NOSECK, U. (2005): Confocal micro- XRF and micro-XAFS studies of uranium speciation in a Tertiary sediment from a waste disposal natural analogue site. Environ. Sci. Technol. 39 (7), 2049–2058.

ERVANNEN, H**.** (2004): Oxidation state analyses of uranium with emphasis on chemical speciation in geological media. Academic disertation. Dept. Of Chemistry, University of Helsinki, Finland

GOMEZ, P., TURRER, M.J., MOULIN, V., MAGONTHIER, M. C. (1992): Characterisation of natural colloids in groundwaters of El Berrocal, Spain. In. Kharaka Y. a Maest A. (eds.): Water Rock Interaction, 797 - 800.

GORBY, Y. A., LOVLEY, D.R (1992): Enzymatic uranium precipitation. Environ, Sci. Tech. 26, 205-207.

GURBAN, I., LAAKSOHARJU, M., LEDOUX, E., MADE, B., SALIGNAC, A. L. (1998): Indications of uranium transport around the reactor zone at Bagombe (Oklo). SKB Technical Report TR 98-06.

HAMMER, Ø., HARPER, D.A.T., RYAN, P.D. (2001): PAST: Paleontologival statistic software package for education and data analyses. Copyright: Palaeontological Association, 2001.

HAVLOVÁ, V., ČERVINKA, R., HAVEL, J. (2009): Interrelation of mobile organic matter and sedimentary organic matter at the Ruprechtov site. Buckau G. and Kienzler B., Duro L., Montoya V., Delos A. (eds.) 4th annual

workshop proceedings of 6th EC FP FUNMIG IP, Karlsruhe November 24–27, 2008. 383-390. Report FZK-INE, FZKA 7461.

HAUSER W., GECKEIS H., GÖTZ R., NOSECK U., LACIOK A. (2006): Colloid Detection in Natural Ground Water from Ruprechtov by Laser-Induced Breakdown Detection. 2nd Annual Meeting of EC Integrated Project FUNMIG, SKB Report TR 07-05.

HAVLOVA, V., NOSECK, U., CERVINKA, R., BRASSER, T, DENECKE, M. HERCIK, M. (2007): Uranium enrichment at Ruprechtov site - Characterisation of key processes. S+T presentation. 3rd annual meeting of IP FUNMIG, Edinborough, GB, Nov. 25 – 29, 2007. NDA report. Available on http://www.nda.gov.uk/documents/upload/3rd-Annual-Workshop-Proceedings-of-the-Integrated-Project-Fundamental-Processes-of-Radionuclide-Migration-6th-EC-FP-IP-FUNMIG.pdf.

HERCÍK, M. (2005): Terénní studium geochemických a transportních procesů na lokalitě Ruprechtov. Úkol Přírodní analog 1999-2005. ÚJV Řež a.s.

IAEA (1989): Natural analogues in performance assessments for the disposal of RAdioactive wastes. IAEA Technical Report, 304, International Atomic Energy Agemcy, Vienna.

IVANOVICH, M. AND HARMON, R.S. (1982): Uranium Series Disequilibrium: Applications to Environmental Problems, Clarendon Press, Oxford, 40p.

KOMÍNEK, J., CHRT, J., AND LANDA, O. (1994): Uranium mineralization in the western Krušné hory Mts. (Erzgebirge) and the Slavkovský les region, Czech Republic.- In: v. Gehlen, K. and Klemm, D.D. (Eds.): Mineral deposits of the Erzgebirge/ Krušné hory (Germany/ Czech Republic,

Monograph Series on Mineral deposits, No. 31, pp.209-230, Gebrüder Bornträger, Berlin – Stuttgart, 1994.

LANGMUIR, D. (1997): Aqueous environmental geochemistry. Prentice Hall, Upper Saddle River, New York, p. 600.

LANGMUIR, D. (1978): Uranium solution-mineral equilibria at low temperatures with applications to sedimentary ore deposits. Geochimica et Cosmochimica Acta, 42, 547-569.

LIESER, K.H. (1995): Radionuclides in the Geosphere: Sources, mobility, retardation. Radchim. Acta, 70/71, 335-375.

LINKLATER, C.M. (Ed.; 1998): A natural analogue study of cement buffered, hyperalkaline groundwaters and their interaction with a repository host rock II. Nirex Report no. S/98/003**,** UKNirex, Harwell, Oxon., UK.

LIU, JINSONG (1995): Development and test of models in the natural analogue studies of the Cigar Lake Uranium deposit. Doctoral thesis. TRITA-KET R24. Dept. of Chemical Engineering and Technology, Royal Institute of Technology, Stockholm, Sweden, 1995.

LOVLEY, D., PHILLIPS, E., GORBY, Y., LANDA, E. (1991): Microbial reduction of uranium. Nature 350 413-416.

LOVLEY, D.R. AND PHILLIPS, E.J.P (1992): Reduction of by Desulfovibrio desulfuricans. Apll. Env. Microbiol., 58, 850-856.

MCKINLEY, I.G. (1989): Applying natural analogues in predictive performance assessment. Unpublished Nagra Internal Report, Nagra, Wettingen, Switzerland.

MILLER, W., ALEXANDER, W., CHAPMAN, N., MCKINLEY, I., AND SMELLIE, J. (2000): Geological disposal of radioactive wastes and natural

analogues. Waste management series, vol. 2, Pergamon, Amsterdam, The Netherlands.

MONTOTO, M., MÉNAGER, M., RODRÍGUEZ-REY, A., MENÉNDEZ, B., MARTÍNEZ-NISTAL, A., FERNÁNDEZ-MERAYO, N. (1996): Uranium transfer phenomena in rock matrix: petrophysical and geochemical study of El Berrocal experimental site, Spain. Journal of Contaminant Hydrology, Vol. 21, Issues 1-4, 35-46.

MURAKAMI, T. OHNUKI, T. ISOBE, H. SATO, T. (1997): Mobility of uranium during weathering. American Mineralogist, 82, 888-899.

NOSECK, U., LAAKSOHARJU, M., SUKSI, J., HAVLOVA, V., DENECKE, M., BUCKAU, G., TULLBORG, E. (2010): Real system analyses / Natural Analogues. Applied Geochemistry, In preparation.

NOSECK, U., SUKSI, J. , HAVLOVA, V., ČERVINKA, R. (2008): Uranium geochemistry at Ruprechtov site. S&T publication. In: Buckau G. and Kienzler B., Duro L., Montoya V., Delos A. (eds.) 4th annual workshop proceedings of 6th EC FP FUNMIG IP, Karlsruhe November 24– 27, 2008. 383-390. Report FZK-INE, FZKA 7461.

NOSECK, U., BRASSER, TH. (2006): Radionuclide transport and retention in natural rock formations – Ruprechtov site.- GRS-218, 157 S. + CD, Köln, 2006.

PEDERSEN, K. (200): Microbial processes in radioactive waste disposal. SKB Technical Report TR-00-04.

PERCIVAL, J. B. (1990): Clay mineralogy, geoochemistry and partitioning of uranium within alternative halo of Cigar Lake Uranium deposit, Saskatchewan, Canada. PhD Thesis. Carleton University.

PHILLIPPI, J., LOGANATHAN, V., MCINDOE, M., BARNETT, M., CLEMENT, T., RODEN, E. (2007): Theoretical Solid/Solution Ratio Effects on Adsorption and Transport Uranium VI and Carbonate. Soil Sci. Soc. Am. J. 71 329_335.

SKB (1999): SR-97 Post closure safety. SKB report TR 99-06. www.skb.se.

SMELLIE, J., KARLSSON, F. (1996): A reappraisal of some Cigar Lake issues of importance to performance assessment. SKB Technical Report TR 96-08.

SMELLIE, J.A.T. (Ed.; 1998): Maqarin natural analogue project: Phase III. SKB Technical Report (TR 98-04**,** Vols I and II), SKB, Stockholm, Sweden.

SUKSI, J., RASILAINEN, K., PITKÄNEN, P. (2006): Variations in the $^{234}U/^{238}U$ activity ratio in groundwater – A key to characterise flow system? Physics and Chemistry of the earth, 31 (10-14), 556-571.

SULOVSKÝ, P. (2005): Expert opinion – Mineralogy on Ruprechtov site. Report. Masaryk University, Brno.

TESSIER A., CAMPBEL P. G. C. AND BOSSON M. (1979): Sequential extraction procedure for the speciation of particulate trace metals. Anal. Chemistry, 51, 844-851.

VOPÁLKA D., HAVLOVÁ V. A ANDRLÍK M. (2008): Characterisation of U(VI) behaviour in the Ruprechtov site (CZ). The 5th conference on Uranium Mining and Hydrogeology, September 14 - 18, Freiberg, 583-590. Springer-Verlag, Berlin, Heidelberg, 2008.

www.funmig.com

www.natural-analogues.com.

ZETTERSTRÖM, L. (2000): Oklo. A review and critical evaluation of literature. SKB Technical report TR-00-17.

APPENDIX:

Scientific publications

[I.]

HAVLOVA, V., LACIOK, A., VOPALKA, D., ANDRLIK, L. (2006):

Geochemical study of Uranium mobility in Tertiary argillaceous systém at Ruprechtov site, Czech Republic.

Czechoslovak Journal of Physics, Vol. 56 (2006), Suppl. D, D1-D

GEOCHEMICAL STUDY OF URANIUM MOBILITY IN TERTIARY ARGILLACEOUS SYSTEM AT RUPRECHTOV SITE, CZECH REPUBLIC

V. Havlová[**], A. Laciok

Nuclear Research Institute Řež plc., CZ-250 68 Řež near Prague, Czech Republic

D. Vopálka, M. Andrlík

Faculty of Nuclear Sciences and Physical Engineering, Czech Technical University, Břehová 7, CZ-115 19 Prague 1, Czech Republic

The natural analogue study at the Ruprechtov site is aimed to investigate and understand the behaviour of natural radioelements in plastic clay formation. Uranium is present predominantly in U(+IV) form, either in secondary uranium minerals (uraninite, ningyoite) or in detrital immobile phases (monazite, rhabdophane, xenotime, zircon) and in hardly characterisable non-crystalline forms as well. Process of uranium accumulation probably proceeded via reduction of U(VI) and U(IV) precipitation with involvement of As. Sorption also played important role in U accumulation formation. The sequential extraction experiments were performed in order to specify phases causing uranium retention and accumulation. The isotopic exchange tests with ^{233}U were used to determine the amount of exchangeable uranium. The contradictions in the extraction schema used for the Ruprechtov sediment samples were found. The results prompt careful approach and potential sequential schema modification.

1 Introduction

Underground repositories of radioactive waste are based on a multibarrier concept. In this concept clay plays important role as either engineered (near field) or natural barrier (clay formations as host rocks, overburden of host rock formations). Detailed study of appropriate natural analogue systems (NAS) may help to better understanding of retardations processes in the vicinity of the deep nuclear waste repository under natural conditions in a long time scale, relevant for performance assessment (PA)

The natural analogue study at the Ruprechtov site was aimed to investigate and understand behaviour of natural radioelements in plastic clay formation. Ruprechtov system was chosen as an analogue for sedimentary overlayers of radioactive waste repository host rocks (salt, granite, clay). Gorleben (Germany) and Mol (Belgium) are the most similar systems studied abroad. The site was investigated within the project of NRI Řez (CZ) and GRS Braunschweig (D) with several other institutions involved in order to identify the main mobilisation/immobilisation processes for PA-relevant elements, namely uranium, thorium and radium [1, 2, 3]. Currently, some specific aspects of Ruprechtov NAS are

[*] The project was supported by RAWRA (CZ), BMWA (D), EC (FUNMIG project – 6th European Framework Programme) and the Czech Ministry of Trade and Industry (in the frame of the POKROK Programme)

[**] hvl@ujv.cz

studied as part of EC PAMINA project. Comprehensive investigation of U-argillized clay-organic matter-granite system-groundwater has been performed so far, including drilling, field tests, groundwater monitoring, sediment and groundwater sampling and characterisation, laboratory experiments and geochemical and hydrogeological modelling.

2 Site Description

The Ruprechtov site is situated in the NW part of the Czech Republic (Fig. 1) in Hroznetin part of Sokolov Basin. The basin is filled with Oligocene and Miocene sediments, represented mainly by argillitized pyroclastical complex (Nové Sedlo Formation) with thickness of 0 – 100 m. Low-grade U accumulation is unevenly distributed within some volcanodetritic layers in the depth of 10 – 40 m. The simplified geological profile is presented on Fig. 2. [2, 3]

Fig. 1. Geographical position of the Ruprechtov site. Czech Republic

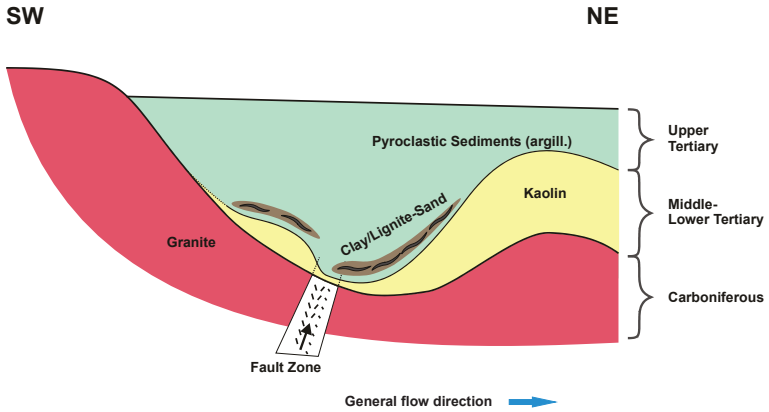

Fig. 2. Schematic geological profile through the rock sequence on the Ruprechtov site (simplified)

Carboniferous age granitic rocks, forming the Karlovy Vary Massif, occur under the sequence of sediments. Granites underwent intensive weathering in Mesozoic ages, causing kaolinization. These granitic bodies are elongated roughly in the NW–SE direction. Two rock types can be distinguished: older Horský granite (325–310 Ma) and younger Krušnohorský granite (< 305 Ma). The Horský granite type is medium grained monzogranite–granodiorite [4]. This shows high average content of Th (23 ppm, up to 42 ppm) at low U (total range 3.4–13.4 ppm) and Th/U > 1 (1.2–8.7, on average 4.0). Krušnohorský granite is extremely structurally variable [4] with higher concentrations of transition metals (Cr, Ni), HREEs and U (maximum 28 ppm) in contradiction with relatively low Th content (median 17 ppm) and significantly lower Th/U (0.5–4.8).

Volcanic material (pyroclastics), deposited in Hroznetin part of Sokolov Basin, originated in Doupovské hory Mts., situated eastward of the Ruprechtov site (basic neovolcanites – alkaline basalts, basanites and olivine nephelinites, with acid volcanites). The age of all volcanic rocks is roughly similar (22–28 Ma). The neovolcanites have low Th concentrations accompanied also by relatively low U contents.

The underlying Krušnohorský granite is the most presumable U source. This is also indicated by relatively high mean primary content of uranium. U concentrations can raise with sharp peaks in the sediment layers and can vary from some tens up to hundreds of ppm.

The current results indicate that U-mineralization is mainly located on the top of kaolin layer usually associated with organic-rich parts, which is – due to strong heterogeneity – usually described as "clay/lignite-sand-layer". The concentration profile of uranium shows a gradient from the top of granite up to the upper part of kaolin, suggesting leaching of uranium from weathered granite followed by diffusive transport through kaolin to the aquiferous horizon. Other processes could have been involved in origin of uranium accumulation, e.g., U transport in solution via fracture/fault zones, transport of U from surrounding granitic bodies by permeable layers, influence of hydrothermal volcanic activity in Tertiary ages.

3 Uranium Mineral Forms

Uranium could be found in the system mainly in U(IV) form. According to the separation experiments, using exchange chromatography, U(IV) forms 80 – 90 % of total uranium content in the enriched parts in the depth (experimental samples from approx. 40 m depth) [5]. That proves reducing conditions under which the U accomulation had been formed.

Mineral phases were studied either using classical methods (XRF, microprobe) and modern microscale surface methods, i.e., micrometer scale X-ray fluorescence and X-ray absorption (μ-XRF and μ-XAFS) [6]. Firstly, detrital immobile uranium phases were found, originated probably from granite source (monazite, rhabdophane, xenotime, zircon). U content in the detrital minerals is usually low and the phases forms minor part of U enrichment. Further, secondary uranium mineral phases of U(IV) predominantly, were identified: uraninite (UO_2), ningyoite (U, Ca, Ce)$_2$(PO_4)$_2$.1-2H_2O, tristamite (Ca, U, Fe)(PO_4, SO_4).2H_2O. According to μ-XRF maps of element distribution, U seems to be accumulated close to Fe nodules where it is associated with As [6]. Content of U in these

phases is high, forming major part of U-mineralisation. There is no spectral evidence for U(VI). Uranium accumulation was probably formed due to reduction of U(VI), that had been remobilized from granitic source and had precipitated with involvement of As.

Important part of accumulation is formed by U phases in non-crystalline form, not being able to be identified with XRF or any other spectral method. They could represent amorphous phases, sorbed U complexes, non-crystalline gel-like substances, etc. Their composition and U content are variable as well as their the occurrence [7]. The non-crystalline phases are not strictly bound neither on organic rich layers nor on pyrite enriched layers.

4 Sequential Extraction and ^{233}U Experiments

The sequential extraction method (SE) is classical approach used in order to found trace metal "forms" in sedimentary rocks. It consists of consecutive extraction steps, leaching the sediment with different extractants in order to define trace metal bonds on/onto sediment. The widely used method was published in [8] and consequently the number of modifications according to purpose of use was made so far, e.g., investigation of Cigar Lake natural analogue (Canada) [9].

To find the U forms on Ruprechtov site following schema was used (simplified):

1. U bound on exchangeable positions (leaching with $MgCl_2$)
2. U bound on carbonates (leaching with ammonium acetate with acetic acid)
3. U on Fe/Mn oxides (leaching with hydroxylamine hydrochloride in acetic acid)
4. U bound onto organic matter (using H_2O_2 and HNO_3)
5. U in residuum (using boiling with HNO_3)

Four samples were selected: NA 10 (kaolinized granite), NA11 and NA12 (argillaceous clay) and NA14 (high content of organic matter and uranium). Boreholes sampled were characterised in [2, 3]. 1 g of grained sample was used in the sequential extraction procedure. After each step the leachate was obtained in which U content was analysed. The fraction of U in each step was recalculated according to the total U content. Results are presented in Table 1 and in Fig. 3.

Simultaneously, easily mobilisable fraction of U was quantified by ^{233}U exchange method, using simulated groundwater from the Ruprechtov site. Methodology was published elsewhere, i.e., in [10].

Table 1. Fractions of U forms bound on the sediment. Samples: NA10 – kaolinized granite, NA 11 and NA 12 argil.clay, NA 14 argil.clay with high content of org. matter and U

Fractions (%)	NA10 A	NA10 B	NA11 A	NA11 B	NA12A	NA12 B	NA 14 A	NA 14 B
U in exch. positions	1.52	0.88	1.50	1.30	1.08	0.47	84.39	83.23
U on carbonates	73.93	72.97	64.42	67.96	12.34	12.62	4.84	5.25
U on Fe/Mn oxides	17.11	19.03	9.74	8.91	7.17	6.66	1.13	1.12
U on organics	4.87	3.99	14.39	11.76	34.97	34.87	7.15	8.03
Residuum	2.57	3.14	9.94	10.08	44.45	45.38	2.49	2.37
q_{ex} ($\mu g.g^{-1}$)	16.95		34.03		<0.238		380.08	

Considering increased content of organic matter, Fe and S (pyrite) in some samples (NA14), it seemed obvious that U should be sorbed on some of those element constituents. Surprisingly, high contents of U bound on carbonates were identified (see Fig. 3). However, XRF or any other method did not prove existence of important amount of carbonates in the sediments. Rarely some siderite concretions were found. This contradiction could be caused by either sorption of U(IV) carbonate complexes on the rock surface or by leaching of other mineral phases present in the sediment but not considered by sequential extraction schema.

Furthermore, the most of U is bound on exchangeable sites for NA14 samples with high content of U, TOC and S. This transfer onto easily removable fraction could be connected with high sulphur content and oxidising conditions under which samples were analysed. The rock samples from the depth (NA 14 60.69 m) were analysed under oxidation conditions. Reduced sulphide compounds (pyrite, etc.) could be therefore oxidised onto sulphates, releasing uranium from the sediment that could re-sorbed on different, easily accessible sites.

Exchangeable U amount, found with ^{233}U experiment, reached almost the same values (comparing concentration in $\mu g.g^{-1}$) as the sum of step 1 and step 2 in SE (U bound on exchangeable sites and on carbonates).

As mentioned above, phosphate U minerals form important portion of mineralisation. However, neither classical nor modified sequential extraction gave hint in which step phosphates were leached and consequently U bound is released. The only possible resolution of the question is to analyse U and P in the leachates from every SE step to identify selectivity of chemical agents.

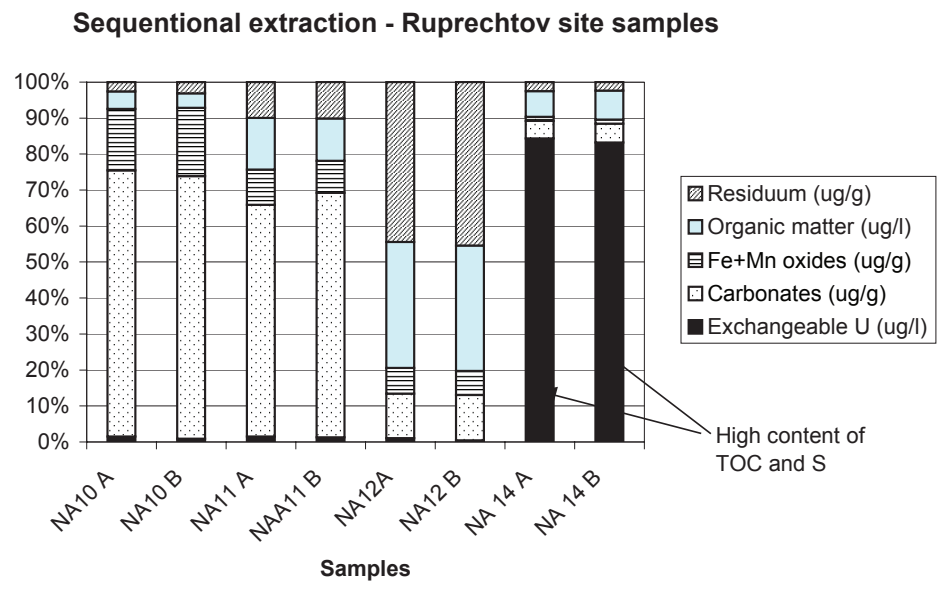

Fig. 3. Fraction of U forms (%) in the sediments from the Ruprechtov site (SE method)

5 Conclusions

The sequential extraction method has been and is still widely used in migration/remobilisation studies. The contradictions in widely used schema were found, analysing the Ruprechtov sediment samples. The discrepancy again drew out necessity that any result should not be taken into account without detailed analyses of phases, really leached out in every SE step. In Ruprechtov case further analyses of U, Th, P, Al, As, Fe, S, K, Ca, Na, K and alkalinity will be performed for each SE step in order to define and model solution/solid system and U forms. Furthermore, this problem proved necessity to use the SE method not as a solitaire and all-to-prove method, but in integration with modern surface and phase analyses methods (XRF, μ-XRF, XAFS…)

References

[1] Noseck U. et al.: *In:* Uranium in Aquatic Environment (Merkel B. el al. ed.) Springer, Berlin, Heidelberg (2002).
[2] Hercík M.: Technická a geologická dokumentace vrtných prací. Přírodní analog. Report ÚJV Řež a.s., 2005.
[3] Hercík M.: Závěrečné shrnutí výsledků projektu Přírodní analog. Report ÚJV Řež a.s., 2005.
[4] Breiter K., Knotek M. and Pokorny L: Folia Musei Rerum Naturalum Bohemia Occidentalis *33* (1991) 1.
[5] Suksi: *In:* Noseck U. et al.: Geochemical behaviour of uranium in a natural argillaceous system at Ruprechtov site. MIGRATION, Avignon, 2005.
[6] Denecke M. et al.: Env. Sci. Technol. *39* (2005) 2049.
[7] Sulovský P.: Mineralogy of Ruprechtov site samples. Expert report. NRI Řež, 2004.
[8] Tessier A., Campbell P. G. C. and Bosson M.: Anal. Chemistry 51 (1979) 844.
[9] Percival J. B. (1990): Clay mineralogy, geochemistry and partitioning of uranium within the alternative halo of Cigar Lake uranium deposit, Saskatchewan, Canada. Carleton University, Ottawa, PhD Thesis.
[10] Sachs S. et al.: FZKA 6969, Wissenschaft Berichte (Buckau G., ed.) Research Centre Karslruhe, Karlsruhe 2004, 79.

[II.]

DENECKE, M. AND HAVLOVA, V. (2007):

Elemental correlations observed in Ruprechtov Tertiary sediment: micro-focus fluorescence mapping and sequential extraction.
S&T publication. In Buckau G. and Kienzler B., Duro L., Montoya V. (eds.): 2rd annual workshop proceedings of 6th EC FP FUNMIG IP, Stockholm, November 21-23, 2006, 315-320. SKB Technical Report, TR-07-05.

ELEMENTAL CORRELATIONS OBSERVED IN RUPRECHTOV TERTIARY SEDIMENT: MICRO-FOCUS FLUORESCENCE MAPPING AND SEQUENTIAL EXTRACTION

Melissa A. Denecke[1*], Václava Havlová[2]

[1] Forschungszentrum Karlsruhe, Institut für Nukleare Entsorgung, P.O. Box 3640, D-76021 Karlsruhe, Germany. Corresponding author.
[2]Nuclear Research Institute Řež plc, Waste and Environmental Management Department, Husinec- Řež, PSČ 250 68, Czech Republic

Abstract

Sequential extraction (SE) is used for determination of U and other elements in a U-rich sediment from the Natural Analogue Site Ruprechtov. In Tertiary clayey samples U is found to be bound onto organic matter and/or be present in reduced form. In granitic samples carbonates/alumosilicates play a more important role in the U distribution.

Extended element analyses (Na, K, S, Fe, As, P) of SE leachates were completed. Cluster analyses of these results are used for identifying possible correlations between elements and for comparing these to previous correlations derived from μ-XRF and μ-XAFS investigations. According to the SE cluster analysis P, As and P can be assigned into one group. Fe and S are separated from U, i.e. we find no direct dependence of U on Fe and S. K and Na are mainly associated with residual minerals. Agreement with micro-scale measurements is observed: U in the sediment is associated with As and is present as phosphate in reduced U(IV) form.

Introduction

The Natural Analogue Study at the Ruprechtov site aims at understanding behaviour of natural radioelements in plastic clay formations. This system is chosen as an analogue for sedimentary overburden of radioactive waste repository host rocks (salt, granite, clay). The most similar proposed repository systems studied are Gorleben (Germany) and Mol (Belgium).

Objectives

The main objective of the Ruprechtov analogue site study is to find and describe the main mobilisation/immobilisation processes for performance assessment

(PA)-relevant elements, namely uranium, thorium and radium. The system consisting of U – argillized clay – organic matter – granite – groundwater is studied both in-situ and in the laboratory in both a macro- and microscale. The investigations include drilling, field tests, geochemical and hydrogeological modelling, as well as monitoring, sampling, both in situ and laboratory characterisation of sediment and groundwater. One of the aims was to study uranium association with other sediment constituents. Modern material surface analyses methods were used: micro x-ray fluorescence (μ-XRF) and micro x-ray absorption fine structure (μ-XAFS) on core sections of Tertiary clay samples images were in this case compared with the results of sequential extraction (SE) of the same material type.

μ-XRF / μ-XAFS is performed in order to assess mechanisms leading to immobilization of the U during diagenesis (Denecke et al., 2005). Sekvential extraction is a widely used tool for speciation of selected elements (in this study, U) bound onto different fractions of sediment (see, e.g., Tessier et al., 1979; Percival 1990, Havlová and Laciok, 2006).

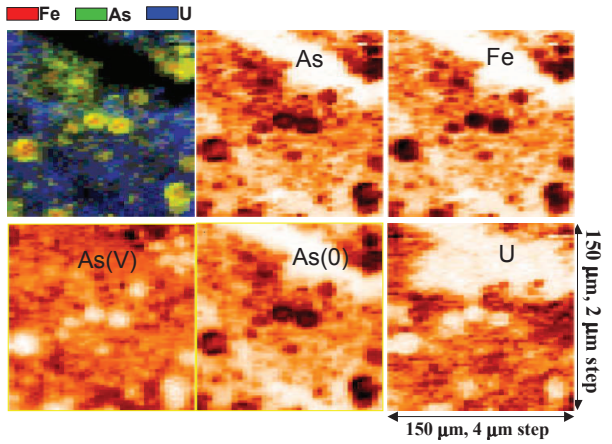

Fig.1: μ-XRF distribution maps for a 150*150 μm^2 area of a thin section of a sample from NA5. The distribution of the total As, Fe and U measured with E_{excite} = 18 keV and its corresponding Red-Blue-Green (Fe, As, and U, respectively) image , as well as the arsenic chemical state distributions for As(V) and As(0) are shown. As(0) is obtained from the As Kα fluorescence recorded using E_{excite} =11.861 keV; As(V) distribution is the difference between As Kα fluorescence recorded using E_{excite} = 11.870 keV and E_{excite} 11.861 keV, i.e. map at 11.87 keV minus the As(0) map

Results and discussion

μ-XRF and μ-XAFS results show uranium to be present as a tetravalent phosphate/sulfate in the regions studied and that U(IV) is associated with As(V) (Denecke, et al., 2006). Arsenic is present in the sediment as either As(V) or As(0);we did not find any evidence for As(III). The As(0) is observed to be intimately associated with the surface of Fe(II) nodules and likely arsenopyrite.

Numerous correlation functions between As and U are determined from measured fluorescence intensities of elemental distribution maps recorded for samples

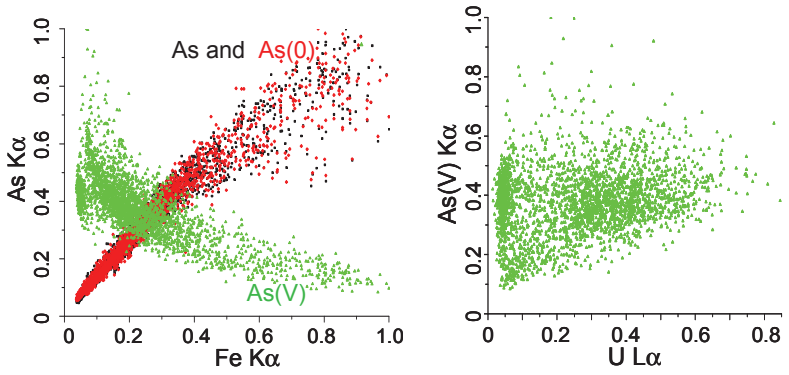

Fig 2: Correlation plots between Fe and As(0) [◆], As(V) [▲], and total As [ ] (left) and between U and As(V) (right).

NA4 and NA5. An example of distribution maps measured for a 150*150 μm^2 area of a thin section of a sample from borehole NA5 is shown in Fig. 1.

In this case it is possible to selectively differentiate between As(0) and As(V) in the maps by tuning the incoming incident photon energy (E_{excite}) to the corresponding ionisation energy. The correlation between U and As(V) and between As (total As, As(0) and As(V)) and Fe is shown in Fig. 2. We observe a correlation between As(V) and U. The linear correlation between As(0) and Fe shows that these are in the same phase, which is another indication of arsenopyrite presence in the sample. The difference between the correlation between As(0) and Fe and between the total As and Fe is hardly different, indicating that As(V) is a minority species.

The sequential extraction (SE) scheme is applied to Ruprechtov samples of different origin (6 boreholes, different depths, different rock types – kaolinized granite/Tertiary argillized clay). Samples are leached using different extractants in order to quantify various forms of U present in the sediment. The SE scheme consists of: following steps:

1. U bound on exchangeable sites (leaching with $MgCl_2$)
2. U bound on carbonates (leaching with ammonium acetate with acetic acid)
3. U bound to Fe/Mn oxides (leaching with hydroxylaminehydrochloride in acetic acid)
4. U bound onto organic matter/in reduced form (using H_2O_2 and HNO_3)
5. U in residuum (using boiling with HNO_3)

SE results of the uranium associated with the various fractions, expressed as percent of total U content are shown on Fig 3.

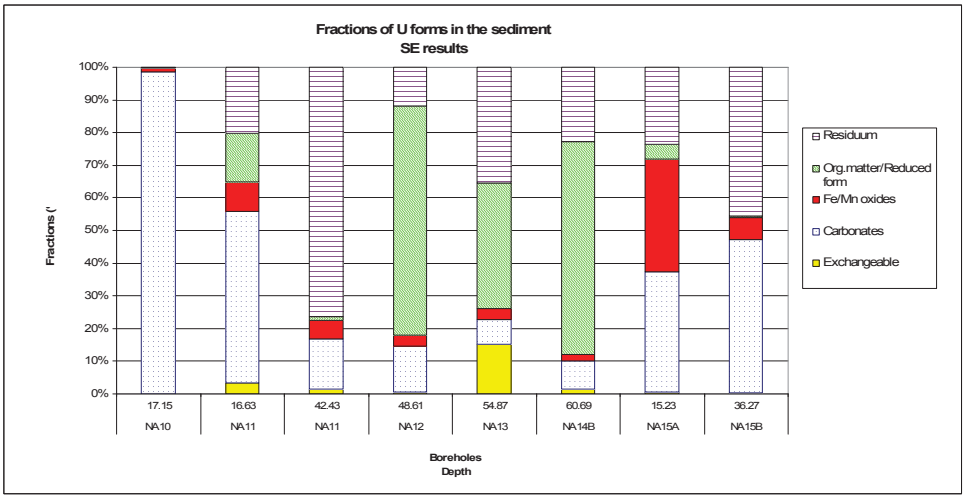

Fig. 3: Fractions (in %) of U in the sediment samples (SE results). NA10&NA15A kaolinized granite, the rest of the samples – argillized Tertiary clay.

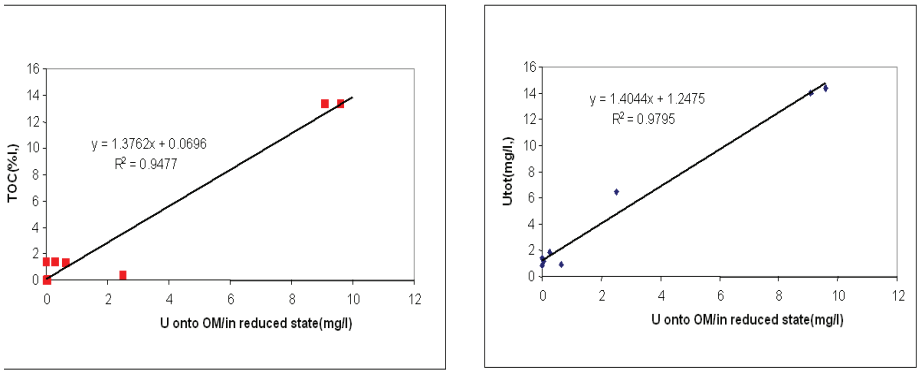

Fig. 4: Dependency of the U fraction bound onto organic matter(OM)/in reduced form in mg/l on TOC in percent (left) and on Utot in mg/l (right). Lines depict linear dependency results, both yielding a slope of around 1.4.

In Tertiary clay samples (all samples except NA10 and NA15B) we find U bound onto organic matter and/or in reduced form to be proportional to the total U content (Utot) and on total organic carbon content (TOC). In other words, observed increases in Utot and TOC are associated with increasing content of U bound to organic matter and/or in reduced form (see Fig. 4). In granitic samples (NA10, NA15B) we find that carbonates/alumosilicates play a more important role in U binding.

Extended element analyses (Na, K, S, Fe, As, P) of SE leachates are completed for two samples in order to define phases dissolving in each extraction step. Therefore, cluster analyses are then used to process the data in order to identify possible interrelations between elements and further prove dissolution/leaching in the sediment. Clustering is one of the most commonly used methods of multivariate data analysis in statistical data processing. The routine produces a dendrogram showing how data points can be clustered (Davis, 1986, Harper et al., 1999). According to that, PAST, paleobiological statistical software package (Hammer and Ryan P.D., 2001) was used for the analyses of trace element content (U, P, As, Na, K, S, Fe) in each SE leachate sample (see Fig. 5). P, As and U can be assigned into one group. This is in agreement with observations derived from the µ-XRF and µ-XAFS measurements. Fe and S are not interrelated with U, i.e. there is no direct evidence of U dependence on Fe and S. The major elements K and Na are mainly bound in residual minerals (SE step 5). As K is also leached in SE step 2 (signed as carbonates, although there is low occurrence of those minerals on the site), we can assume that alumosilicates and/or carbonate complexes are more responsible for U distribution than carbonate minerals themselves.

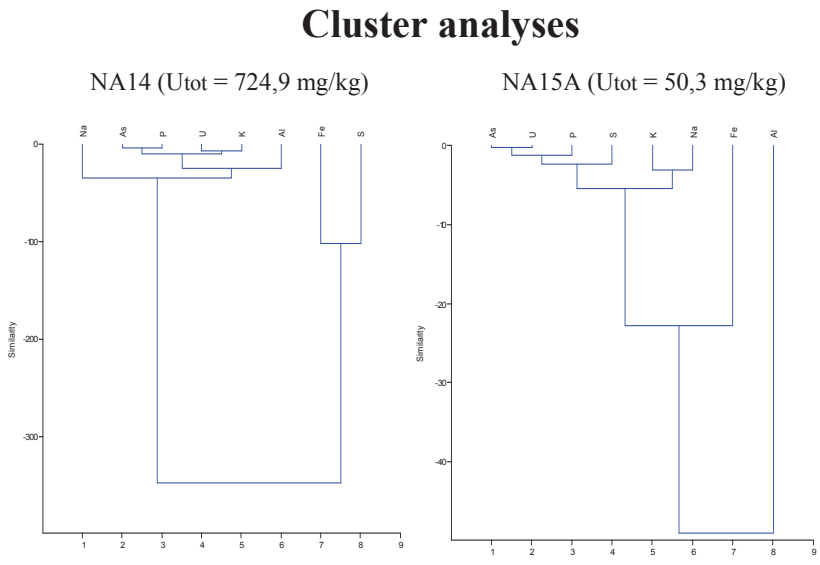

Fig. 5: Cluster analyses (PAST) for trace element content in each sequential extraction leachate for 2 Tertiary clay samples from the Ruprechtov site. NA14 - Tertiary clay, rich in organic matter, high U content, NA11 - Tertiary clay, low organic matter and U content. PAST, paleobiological statistical software package (Hammer and Ryan P.D., 2001)

Conclusions

Both micro-focus fluorescence mapping and sequential extraction of Ruprechtov clay samples showed that U accumulation in the sediment is associated with

As. Analysis of μ-XAFS reveals the presence of U-phosphate phases in the sediment, corroborated by the cluster analysis showing a correlation between U and P. Cluster analysis further shows that there was no direct interrelation between U and Fe and S. This is in agreement with the observation in the elemental distributions for Fe and U by μ-XRF/μ-XAFS. U is observed to be located in sample areas void of Fe. In this comparative study the application of independent methods, i.e. SE and μ-XRF/μ-XAFS, yields complementary results. This is important as we find similar elemental correlation results using the x-ray based methods as in SE. This indicates that SE results are not erroneously fraught with artefacts caused by speciation changes during the extraction processes.

References

Davis, J.C. 1986. Statistics and Data Analysis in Geology. John Wiley & Sons, New York.

Denecke, M.A., Janssens, K., Proost, K., Rothe, J., Noseck, U. (2005) *Environ. Sci. Technol.* **39**(7), 2049-2058.

Denecke, M.A., Somogyi, A., Janssens, K., Simon, R., Dardenne, K., Noseck, U**.** (2006) *Microscopy Microanal*. (invited contribution; accepted)

Harper, D.A.T. (ed.). 1999. Numerical Palaeobiology. John Wiley & Sons, New York

Hammer Ø., Harper D.A.T., Ryan P.D. (2001): PAST: PALEONTOLOGICAL STATISTICS SOFTWARE PACKAGE FOR EDUCATION AND DATA ANALYSIS. Copyright: Palaeontological Association, 2001.

Havlová V., Laciok A. (2006): Geochemical study of uranium mobility in Tertiary argillaceous system at Ruprechtov site, Czech Republic. *Czech Journal of Physics*, Vol. 56, Suppl. D. (in press).

Percival J. B. (1990): Clay mineralogy, geochemistry and partitioning of uranium within the alternative halo of Cigar Lake uranium deposit, Saskatchewan, Canada. Carleton University, Ottawa, PhD thesis.

Tessier A., Campbell P.G.C. and Bosson M.(1979): Sequential extraction procedure for the speciation of particulate trace metals**.** *Anal. Chemistry* **51** 844-851.

[III.]

NOSECK U., SUKSI, J. , HAVLOVA, V., BRASSER, T. (2007):

Uranium enrichment at Ruprechtov site . Uranium disequilibrium series and geological development.

S&T publication. In: Buckau G. and Kienzler B., Duro L., Montoya V., Delos A. (eds.) 3rd annual workshop proceedings of 6th EC FP FUNMIG IP, Edinborough, GB, Nov. 25 . 29, 2007, 317-325. Report NDA 2007.

URANIUM ENRICHMENT AT RUPRECHTOV SITE – URANIUM DISEQUILIBRIUM SERIES AND GEOLOGICAL DEVELOPMENT

Ulrich Noseck[1*], Juhani Suksi [2], Vaclava Havlova [3], Thomas Brasser[1]

[1] Gesellschaft für Anlagen- und Reaktorsicherheit (GRS) mbH (D)
[2] University of Helsinki (FIN)
[3] Nuclear Research Institute (NRI) (CZ)

* Corresponding author: Ulrich.Noseck@grs.de

Abstract

As part of the characterisation of immobile uranium forms at Ruprechtov site uranium disequilibrium series, as well as separation of U(IV) / U(VI) and sequential extraction with subsequent analysis of the $^{234}U/^{238}U$ activity ratio in the distinctive phases are performed on samples from the uranium-enriched clay/lignite layers. The observations of $^{234}U/^{238}U$ and $^{230}Th/^{238}U$ activity ratios below unity and very low $^{234}U/^{238}U$ ratios between 0.14 and 0.8 in the U(IV)-bearing fractions in the majority of samples clearly show that the predominant part of uranium was fixed over very long time scales in the form of U(IV) minerals. This finding is in agreement with results from other analyses and supports the scenario outcome of the geological development of the site assuming that uranium input occurred preferentially during the Upper Tertiary. The occurrence of immobile U(VI) with activity ratios above one indicates some recent uranium input.

Introduction

Major focus on the investigations at Ruprechtov site is put on the uranium accumulation in clay/lignite layers at the interface of kaolin and pyroclastic sediments (e.g. Noseck et al. 2007). By application of different microscopic and macroscopic methods immobile uranium phases are characterised in order to understand the whole uranium enrichment scenario. In particular, analyses of uranium disequilibrium series and $^{234}U/^{238}U$ activity ratios (ARs) in different phases separated by wet chemical U(IV)/U(VI) separation and sequential extraction methods give insight into time frames of enrichment and stability of distinct uranium forms. First results of U(IV)/U(VI) separation have been discussed at the 2nd annual workshop. In this presentation new results are presented and it is shown how these results correlate to the assumed geological development of the site.

Experimental Method

U series disequilibrium measurements have been performed over several years to date bulk U accumulations. The sample material was extracted in boiling concentrated HNO_3

to dissolve U. ^{238}U, ^{234}U and ^{230}Th were analysed applying both liquid-liquid extraction and ion exchange methods. Radionuclide concentrations were measured by α-spectrometry.
Oxidation states U(IV) and U(VI) were determined using a wet chemical method as decscribed in (Noseck et al. 2007). Dissolution of U(IV) and U(VI) phases was performed by extracting the sample material under anoxic conditions in an ultrasonic bath with a mixture of 4 M HCl and 0.03 M HF under Ar-atmosphere for 10 min. The solid to solution ratio was adjusted to about ~0.1. The solution obtained was fed into an anion-exchange column. U(IV) passes the column, whereas U(VI) is retained. U(IV) was collected in the first 20 ml and U(VI) then eluted with 20 ml of 0.1 M HCl. Separation is quantitative and no overlap of U(IV) and U(VI) fractions has been observed in tracer experiments. Concentration of ^{234}U and ^{238}U in the U(IV) and U(VI) fractions were determined using the procedure described above.

A sequential extraction (SE) scheme consisting of five steps was applied to samples from the clay/lignite horizon. The samples were leached using the following different extractants to identify and quantify uranium association in the sediment:

1. U bound onto exchangeable sites (leaching with magnesium chloride)
2. U bound to carbonates (leaching with ammonium acetate with acetic acid)
3. U associated with Fe/Mn oxides (leaching with hydroxylamine hydrochloride in acetic acid)
4. U bound in reduced form/onto organic matter (leaching with H_2O_2 and HNO_3)
5. U in residuum (boiling in HNO_3)

Uranium concentrations and isotope activities in different steps were determined as described above.

Results and Discussion

U series data obtained from analyses of clay/lignite samples from several boreholes are presented in Fig. 1 in the form of Thiel's diagram. By considering a closed system, the diagram can be divided into four segments, which are determined on the one hand by the $^{234}U/^{238}U$ equilibrium line (i.e. AR =1) and on the other hand by a line obtained when a tangent is drawn on the closed system chain decay curves evolving towards radioactive equilibrium ($^{230}Th/^{238}U$=1 and $^{234}U/^{238}U$=1) after sudden accumulation and removal of U. The segments denoted S1 and S2, between the U addition and removal areas, cannot be reached by closed system chain decay. Data plots in segment S1 represent samples in an open system from which ^{234}U has been selectively removed. Segment S2 can be reached if samples with recently accumulated U (within the last million years) have subsequently experienced U removal.
Most of the data points appear in segment S1, indicating that the system in the clay/lignite layers has been open but stable conditions with respect to bulk U occurred. AR<1 is caused by ^{234}U removal from the system as a consequence of α–recoil and related processes. Thus at least a significant fraction of uranium in the clay/lignite horizon is more than 1 Million years old, i.e. beyond the time range of the U series method. A number of data points in the bulk U addition area give rise that some uranium accumulation is still in progress.

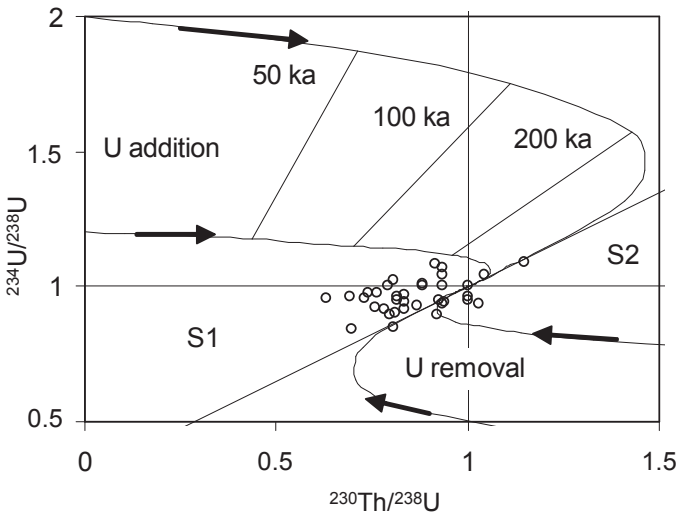

Fig. 1: *$^{230}Th/^{238}U$ and $^{234}U/^{238}U$ activity ratios of samples from the clay/lignite horizon plotted in Thiel's diagram with isochrones. Curves started from $^{230}Th/^{238}U=0$ and $^{234}U/^{238}U=1.2$ and 2 in the U addition area have been taken as examples to show how activity ratios change as a function of time in the closed system after sudden U accumulation. Curves in the U removal sector describe changes in isotope ratios back to secular equilibrium after sudden U removal.*

In order to better understand the uranium enrichment and distinguish between different immobile phases, a separation method for U(IV) and U(VI) (Ervanne et al. 1996) has been modified and applied to samples from the clay/lignite layers from different boreholes NA6, NA11, NA12, NA13 and NA14. The results are listed in Table 1. The analytical error of the measured activity ratios is usually in the range of 1 to 5 %, and only in exceptional cases up to 10 %.
Total uranium content in the samples ranges from 27 to 468 ppm, with lowest uranium content in sample NA12. High uranium content is observed in samples NA13, NA14 and NA6 from app. 35 m depth, with the highest value of 468 ppm in NA6. We observe that uranium in the borecore samples consists of both U(IV) and U(VI). The extraction does not dissolve all uranium. The content of uranium in this insoluble phase is denoted as U(res).
The AR differs significantly in the U(IV) and U(VI) phases, with ratios <1 in the U(IV) phase and ratios >1 in the U(VI) phase in nearly all samples. The AR of the U(res) phase is with exception of NA12 similar to that observed in the U(IV) phase. Different (higher) AR in the NA12 residue may indicate involvement of different U compounds in the sample material, i.e. U(IV) and insoluble U(res) represent different compounds. Taking into account the higher stability of U(IV) phases we assume that insoluble uranium exists as a stable mineral phase in oxidation state IV. Most uranium in all samples is U(IV), with contents between 50 and 90 wt.%. The highest U(IV) fraction is found in sample NA6-37.

That U(res) and U(IV) exhibit in nearly all samples an AR below one is a strong indicator for their long-term stability. AR values significantly below unity are caused by

the preferential release of ^{234}U, which is facilitated by α-recoil process and subsequent ^{234}U oxidation (see, e.g., Suksi et al. 2006). In order to attain low AR values of approx. 0.2 in the U(IV) phase, it must have been stable for a sufficiently long time, i.e. no significant release of bulk uranium has occurred during the last million years. This is in agreement with the hypothesis that the major uranium input into the clay/lignite horizon occurred during Tertiary, more than 10 My ago as described in the next chapter and in (Noseck et al. 2006). The prevailing groundwater conditions, with low Eh values especially in the clay-lignite horizon of borehole NA6, is another indication that stable, insoluble U(IV) phases such as uraninite can be expected under the present conditions. The AR in groundwater generally reflects the nature of water-rock interaction and is therefore sensitive to groundwater conditions (see Suksi et al. 2006). Under oxidising conditions both isotopes are released into the groundwater with the ratio they occur in the uranium source. Under anoxic conditions, where bulk uranium release is strongly suppressed, the release of the more mobile $^{234}U(VI)$ is favoured. The low ARs in the U(IV) phase observed in this study are correlated with AR values >1 in pore and groundwater from the clay/lignite horizon (Noseck et al. 2007). This is expected because of the anoxic sediment conditions and preferred mobilisation of ^{234}U.

Tab. 1: *Amount of uranium and $^{234}U/^{238}U$-activity ratios (ARs) in the different phases from uranium separation*

sample	U [ppm]	U(IV)		U(VI)		U(res, IV)		U(IV) total
		[%]	$^{234}U/^{238}U$	[%]	$^{234}U/^{238}U$	[%]	$^{234}U/^{238}U$	[%]
NA6 35a	356±7	28.7	0.54 ± 0.01	41.9	1.42 ± 0.02	29.5	0.65± 0.01	58.1
NA6 35b	468±9	45.9	0.56± 0.01	33.3	1.69 ± 0.03	20.7	0.64± 0.02	66.7
NA6 35c	369±8	23.3	0.47± 0.01	47.4	1.16± 0.02	29.3	0.67± 0.01	52.6
NA6 37a	37.3±2	73.7	0.79 ± 0.03	15.7	2.66± 0.07	10.6	0.73± 0.01	84.3
NA6 37b	47.5±1,5	66.2	0.52± 0.01	9.0	3.37± 0.15	24.8	0.86± 0.02	91.0
NA6 37c	35.7±2	51.3	0.58± 0.01	19.8	2.56 ±0.08	28.9	0.71± 0.04	80.2
NA11 a	52.5±2,2	4.2	0.44± 0.02	34.1	0.94± 0.01	61.7	0.55± 0.02	65.9
NA11 b	53.6±2,5	6.1	0.39± 0.02	49.6	0.94± 0.025	44.3	0.67± 0.02	50.4
NA12 a	27.2±1,4	3.9	0.26± 0.02	47.5	1.31± 0.04	48.6	1.22± 0.03	52.5
NA12 b	31.4±2,1	4.2	0.13± 0.02	57.4	1.25± 0.04	38.4	1.04± 0.03	42.6
NA13 a	216±7	5.4	0.53± 0.02	46.8	1.15 ± 0.02	47.8	0.55± 0.01	53.2
NA13 b	230±9	1.6	0.58± 0.03	46.2	1.15± 0.02	52.2	0.53± 0.01	53.8
NA14 b	317±10	13.3	0.87± 0.02	68.8	1.28± 0.02	18.0	0.44± 0.01	31.2
NA14 c	354±11	25.4	0.88± 0.02	39.6	1.11± 0.01	41.5	0.54± 0.01	58.5

Results from SE are described elsewhere (Denecke et al. 2007, Noseck et al. 2007). In general those results correlate well with the U(IV)/U(VI)-separation results, since both methods observed the major part of uranium to be associated with the U(IV) phase, which are expected in step 4 and 5 from sequential extraction (U bound in reduced form/onto organic matter and U in residuum).
In order to confirm that uranium in steps 4 and 5 is really in the tetravalent state, analyses of AR in the different SE leachates from sample NA13 were performed. The analyses were limited to the leachates from step 1, 2, 4 and 5, since the uranium content in the third step is always very low, < 3 % of total uranium. The results are shown for sample NA13 in Fig. 2. AR values in steps 1 and 2 are quite similar, with values above

1.75. Upon comparing this value with results from U(IV)/U(VI)-separation we conclude that uranium extracted in these first two steps was U(VI). In contrast, ARs in leachates from steps 4 and 5 are around 0.5 to 0.6, which matches well the values observed in the U(IV) and U(res) fractions from U(IV)/U(VI)-separation. This confirms that uranium extracted in steps 4 and 5 was U(IV).
The amount of U(VI) determined by the two methods differs. From the U(IV)/U(VI)-separation, 44 % U(VI) was found, whereas uranium extracted by steps 1 and 2 consists of only 22.5 % U(VI). One possible explanation for this discrepancy is that part of the U(IV) in the sample was oxidised during the U(IV)/U(VI)-separation. We expect such an oxidation to affect a AR decrease in the U(VI) phase by dilution with originally U(IV) having a lower AR. The lower value of 1.2 observed in the separation, compared to values of 1.75 and 1.76 from steps 1 and 2, might be an indication that partial oxidation of U(IV) to U(VI) actually occurred. In order to reliably use the U(IV)/U(VI)-separation method for quantification of uranium redox state, a more systematic work on determining redox states during uranium dissolution is necessary.

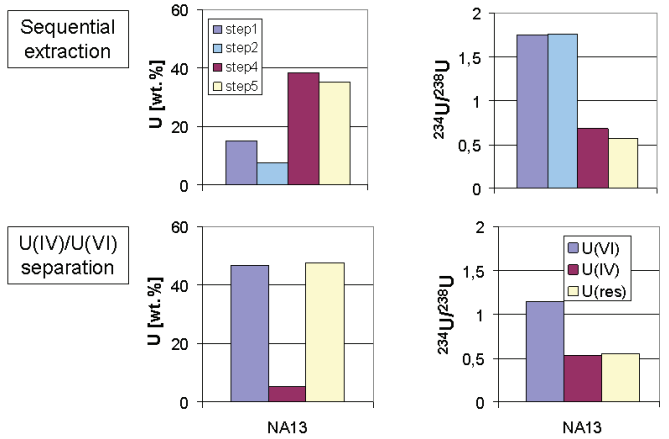

Figure 2: *Uranium content and $^{234}U/^{238}U$ activity ratios in SE leachates from steps 1, 2, 4 and 5 (top) compared to U(IV), U(VI) and U(res) fractions (bottom) in sample NA13*

Geological development and uranium enrichment scenario

In order to evaluate how the results support the ideas about uranium enrichment at Ruprechtov site, firstly the geological development is described. Recent studies about the geological evolution of the Ruprechtov area have shown that the bedding conditions are governed by a strong morphology of the Pre-Oligocene surface (now transition between kaolin and pyroclastics, e.g. Noseck et al. 2006). This morphology is a key feature for the analysis of the geological development. The assumptions about the major steps, based on current knowledge, comprise 5 main phases a–e as illustrated in Fig. 3. A major contribution to the uranium accumulation occurred in phase "c" which is shown in Fig. 4. Preceding the sedimentation of the pyroclastics, weathering of the underlying granite in particular took place as a result of the reaction of feldspars with CO_2-rich groundwater and the formation of kaolin. CO_2-rich groundwater furthermore

initiated the mobilisation of uranium from accessory minerals by formation of soluble UO_2-carbonate complexes. Within the kaolin, uranium was mainly transported by diffusion. At the boundary layer between kaolin and overlying pyroclastic sediments, advective transport was also possible over short distances in a local horizon with increased hydraulic conductivity. The main immobilisation processes occurred in/close to lignite-rich sediments. The key processes contributing to the uranium immobilisation are described in the contribution of Havlova et al. 2007 to the 3rd annual FUNMIG workshop. Hexavalent uranium was reduced and U(IV) was immobilised in secondary uranium phases ningyoite and uraninite due to processes connected with microbial reduction of organic matter and arsenopyrite formation.

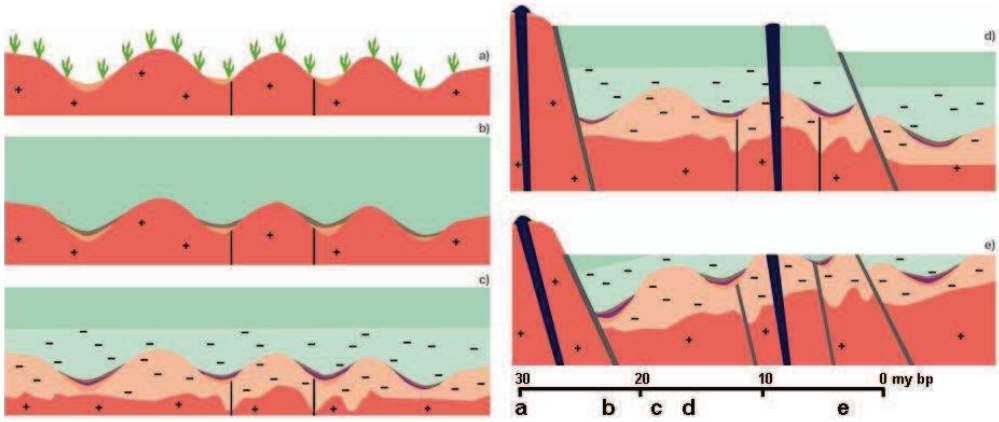

Figure 3: *Schematic representation of relevant phases of the geological evolution of the Sokolov basin: a) Pre-Oligocene,> 30 My: influx of detritic material (orange) by physical weathering of the granite present at the surface (red); b) Lower Oligocene – Miocene, 30-16 My: deposition of organic material (brown) in trough areas; after that, main phase of volcanic activity with wide-area sedimentation of pyroclastics / tuff (green); c) Lower Oligocene – Miocene, 30-16 My: alteration of granite (kaolinisation - light red, dashed) and tuff (bentonisation - light green, dashed); d) Miocene (16-15 My): rift formation, combined with fault zones (grey) and basalt intrusions (dark blue) e); Pliocene - Quaternary (< 5 My): further evolution of the Ohre rift and partial erosion of the pyroclastic sediments (after Noseck et al. 2006)*

Uranium series disequilibria results and results from U(IV)/U(VI) separation support the hypothesis that a major part of uranium has formed more than a million years ago. The results also show that to some extent a transport and immobilization of uranium in the clay/lignite layers continued following the major influx during Tertiary. This more recently enriched uranium seems to occur at least partially in the U(VI) state. However, we have not yet been able to identify the form of this uranium. We assume that it occurs adsorbed on clay or organic material or in an amorphous mineral phase.
The impact of the major uranium input processes on AR in sediment and groundwater is illustrated in Fig. 5. We assume that at the time of major uranium influx during Upper Tertiary the AR in infiltrating groundwater was unity as it is observed today. Inflowing U(VI) was reduced in the clay/lignite horizon and immobilised in secondary minerals (Havlova et al. 2007). Thus, the immobile U(IV) phase formed had the same ratio of 1.

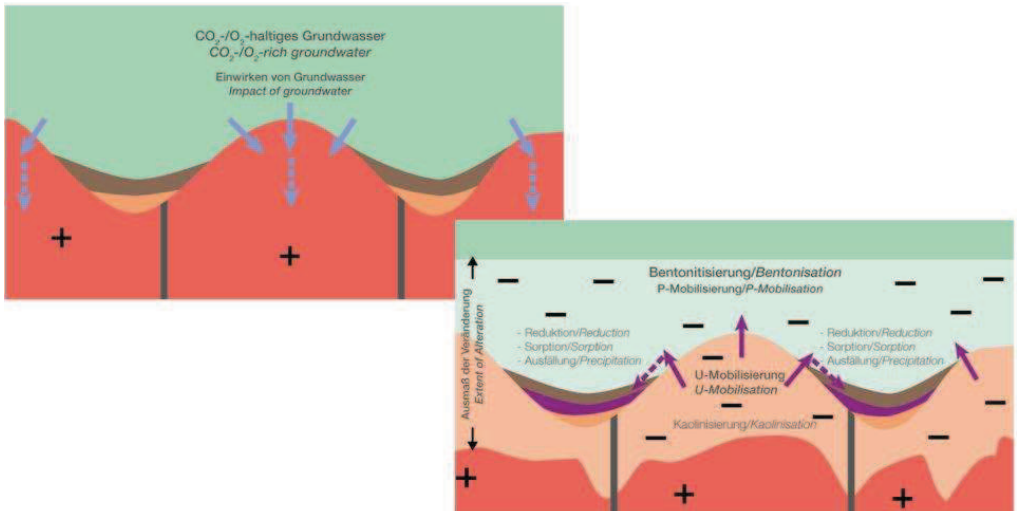

Figure 4: *Schematic illustration of the alteration processes in granite (kaolinisation) and tuff (bentonisation) by impact of CO_2- and O_2-rich groundwaters in phase "c" of the geological evolution. Kaolin is largest at previously morphological elevations of the granite due to Previous sedimentation of pyroclastic sediments. Uranium (magenta) is accumulated in those former valleys in which lignite or lignitic clay also accumulated*

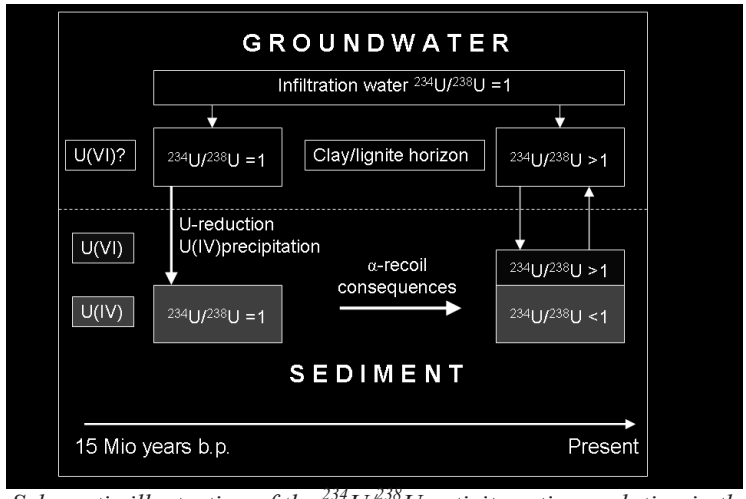

Figure 5: *Schematic illustration of the $^{234}U/^{238}U$ activity ratios evolution in the immobile secondary uranium phases and groundwater*

Due to α-recoil related processes, selective leaching of ^{234}U decreases AR in the stable secondary U(IV) phase. The preferred mobilisation of ^{234}U over ^{238}U also leads to an AR increase in the porewater and the groundwater-bearing layers with low flow velocity in the clay/lignite horizon. The AR in the porewater and groundwater-bearing layers is also affected by slow inflow of water from the infiltration area, containing uranium with AR around 1. Typical AR values in the clay/lignite layer water lie in the range between

2 and 4. Similar values are found in more accessible uranium fractions in the immobile phase, which have been more recently accumulated in the clay/lignite horizon.

Summary and Conclusions

Uranium series disequilibria and analyses of ARs in immobile uranium phases with different redox state contribute to the understanding of uranium enrichment at Ruprechtov site in the geological past. Using U(IV)/U(VI)-separation and SE coupled with analysis of AR in each phase, both U(IV) and U(VI) forms were identified in the clay/lignite horizon. We also found that the U(IV) phase has been stable over geological time frames, whereas the U(VI) phase was formed more recently. This is in accordance with the current understanding of the geological development of the site.
The wet chemical method to separate U(IV) and U(VI) was applied for the first time to the samples from Ruprechtov site. The results are very promising but the quantification of U(IV) and U(VI) phases using the separation method needs to be assessed, to ascertain if possible redox disturbances are caused by the uranium dissolution. Systematic investigations to compare U(IV)/U(VI)-separation and SE methods with homogenised samples are planned. In addition, the effect of iron present in the samples on the redox state of uranium during the sample dissolution will be investigated.

Acknowledgement

This work has been financed by the German Federal Ministry of Economics (BMWi) under contract no 02E 9995, by RAWRA and Czech Ministry of Trade and Industry (Pokrok 1H-PK25) and by the European Commission within the IP FUNMIG.

References

Denecke M, Havlova V (2007): Elemental correlations observed in Ruprechtov tertiary sediment: micro-focus fluorescence mapping and sequential extraction. In Buckau G., Kienzler B., Duro L., Montoya V. (eds.): 2nd Annual Workshop Proceedings of the IP Project FUNMIG", 315 ppt. SKB Technical Report, TR-07-05.

Havlová V., Brasser Th., Cervinka R., Noseck U., Denecke M., Suksi J (2007). Uranium enrichment at Ruprechtov site – Characterisation of key processes. S&T contribution to the 3rd annual workshop of the IP FUNMIG, 26.-29. November 2007.

Noseck U, Brasser Th, Suksi J, Havlova V, Hercik M, Denecke MA, Förster HJ (2007): Identification of Uranium enrichment Scenarios by Multi-Method Characterization of Immobile Uranium phases. Submitted to Physics and Chemistry of the Earth.

Noseck U, Brasser Th (2006): Application of transport models on radionuclide migration in natural rock formations - Ruprechtov site. Gesellschaft für Anlagen- und Reaktorsicherheit (GRS) mbH, GRS-218, Braunschweig.

Suksi J, Rasilainen K, Pitkänen P (2006): Variations in the $^{234}U/^{238}U$ activity ratio in groundwater – A key to characterise flow system? Physics and Chemistry of the earth, 31 (10-14), 556-571.

[IV.]

HAVLOVÁ, V., BRASSER, TH., CERVINKA, R., NOSECK, U., LACIOK, A., HERCIK, M., DENECKE, M., SUKSI, J., DULINSKI, M., ROZANSKI, K. (2007):

Ruprechtov Site (CZ): Geological Evolution, Uranium Forms, Role of Organic Matter and Suitability as a Natural Analogue for RN Transport and Retention in Lignitic Clay.

Proc. of Reposafe Conference, Braunschweig Nov. 6.9, 2007, 203-212, GRS-S-49.

REPOSAFE 2007
International Conference
on Radioactive Waste Disposal
in Geological Formations

Braunschweig ("City of Science 2007")
November 6 – 9, 2007

Ruprechtov Site (CZ): Geological Evolution, Uranium Forms, Role of Organic Matter and Suitability as a Natural Analogue for RN Transport and Retention in Lignitic Clay

V. Havlova*, Th. Brasser**, R. Cervinka*, U. Noseck**, A. Laciok*, M. Hercik*, M.A. Denecke***, J. Suksi****, M. Dulinski*****, K. Rozanski*****

**Nuclear Research Institute Řež plc, Husinec - Řež 130, 250 68 Řež, Czech Republic*
*** Gesellschaft für Anlagen- und Reaktorsicherheit (GRS) mbH, Theodor-Heuss-Strasse 4, 39122 Braunschweig, Germany*
**** Forschungszentrum Karlsruhe GmbH, Institut für Nukleare Entsorgung, Postfach 3640, 76021 Karlsruhe, Germany*
***** Department of Chemistry, A.I.Virtasen aukio 1, PL 55, 00014 University of Helsinki, Finland*
****** AGH University of Science and Technology, Faculty of Physics and Applied Computer Science, Al. Mickiewicza 30, 30-059 Krakow, Poland*

Abstract:
Ruprechtov natural analogue site, notably for its unique association of U-rich and organic layers within clay sediments, being underlain by granite, is studied in order to understand the processes of U-enrichment as a natural analogue for radionuclide transport and retention in lignitic clay formations, which often represent constituent parts of the overburden of potential host rocks for radioactive waste disposal. The site investigations focus on the detailed characterization of immobile uranium phases methods. Based on all available results a model for the geological evolution of the site including the different processes of uranium enrichment is developed. Special focus is laid on investigation of organic rich layers (lignite) within clayey sediments with carbon content up to 40 %. The results show that organic matter plays a more important role in establishing a reducing environment than as U sorbent.

1 INTRODUCTION

To assess the safety of a repository for radioactive waste, one needs to look at the important aspect of the barrier function of surrounding geological environment, i.e. the host rock and overlying and the overburden. Possible future developments are simulated with the help of long-term safety analyses, which in turn are based on assumptions that have to be verified. So-called "Natural Analogues" are a particularly suitable instrument for such verification purposes as they represent naturally occurring systems in which physical and/or chemical processes that can be expected in repository systems (or parts thereof) are developing (or have developed) over geological time periods. In particular, the study of geochemical long-term processes in rock types with increased natural radionuclide content represents an important supplement to laboratory experiments, which for reasons of setup and realisable time periods are subject to many limitations. Natural analogues can be also a very useful tool for methodology development, scientific team building and communication with the public.

Starting from the general geological situation in the environment of possible repository sites in northern Germany, with their characteristic sequence of clayey-silty and sandy sediments as well as lignite sands, approx. 40 uranium ore deposits in Germany were studied initially by way of an evaluation of the relevant literature. Due to their high potential suitability (genesis, lithology, age), two localities were finally chosen for a more detailed investigation programme: a) Heselbach near Schwandorf/Upper Palatinate (north-eastern Bavaria) and b) Ruprechtov in the north-east of the Czech Republic (between Jáchymov and Karlovy Vary). The latter is subject of the present paper. The investigations at both localities have been aimed to broaden the understanding of complex geochemical behaviour of radionuclides during transport and sorption in argillaceous sandy sediment under the influence of lignite horizons, affecting the geochemical milieu.

2 GEOLOGICAL EVOLUTION AND URANIUM ACCUMULATION

The overall geological situation of the Ruprechtov NA site is characterised by its position within the Sokolov basin, which forms part of the Ohre rift, a rift structure running in SW-NE direction and parallel to the Erzgebirge / Krušné hory mountains. This rift structure is filled with tertiary sediments (in the region of Ruprechtov mainly of volcanic origin) (Figure 1).

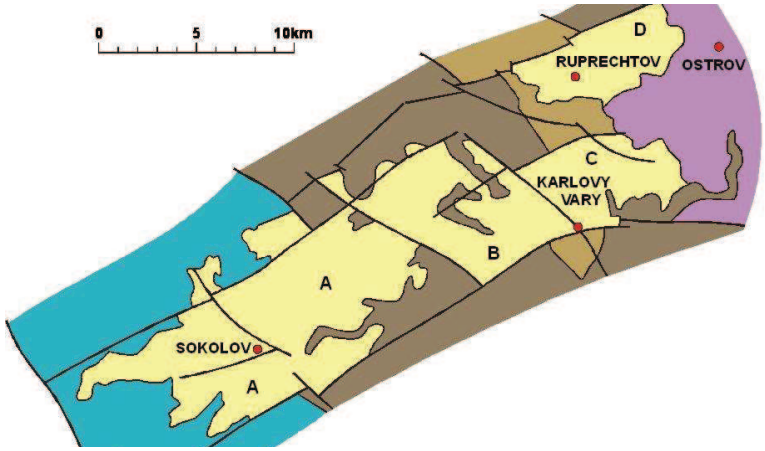

Figure 1: Geological sketch map of Sokolov basin (part of the Ohre rift). Tertiary sediments are plotted in yellow, granitic rocks in brown, metamorphic rocks in cyan and the tertiary volcanic rocks of the Doupovské hory stratovolcano in purple colour. Characters A-D mark several sub-basins

In the investigation area the following stratification is represented (from top to bottom):

- Quaternary cover (soil, loam – up to 2 m deep)
- Pyroclastic sediments (tuff, mostly argillised into bentonitic clay - maximum thickness up to 50 m)
- Clay/Lignite-sand horizon (with the most important uranium accumulation – thickness of stratum approx. 1-2 m)
- Kaolin (weathering product of the underlying granite – thickness up to approx. 40 m)
- Granite (partially also outcropping).

A first, in an early stage developed, relatively simple model of uranium mobilisation [1] was based on information found in the literature and on the results of a few drillings that had been restricted to the area of the uranium accumulation known at this time. This model involved the dissolution of uranium under oxidising conditions from the surrounding granite, its transport via groundwater in sediments with increased hydraulic conductivity, and its precipitation/sorption on lignite intercalations under reducing conditions in the form of a roll-front deposit.

More recent studies supported by drilling programmes spread over wider areas and involved more detailed laboratory tests have now shown that the bedding conditions are governed by strong morphology at the Tertiary base and that the uranium accumulations found in the clay/lignite-sand horizon have not been formed by one single process but by several different causes:

- Synsedimentary influx of detritic uranium minerals,
- Spatially limited mobilisation of uranium from the surrounding granite during the kaolinisation of the latter, diffusion and retardation (reduction, sorption, precipitation) within the clay/lignite-sand horizon,
- Influx from the underlying granite in zones of low kaolin thickness and/or via fault zones and retardation (reduction, sorption, precipitation) in the zone of the clay/lignite-sand horizon.

The assumptions based on current knowledge regarding the geological evolution of the Ruprechtov locality (as far as an U-accumulation is concerned) now comprise five main phases a – e (Figure 2).

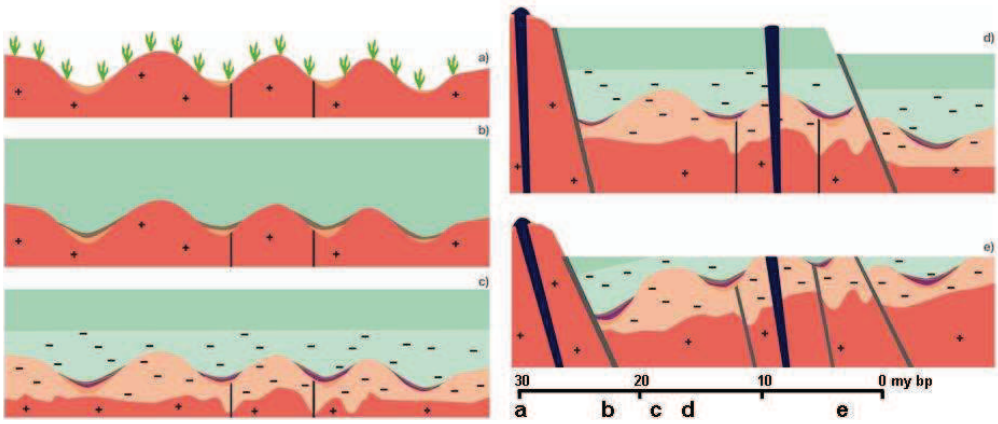

Figure 2: Schematical representation of relevant phases of the geological evolution of the Sokolov basin: a) Pre-Oligocene (> 30 My): influx of detritic material (orange) through physical weathering of the granite present at the surface (red); b) Lower Oligocene - Miocene (30-16 My): deposition of organic material (brown) in trough areas; after that, main phase of volcanic activity with wide-area sedimentation of pyroclastics / tuff (green); c) Lower Oligocene - Miocene (30-16 My): alteration of granite (kaolinisation - light red, dashed) and tuff (bentonisation - light green, dashed); d) Miocene (16-15 My): rift formation, combined with fault zones (grey) and basalt intrusions (dark blue) e); Pliocene - Quaternary (< 5 My): further evolution of the Ohre rift and partial erosion of the pyroclastic sediments

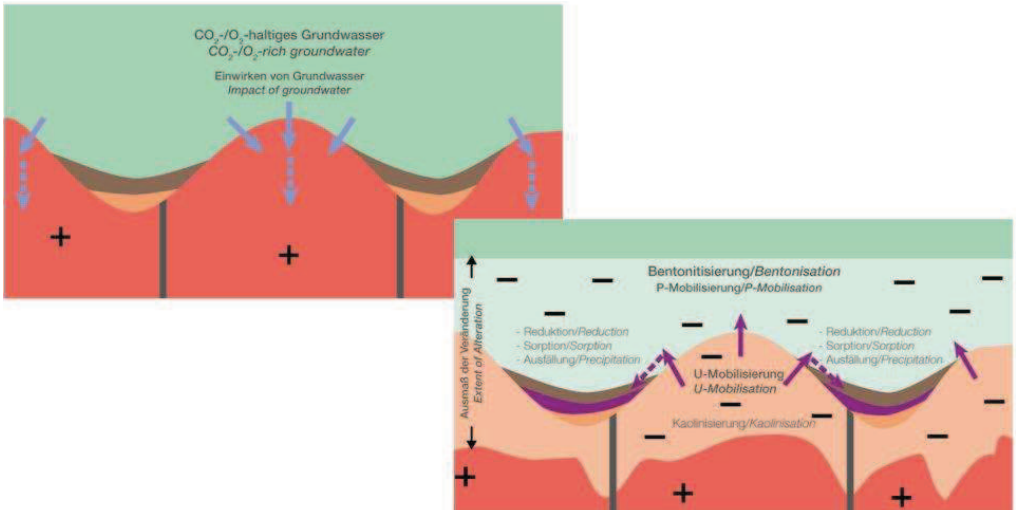

Figure 3: Schematical representation of the alteration processes in granite (kaolinisation) and tuff (bentonisation) through the impact of CO_2- and O_2-rich groundwaters in phase "c" of the geological evolution. The previous wide area sedimentation of pyroclastic sediments has led to the condition that the thickness of kaolin is greatest where the granite previously showed morphological elevations. Uranium (magenta) is accumulated in those former valleys in which lignite or lignitic clay also have accumulated

Here, it is above all phase "c" (Figure 3) that makes a major contribution to uranium accumulation: Following the sedimentation of the pyroclastics, weathering of the underlying granite mainly took place as a result of the reaction of feldspars with CO_2-rich groundwaters and the formation of kaolin. CO_2-rich groundwaters furthermore initiated the mobilisation of the uranium from accessory minerals by formation of soluble UO_2-carbonate complexes. Within the kaolin, uranium was mainly transported through diffusion. At the boundary layer between the kaolin and the overlying pyroclastic sediments, advective transport was also possible over short distances in a local horizon with increased hydraulic conductivity. The main immobilisation processes that could be considered were uranium reduction in/close to lignite-rich sediments, combined with formation of secondary uranium(IV) minerals such as uraninite and ningyoite.

The strongly reducing conditions in lignite-rich horizons could be verified by means of pH-Eh measurements in the corresponding groundwaters. The Eh-values of the groundwaters in clay sediments are clearly below those of granitic waters. According to that uranium can be supposed to exist in immobile U(IV) form that could be also declared by low U groundwater concentration (see Figure 4).

The individual retention processes are currently quantified within the framework of FUNMIG EC Project (see http://www.funmig.com/). Here, the focus was paid on the in-depth study of the immobile uranium phases by means of different surface-spectroscopic methods, adsorption and desorption experiments, as well as geochemical studies.

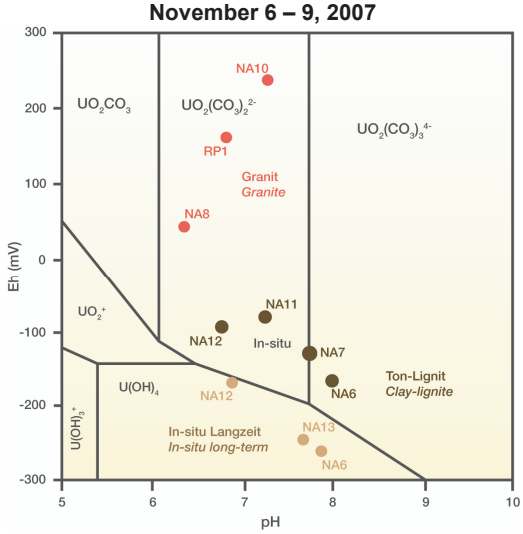

Figure 4: pH-Eh-phase diagram of aqueous uranium species. The coloured dots represent groundwater measurements and illustrate the differences in the geochemical environment between granite (red) and the lignite-clay/sand horizon (dark brown) as well as problems associated with qualified pH-Eh-measurements: regarding the drillings NA6, NA12 and NA13, only in-situ long-term measurements (light brown) at a depth of approx. 40 m have shown that uranium(IV) can be expected to be the dominant species in the aqueous phase

The very thin clay/lignite-sand horizon therefore can act as a highly effective transport barrier for uranium. There are no indications whatsoever to a renewed release of uranium from the accumulation horizons. Details concerning the studies and the results are summarised in the recently published final report "Radionuclide Transport and Retention in Natural Rock Formations - Ruprechtov Site" [2].

3 URANIUM FORMS

Organic rich layers (up to 40 wt% of TOC) were localised within the sedimentary system, being heterogeneously distributed. Uranium enrichment found showed also heterogeneous distribution, however it was usually not directly incorporated within lignite-like matter, but in vicinity.

Therefore, uranium forms in the sediment system and its relation to organic matter composition and degradation were extensively studied. In a first step, modern material surface analyses methods, i.e. micro X-ray fluorescence (µ-XRF) and micro x-ray absorption fine structure (µ-XAFS) on several core sections were employed [3]. Those were compared with the classical sequential extraction method, used up for trace element fractionation and form determination. The results showed uranium to be present as a U(IV) phosphate in association with As (see Figure 5 and Figure 6).

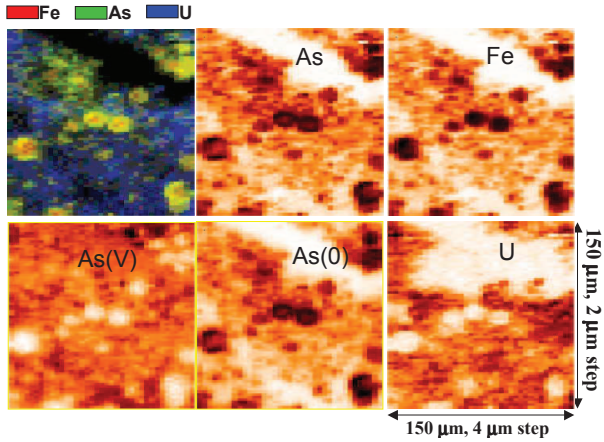

Figure 5: µ-XRF distribution maps for a 150*150 µm^2 area of a thin section of a sample from NA5. The distribution of the total As, Fe and U measured with Eexcite = 18 keV and its corresponding red-blue-green (Fe, As, and U, respectively) image, as well as the arsenic chemical state distributions for As(V) and As(0) are shown [3]

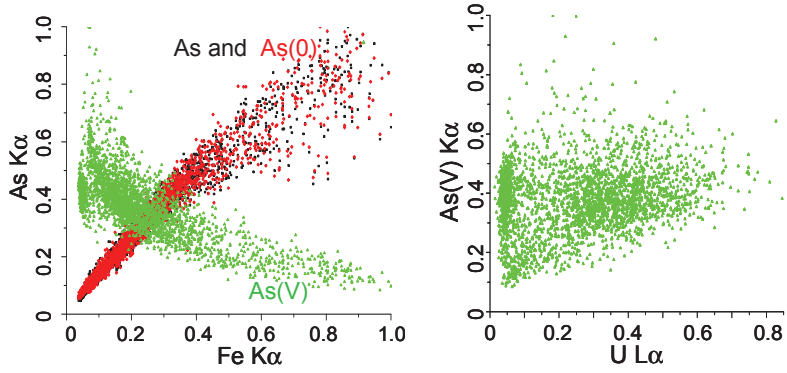

Figure 6: Correlation plots between Fe and As(0) [◆], As(V) [▲], and total As [ ] (left) and between U and As(V) (right) [3]

Simultaneously the sequential extraction (SE) scheme was applied to Ruprechtov samples of different origin (six boreholes, different depths, different rock types - kaolinised granite or tertiary clay). Samples were leached using different extractants in order to quantify various forms of U present. The SE scheme consists of alltogether 5 successive steps [4].

In tertiary clay samples (all samples except NA10 and NA15B) U in reduced form/bound onto organic matter was proportional to the total U content (U_{tot}) and on total organic carbon content (TOC). Those lead to conclusion U in reduced form was dependent on organic matter presence. Moreover, increased U total content only increased with more reduced U(IV) present. In granitic samples (NA10, NA15B) U was significantly bound either into residual phase or bound onto carbonate (Figure 7).

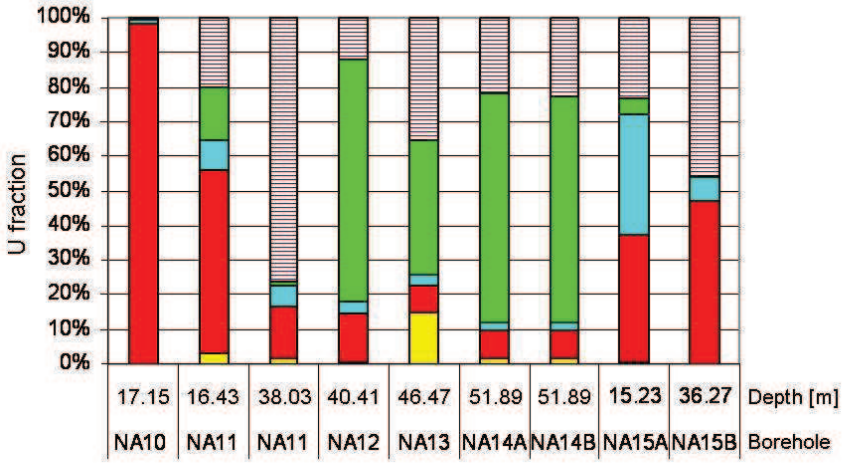

Figure 7: Uranium form fraction representation (in %) within Ruprechtov sediment samples as result of SE-experiments (step 1 [yellow] = exchangeable; step 2 [red] = carbonates; step 3 [cyan] = Fe/Mn oxides; step 4 [green] = U(IV) / reduced form; step 5 [dotted] = residuum)

Following these observations extended element analyses (Na, K, S, Fe, As, P) of SE-leachates were performed for two samples (NA14 and NA15A) in order to define phases dissolving in each extraction step. Cluster analyses could then be used to process the data in order to identify possible interrelations between elements and define phase dissolution/leaching within the sediment. [5] was used for the statistical procedure of U, P, As, Na, K, S, Fe in each SE-leachate sample (see Figure 8).

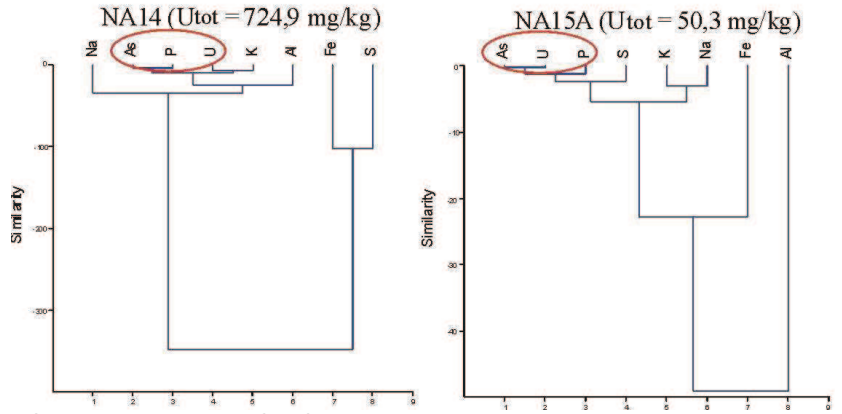

Figure 8: Cluster analyses (PAST) for trace element content in each sequential extraction leachate for two tertiary clay samples from Ruprechtov site. NA14 - tertiary clay, rich in organic matter (left), high U content, NA15A - tertiary clay, low organic matter and U content (right)

The results revealed that P, As and U were assigned into one group. This was in direct agreement with the µ-XRF and µ-XAFS measurement results. Fe and S were not interrelated with U, i.e. after all, there was no direct evidence of U dependence on Fe and S, although

high content of those two elements were identified within the sediment. The major elements K and Na were mainly fixed in residual mineral phase (SE step 5, silicate origin).

As K was identified to be leached in SE step 2, originally signed as carbonate bound form, although there is limited occurrence of carbonate minerals, we can assume that alumosilicates and/or carbonate complexes are more responsible for U distribution than carbonate minerals themselves.

In the same time, results of both microstructural analyses and sequential extraction were compared with mineralogical and microscopic study [6]. Here, U was identified in the forms of either primary U-bearing detritic minerals (xenotime, zircon, monazite) or secondary minerals (ningyoite, uraninite). In addition, very rare grains of non-identified uranium phases were observed. Ningyoite was also detected by micro structural analyses as small crystals, with dimensions around 5 μm, most commonly in association with iron sulphides (μ-XRF, μ-XANES, μ-EXAFS measurement [3]).

To identify uranium oxidation state fraction detailed complementary method for analysing uranium (IV) and uranium (VI) was applied for samples with different uranium content from different boreholes [7]. Both forms U(IV) and U(VI) existed in the tertiary clay horizon. The major part of uranium was U(IV) and its fraction varied from 55 to 90 % in the investigated samples. The generally low $^{234}U/^{238}U$-activity ratios (< 1) in the uranium(IV) fraction gave the evidence that this phase was rather stable and immobile over geological time scales (Figure 9). This evidence was confirmed by content of uranium in groundwater: even though U content in sediments was relatively high (up to 600 ppm), U concentration measured in groundwater was very low (app. 10 μg/l in granitic water, 0.5 μg/l in waters from Tertiary).

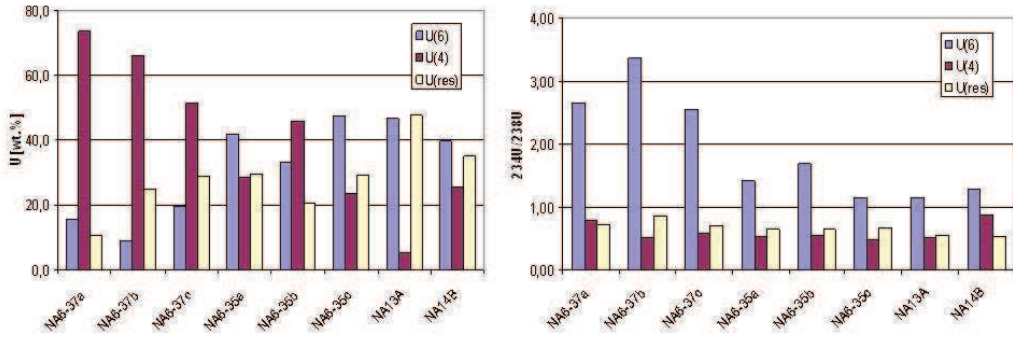

Figure 9: Fraction of uranium in U(IV), U(VI) and U(res) phase (left) and corresponding $^{234}U/^{238}U$ isotope ratios (right). Insoluble U(res) is assumed to be U(IV)

4 SEDIMENTARY ORGANIC CARBON CYCLE

Natural isotopic data were used for identification of the hydrogeological flow regime and the processes on the site, including carbon and sulphur cycle within the Ruprechtov system (e.g. [2]). Moreover, sedimentary organic matter composition and humic substances content were studied.

Despite the high sedimentary organic carbon (SOC) content in the clay/lignite-sand horizon (up to 40 wt%), the concentration of dissolved organic carbon (DOC) in Ruprechtov groundwater was generally low (app. 4 mg/l). Comparing the system with conditions at Gorleben, striking difference was evident: The highest DOC concentrations at Gorleben reached up to 200 ppm [8]. If humic substances were present, those were identified as fulvic acids. Studying composition of SOC, humic acids formed only 0.15 wt% of SOC [9].

Preliminary results indicated that microbial SOC degradation probably takes place at Ruprechtov site [2]. The conceptual model of sedimentary organic matter (SOC) decomposition was described elsewhere. Microbial processes lead to oxidation of SOC and reduction of oxidising agents, like SO_4^{2-} or NO_3^-. SOC is then partly oxidised to dissolved inorganic carbon (DIC) but part is also released as DOC, i.e. humic, fulvic and hydrophilic acids. However, those degradation products could then be sorbed on clayish sedimentary material and got fixed as reported in [10]. Such effects could result in a DOC content decrease in Ruprechtov groundwaters and the lack of humic substances [8].

In the next stage of degradation process more DIC is released followed by an increasing DOC oxidation. The formation of carbonic acid releases one proton and dissolves as HCO_3. In contact with carbonate containing sediments (sedimentary inorganic carbon - SIC) this process results in its dissolution and additional release of DIC of sedimentary origin.

The first indication of the microbially mediated process at Ruprechtov site is presented in Figure 10. Dissolved inorganic carbon concentration increase, particularly in clay/lignite horizon, is generally followed by increased DOC release (extraordinary NA8 borehole is the one with outcropping granite)

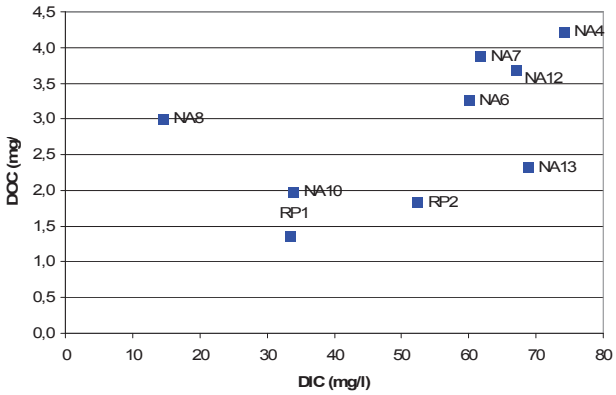

Figure 10: DIC concentration vers. DOC concentration in Ruprechtov groundwater wells

Furthermore, mineralisation (oxidation) of SOC can be accompanied by reduction of oxidising agents (SO_4^{2-} and NO_3^-), i.e. decrease of the species concentration with increasing DOC. The general trend is traceable within species concentration analyses in the Ruprechtov groundwater (see Figure 11). On the other hand, general reverse increasing trend can be spotted for phosphates (PO_4^{3-}). Those are produced by microbial mediated SOC metabolisation, causing reduction of sulphates and nitrates and release of originally SOC-bound phosphates into the solution.

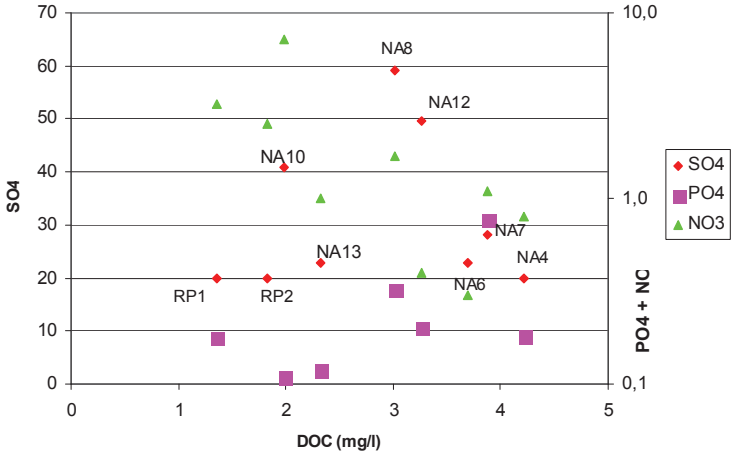

Figure 11: SO_4^{2-}, NO_3^- and PO_4^{3-} concentration vers. DOC groundwater (RP1 and RP2 boreholes were not drilled as part of the research project and are not filtered in a distinct horizon as the other ones)

Moreover, considering sulphur isotopic signatures, a complete oxidation of organic matter and the sulphate reduction can be written as $SO_4^{2-} + 2\ CH_2O = H_2S + HCO_3^-$. In presence of iron the reaction product will be fixed as mono-sulphide and afterwards be transformed into pyrite. The microbial sulphate reduction is accompanied by isotope fractionation. The lighter isotope ^{32}S is preferentially metabolised by microbes and therefore residual sulphate molecules in groundwater become enriched in the isotope ^{34}S, whereas $\delta^{34}S$ values in sulphides decrease. The groundwaters from the clay/lignite-sand layer show increased $\delta^{34}S$-values in the range of 16.43 to 24.63 ‰ that is clear indication of microbial sulphate reduction. The results of $\delta^{34}S$ analyses in water samples are shown in Figure 12.

Considering the results of uranium form identification and organic carbon behaviour on the site, there are indications for proposed uranium immobilisation at Ruprechtov site. Organic matter degradation was a microbial mediated process contributing to U(VI) reduction and U(IV) immobilisation into secondary phases.

SOC within the sedimentary layers was microbially oxidised, releasing DOC and providing protons to dissolve SIC. Oxidation agents (SO_4^{2-} and NO_3^-) were reduced and reduction of sulphate caused FeS_2 formation. Dissolved As got sorbed onto FeS_2, forming FeAsS precipitate. Uranium, having source in the underlying granite, was reduced on FeAsS surface to U(IV) and reacted with phosphates PO_4^{3-}, produced by microbial SOC oxidation. Uranium phosphates (ningyoite) were thus formed. Uranium is predominantly in U(IV), stable and immobile.

Low content of DOC in the groundwater identified could be caused either by high sorptive affinity of clay for organic degradation products or low SOC availability for degradation. Organic degradation products, considered in PA as potentially strong complexing agent, causing colloidal facilitated transport of radionuclides, then could be effectively fixed in the sedimentary system and reduce probability of radionuclide release into the environment. The research on sorptive properties of Ruprechtov tertiary clay sediments for natural humic acids and their complexation are in progress within the frame of FUNMIG project.

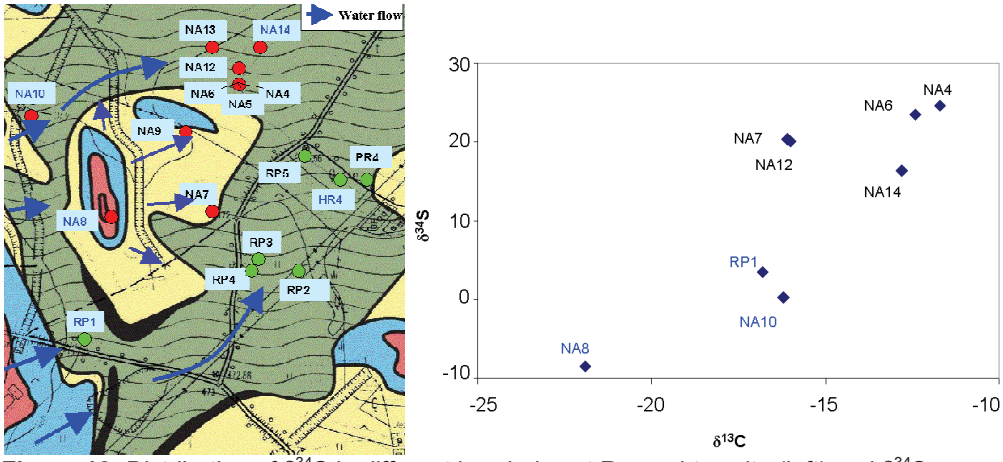

Figure 12: Distribution of $\delta^{34}S$ in different boreholes at Ruprechtov site (left) and $\delta^{34}S$ vs δ13C (right)

5 CONCLUSIONS AND OUTLOOK

Ruprechtov site is a good example to demonstrate that tertiary argillaceous sediments can exert a strong barrier function for uranium migration, when specific prerequisites are fulfilled. Major uranium transport occurred over distances of about tens to max. some 100 m only during Tertiary. Uranium was transported as U(VI) and was reduced in a lignite rich clay horizon with occurrence of pyrite and arsenopyrite minerals. It was immobilised by forming uraninite, and phosphate bearing minerals like ningyoite. There is no evidence of uranium mobilisation during the last million years. But there is indication that still during the last several 100'000 years further uranium enrichment occurred in this lignite rich clay horizon. This is probably due to transport from underlying granite through zones of low kaolin thickness and/or fault zones. The uranium concentrations in groundwater of the clay/lignite-sand horizon are low in the range of 0.5 µg/l although this horizon is only 25 to 65 m below the surface.

There are still several open questions to be answered at Ruprechtov site. In the frame of the integrated project FUNMIG, which is carried out from 2005 until 2008, some of these questions are addressed (e.g. role of organic matter, immobile uranium phases). Further interest is also given to an easier accessible uranium phase, which makes up about 10-20 % of uranium in the enriched horizon and probably represents a uranium(VI) phase, which is sorbed to organic material. This will be investigated by optimization of the U(IV)/U(VI)-separation method and application to further samples. All analyses of immobile uranium phases will be accompanied by further specific sequential extraction methods and specific uranium desorption (exchange) measurements with the non-naturally occurring 236U tracer. Application of surface complexation models are planned to quantify the sorption process.

It is still not proved that the current model assumptions are complete and describe all relevant processes. The recently started kaolin open cast mining now offers the unique chance, to review the state of knowledge concerning genesis of uranium accumulation and model assumptions by a large-scale and 3-dimensional exposure of geological conditions of

the site and therewith allows the proof of assumptions and amendment of model assumptions (if necessary). Furthermore, the scientific attendance of kaolin mining with its alterations of hydrogeological and hydrogeochemical conditions enables the investigation of the impact of such sudden changes (especially redox potential and pH- value) on the mobility of uranium and – in addition – may give hints on the demand of investigations needed to characterise a potential site for geological disposal of radioactive waste. Thus, it could help to improve the public acceptance of long-term safety assessments also.

References

[1] Noseck, U., Brasser, Th. & Pohl, W.: Tertiäre Sedimente als Barriere für die U-/Th-Migration im Fernfeld von Endlagern.- GRS-176, 295 S., Köln, 2002.

[2] Noseck, U. & Brasser, Th.: Radionuclide transport and retention in natural rock formations – Ruprechtov site.- GRS-218, 157 S. + CD, Köln, 2006.

[3] Denecke, M.A., Janssens, K., Proost, K., Rothe, J. & Noseck, U.: Confocal Micrometer-Scale X-ray Fluorescence and X-ray Absorption Fine Structure Studies of Uranium Speciation in a Tertiary Sediment from a Waste Disposal Natural Analogue Site.- Environ. Sci. Technol. 39 (7), pp. 2049-2058, 2005.

[4] Havlová, V. & Laciok, A.: Geochemical study of uranium mobility in tertiary argillaceous system at Ruprechtov site, Czech Republic. Czech Journal of Physics, Vol. 56, Suppl. D, 2006.

[5] Hammer, Ø., Harper, D.A.T. & Ryan; P.D.: PAST: Paleontological statistical software package for education and data analysis.- Palaeontological Association, 2001.

[6] Sulovsky, P.: Mineralogy on the site. Expert report by the faculty of natural sciences of Masaryk university, Brno (under the authority of NRI, Řež), 2004.

[7] Suksi, J., Noseck, U., Fachinger, J. & Salminen, S.: Uranium Redox State and $^{234}U/^{238}U$ Ratio Analyses in Uranium Rich Samples from Ruprechtov Site.- Proceedings of the 2nd Annual FUNMIG Workshop, Stockholm, Sweden 21.11-23.11.2006.

[8] Buckau G. et al.: Groundwater in-situ generation of aquatic humic and fulvic acids and the mineralization of sedimentary organic carbon.- Applied Geochemistry, 15, pp. 819-832, 2000.

[9] Červinka et al.: Report on natural radioelements U(VI) sorption and complexation properties of immobile OM extracted from real site conditions.- PID2.2.15 FUNMIG report, submitted, 2007.

[10] Sutton, S. & Sposito, G.: Molecular simulation of humic substance–Ca-montmorillonite complexes.- Geochimica et Cosmochimica Acta, 70, pp. 3566-3581, 2006.

Acknowledgements

The work was funded by the German Federal Ministry of Economics and Technology (02E9551, 02E9995), RAWRA, EC (IP FUNMIG) and the Czech Ministry of Trade and Industry (POKROK 1H-PK25)

[V.]
NOSECK, U., BRASSER, TH., SUKSI, J., HAVLOVA, V., HERCIK, M., DENECKE, M.A., FÖRSTER, H.J. (2008):

Identification of Uranium enrichment scenarios by multi-method characterisation of immobile Uranium phases.

J. Phys. Chem. Earth, Vol. 33, Issue 14-16, 961-977.

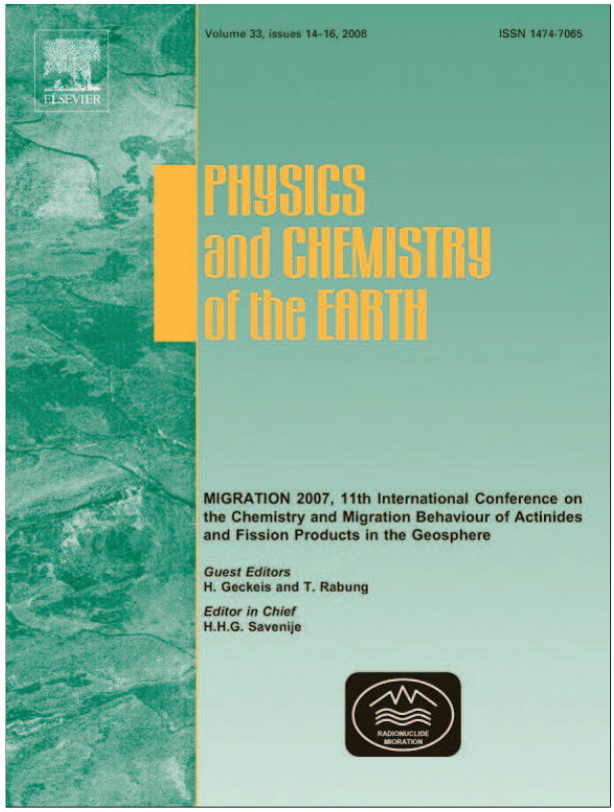

Physics and Chemistry of the Earth 33 (2008) 969–977

Contents lists available at ScienceDirect

Physics and Chemistry of the Earth

journal homepage: www.elsevier.com/locate/pce

Identification of uranium enrichment scenarios by multi-method characterisation of immobile uranium phases

Ulrich Noseck [a,*], Thomas Brasser [a], Juhani Suksi [b], Václava Havlová [c], Mirek Hercik [c], Melissa A. Denecke [d], Hans-Jürgen Förster [e]

[a] Gesellschaft für Anlagen-und Reaktorsicherheit (GRS) mbH, Theodor-Heuss-Str. 4, 38122 Braunschweig, Germany
[b] University of Helsinki, Department of Chemistry, P.O. Box 55, 00014 University of Helsinki, Finland
[c] Nuclear Research Institute (NRI), 250 68 Řež, Czech Republic
[d] Forschungszentrum Karlsruhe, Institut für Nukleare Entsorgung, P.O. Box 3640, 76021 Karlsruhe, Germany
[e] University of Potsdam, Institute of Earth Sciences, P.O. Box 601553, 14415 Potsdam, Germany

ARTICLE INFO

Article history:
Available online 10 June 2008

Keywords:
Natural analogue
Hydrogeology
Uranium
Enrichment

ABSTRACT

We investigate natural uranium occurrences as analogues for uranium migration and immobilisation in the post-operational phase of a radioactive waste repository. These investigations are aimed at gaining insight into the behaviour of uranium in a complex natural system. We characterise the immobile uranium phase and trace elements distributions in argillaceous uranium-rich samples from the Ruprechtov site, Czech Republic, applying a combination of different analytical methods. We use wet chemistry to determine the distribution of U(IV) and U(VI), sequential extraction to characterise different uranium phases, and $^{234}U/^{238}U$-activity ratios to correlate results between U(IV) and U(VI) distributions and the various uranium phases. Most of the uranium was determined to occur in a very long-term stable, tetravalent phase. Results from chemical methods are in good agreement with the results from spectroscopic methods. U(IV) mineral phases are identified by SEM–EDX spectroscopy and synchrotron-based μ-EXAFS. Electron-microprobe analysis confirmed that uraninite is newly formed and not a relictic phase from the altered granite. Correlation of uranium with As(V) located on thin As-rich layers on pyrite surfaces determined by confocal μ-XRF supports element correlations obtained by the sequential extraction. The key processes involved in uranium immobilisation in the argillaceous layers have been identified and can be used to reconstruct the geological history at the site.

1. Introduction

The Ruprechtov site, located in the north-western part of the Czech Republic, is geologically situated in a Tertiary basin, which forms part of the Ohře rift (Noseck et al., 2004; Noseck and Brasser, 2006). The study area itself is characterised by a granite, which partly crops out in the west and in the south, but is covered by kaolin layers of varying thickness (up to several tens of metres) in the central part. Large parts of the basin are overlain by pyroclastic Tertiary sediments. A multi-method study of these, now argillised sediments – in combination with lignitic intercalations and uranium enrichments close to such intercalations – permitted to gain a better understanding of the complex interrelations between transport and retention of radionuclides in argillaceous media with considerable amounts of organic matter under natural conditions, especially on very long-term scales relevant for performance assessment.

The interface between the kaolinised granite and the overlain pyroclastic sediments mimics the surface of the region in Tertiary time. Its strong morphology, i.e. former humps and hollows, is still preserved underground, with variations in altitude of more than 60 m. The horizon of major scientific interest is a clay/lignite layer at this interface at hollow positions, with a high content of sedimentary organic carbon (SOC), zones of uranium enrichment, and local zones of higher hydraulic conductivity (Noseck and Brasser, 2006). The occurrence of pyrite and siderite reflects the reducing conditions in this horizon containing up to 400 ppm U.

Previous investigations identified the sources of uranium and its transport pathways (Noseck et al., 2004). Adopting the strategy of combining analytical methods, as described subsequently in this paper, enables understanding of, and differentiating between individual uranium enrichment mechanisms at the site and provides information about their age and duration and the long-term stability of the respective uranium-bearing phases.

2. Experimental

Fig. 1 shows a sketch of the area and the location of the boreholes, from which drill-core samples have been collected for

* Corresponding author. Tel.: +49 531 8012247; fax: +49 531 8012200.
E-mail address: ulrich.noseck@grs.de (U. Noseck).

1474-7065/$ - see front matter © 2008 Elsevier Ltd. All rights reserved.
doi:10.1016/j.pce.2008.05.018

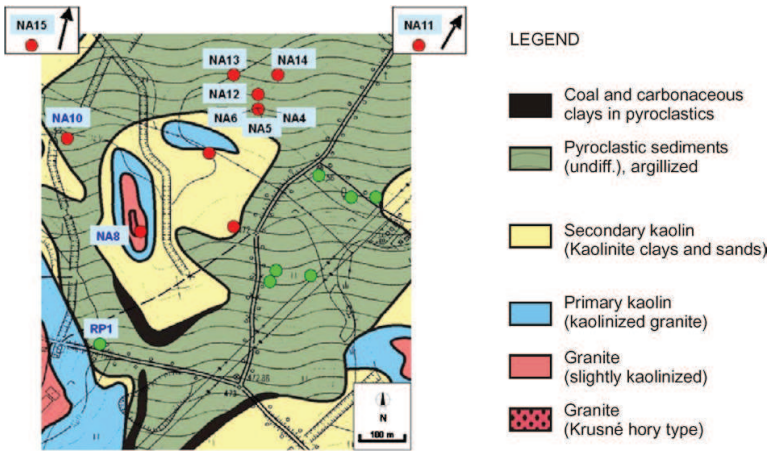

Fig. 1. Location of the boreholes, from which the core samples used in this paper were collected. NA11 and NA15 are approx. 1 km outside of the depicted area, in the north and north-east, respectively.

analyses. RP1, NA8, and NA10 are boreholes located in the outcropping granite, in the western and south-western part of the study area. The clay/lignite samples originate from the northern and north-eastern part of the area. Due to the morphology of the kaolin and underlying granite the depth of the uranium enriched clay/lignite layers varies between approx. 10 m and 60 m, as indicated by the gamma spectra for the drill-cores in Fig. 2.

Different macroscopic and microscopic methods, summarised in Table 1, have been applied to samples from the boreholes and are briefly described here.

2.1. U series measurements

U series disequilibrium measurements were performed to date bulk U accumulations. The sample material was dissolved in boiling concentrated HNO_3. ^{238}U, ^{234}U and ^{230}Th were analysed applying both liquid–liquid extraction and ion exchange methods. Radionuclide concentrations were measured by α-spectrometry.

2.2. U(IV)/U(VI)-separation and $^{234}U/^{238}U$-activity ratios

The oxidation states U(IV) and U(VI) were determined using a method slightly modified from that presented in Ervanne and Suksi (1996). U(IV) and U(VI) phases were dissolved simultaneously by extracting the sample material in anoxic conditions with a mixture of 4 M HCl and 0.03 M HF under Ar atmosphere for 10 min. The solid to solution ratio was adjusted to about ~0.1. Uranium dissolution was intensified by performing extractions in an ultrasonic bath, while mixing the solution with Ar bubbling. Uranium was not totally dissolved during the extraction; the dissolution yield

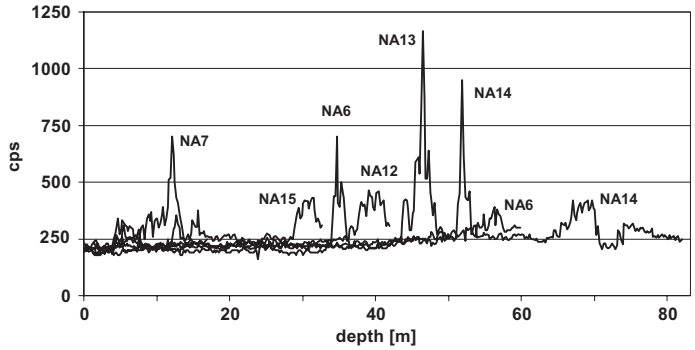

Fig. 2. Uranium concentrations in different drill-cores detected by the on-site gamma log with a differential gamma ray spectrometer.

Table 1
Different methods applied to clay/lignite samples from different boreholes

Method applied	NA4	NA5	NA6	NA11	NA12	NA13	NA14	NA15
U series measurement	×	×	×	×	×	×	×	×
$^{234}U/^{238}U$-activity ratios			×	×	×	×	×	×
U(IV)/U(VI)-separation			×	×	×	×	×	×
Sequential extraction				×	×	×	×	×
ASEM	×	×	×					
Electron microprobe	×		×					
μ-XRF, μ-XAFS	×		×					

varied between 50% and 90%, indicating the presence of U-bearing minerals resistant to the used acid mixture. The extraction solution containing dissolved U(IV) and U(VI) was fed into a Dowex 1x4 (in Cl-form) anion-exchange column, which was regenerated with the same solution used for extraction. U(IV) passes the column, whereas U(VI) is retained. U(IV) was collected in the first 20 ml and U(VI) then eluted with 20 ml of 0.1 M HCl. Separation is quantitative and no overlap of U(IV) and U(VI) fractions has been observed in the tracer experiments. Uranium concentrations in the U(IV) and U(VI) fractions were determined using the procedure described in the context of U series measurements.

2.3. Sequential extraction

Sequential extraction (SE) is a widely used tool for studying the geochemical distribution of elements (e.g., Tessier et al., 1979; Percival, 1990; Havlová and Laciok, 2006). In practice, operationally defined phases and their elemental content are dissolved and separated with specific reagents. The following SE scheme was applied to the Ruprechtov samples from the clay/lignite horizon:

1. U bound onto exchangeable sites (leaching with 1 M $MgCl_2$ for 1 h, pH 4–5).
2. U bound to carbonates (leaching with 1 M ammonium acetate in 25% acetic acid for 5 h, pH 4.8).
3. U associated with Fe/Mn oxides (leaching with 1 M hydroxylamine hydrochloride in 25% acetic acid for 12 h, pH 2).
4. U as U(IV) and/or onto organic matter (leaching with 30% H_2O_2 and 0.02 M HNO_3 for 5 h, continuously heating, pH 2).
5. U in residuum (boiling with 8 M HNO_3) at least for 2 h).

In each step the solid residuum and the leachate were separated by 4000 rpm centrifugation for 10 min. The uranium content in the leachate solutions was determined by ICP-MS. Multi-element analyses (Na, K, S, Fe, As, P) of SE leachates were performed for two samples (NA14 and NA15), in order to better define the phases dissolved in each extraction step. A statistical procedure, i.e. cluster analysis, was used to identify possible correlations between elements and the dissolving/leaching phases of the sediment (Denecke and Havlová, 2006).

2.4. ASEM and electron microprobe

Analytical scanning electron microscope (ASEM) observations were made using a ESEM-XL30TMP (Philips/Fei) instrument scanning electron microscope equipped with an EDAX detector. Quantitative analyses of accessory minerals were performed using CAMEBAX SX-50 and SX-100 electron microprobes operating in the wavelength-dispersive mode. The operating conditions during analysis of accessory minerals were as follows: accelerating voltage 20 kV, beam current 40–60 nA, and beam diameter 1–2 μm. Counting times, data reduction, analyzing crystals, standards, analytical precision and detection limits are described in detail in Förster (1998a,b).

2.5. μ-XRF/μ-XAFS

The main feature of the set up used is two polycapillary halflenses in a confocal geometry. This confocal set up allows probing defined volumes below the surface of the sample with a μm-scale resolution. By scanning arbitrary sample areas (x, y scans) at different depths (z), stacks of tomographic cross-sections can be recorded. A detailed description of the method is given by Denecke et al. (2005).

Micro-X-ray fluorescence (μ-XRF) measurements, using a band pass of wavelengths, are made at the Fluo-Topo Beamline (ANKA) and at Beamline L (HASYLAB). Monochromatic X-rays are used for collecting some μ-XRF data and all micro-X-ray absorption fine structure (μ-XAFS, consisting of XANES and EXAFS) spectra at Beamline L. The measurements focused on uranium hot spots identified previously by autoradiography. All results reported in this paper originate from core samples of the U-enriched horizon in borehole NA4 and NA6.

3. Results and discussion

3.1. U series activity ratios and U(IV)/U(VI)-separation

Uranium series data are presented in the form of a Thiel's diagram (Thiel et al., 1983), which is generally used to interpret U series disequilibria (Fig. 3). The diagram is divided into segments determined by (i) the $^{234}U/^{238}U$ equilibrium line (i.e. AR = 1) and (ii) the line obtained when a tangent is drawn on the closed system chain decay curves evolving towards radioactive equilibrium ($^{230}Th/^{238}U = 1$ and $^{234}U/^{238}U = 1$) after sudden accumulation and removal of U. The segments S1 and S2 between the U addition and removal areas represent U series disequilibria, which cannot be created by closed system chain decay. Data plots in segment S1 are interpreted to represent an open system, where selective ^{234}U removal is favoured. U series disequilibria determined by the segment S2 are interpreted to represent an open system affecting bulk U. Data plots in this segment represent samples with recently accumulated U (within the last million years) and subsequent U removal.

Most of the data points plot in segment S1, indicating stable conditions with respect to bulk U. The ages of U phases in the respective samples are beyond the U series method. Thus, at least a significant fraction of U in the clay/lignite horizon is more than one million years old. The number of data points in the bulk U addition area indicates that some U accumulation is still in progress. In order to better characterise the different U forms and to distinguish between U valencies, different separation methods were applied.

U(IV)/U(VI)-separation was performed on four samples from three different boreholes (NA6, NA13, NA14). Two samples were taken from borehole NA6, one from the major U-peak at 35 m depth and one from a second, smaller peak at 37 m depth. The other two

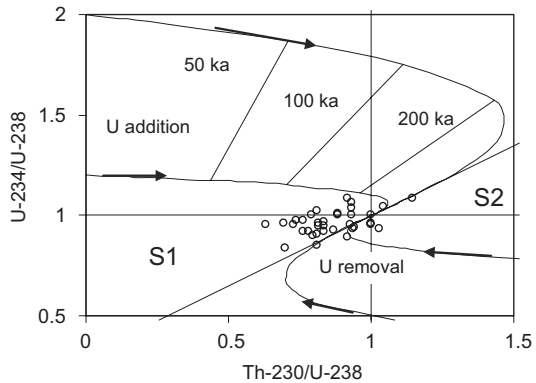

Fig. 3. $^{230}Th/^{238}U$ and $^{234}U/^{238}U$-activity ratios of bulk samples from the clay/lignite horizon plotted in Thiel's diagram, with isochrones. Curves started from $^{230}Th/^{238}U = 0$ and $^{234}U/^{238}U = 1.2$ and 2 in the U addition area have been taken as examples to show how activity ratios change as a function of time in the closed system after sudden U accumulation with the $^{234}U/^{238}U$-activity ratios 1.2 and 2. Curves in the U removal sector describe changes in isotope ratios back to secular equilibrium after sudden U removal. Segments S1 and S2 between U removal and addition areas represent open system (see text).

Table 2
Amount of uranium and $^{234}U/^{238}U$-activity ratios in the different phases from U(IV)/U(VI)-separation

Sample	U (ppm)	U(IV)		U(VI)		U(res)	
		(%)	$^{234}U/^{238}U$	(%)	$^{234}U/^{238}U$	(%)	$^{234}U/^{238}U$
NA6-35a	356±7	28.7	0.54±0.01	41.9	1.42±0.02	29.5	0.65±0.01
NA6-35b	468±9	45.9	0.56±0.01	33.3	1.69±0.03	20.7	0.64±0.02
NA6-35c	369±8	23.3	0.47±0.01	47.4	1.16±0.02	29.3	0.67±0.01
NA6-37a	37.3±2	73.7	0.79±0.03	15.7	2.66±0.07	10.6	0.73±0.01
NA6-37b	47.5±2	66.2	0.52±0.01	9.0	3.37±0.15	24.8	0.86±0.02
NA6-37c	35.7±2	51.3	0.58±0.01	19.8	2.56±0.08	28.9	0.71±0.04
NA13-46	216±5	5.8	0.53±0.02	43.9	1.15±0.02	40.3	0,55±0.01
NA14-51	354±9	25.5	0.88±0.02	39.5	1.28±0.02	35.0	0.54±0.01

U(res) is assumed to be U(IV) (see text for explanation).

samples were taken from depths with the highest U concentration in boreholes NA13 and NA14. The distance between each borehole is approx. 50 m.

The U(IV)/U(VI)-separation results are listed in Table 2. The analytical error of the measured activity ratios (denoted AR) is usually in the range of 1–5%, and only in exceptional cases up to 10%.

The total U concentration in the samples ranges from 35 to 468 ppm, with the lowest concentration in sample NA6, from a depth of 37 m (35–48 ppm). In all other samples, U concentrations are significantly higher, with the largest value of 468 ppm in NA6 from 36 m depth. We observe that U in the core samples consists of both U(IV) and U(VI). Note that the extraction does not dissolve all U. The U content in this insoluble phase is denoted as U(res).

The $^{234}U/^{238}U$-AR differs significantly in the U(IV) and U(VI) phases, with ratios <1 in the U(IV) phase and ratios >1 in the U(VI) phase. The AR of the U(res) phase is similar to that observed in the U(IV) phase. Taking into account the higher stability of U(IV) phases, we suppose that U(res) exists as a stable mineral phase in oxidation state IV. Most U in all samples is U(IV), with fractions between 52 and 90 wt.%. The largest U(IV) fraction is found in sample NA6-37, which also displays the lowest total U concentration.

That U(res) and U(IV) exhibit an AR below one is a strong indicator for their stability. AR values significantly below unity are caused by the preferential release of ^{234}U, which is facilitated by α-recoil process and subsequent ^{234}U oxidation (e.g., Suksi et al., 2006). In order to attain low AR values of approx. 0.5 in the U(IV) phase, the phase must have been stable for a sufficiently long time, i.e. no significant release of bulk U has occurred during the last million years. This is in agreement with the hypothesis that the major U input into the clay/lignite horizon occurred during the Tertiary, more than 10 million years ago (Noseck and Brasser, 2006). The prevailing groundwater conditions, with low Eh values especially in the clay/lignite horizon of borehole NA6, is another indication that stable, insoluble U(IV) phases such as uraninite can be expected under the present physicochemical conditions (cf. Section 4).

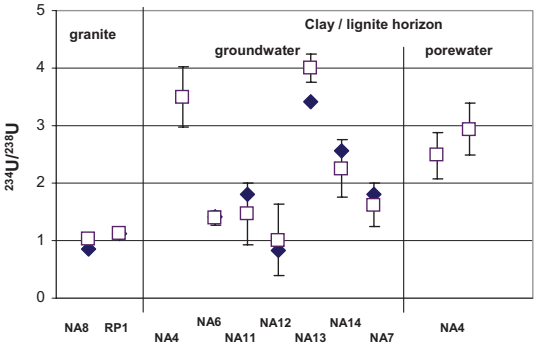

Fig. 4. $^{234}U/^{238}U$-activity ratios in groundwater from outcropping granite boreholes with high water flow and from groundwater/pore-water from the clay/lignite horizon measured by α-spectrometry (open symbols) and ICP-MS (filled symbols).

The AR in groundwater generally reflects the nature of water–rock interaction and is, therefore, sensitive to groundwater conditions (see Suksi et al., 2006). At oxidising conditions, both isotopes are released into the groundwater in the ratio they have in the U source. At anoxic conditions, where the bulk U release is strongly suppressed, the release of the more mobile ^{234}U(VI) is favoured. The low AR in the U(IV) phase observed in this study is correlated with AR values >1 in pore and groundwater from the clay/lignite horizon (Fig. 4). This is expected because of the anoxic sediment conditions and preferred mobilisation of ^{234}U.

3.2. Sequential extraction

The distribution patterns of U obtained from the five SE steps are illustrated in Fig. 5. All samples stem from the clay/lignite horizon at the interface kaolin/pyroclastic rock and show remarkable similarities in that all released only a small amount of U in step 1 and step 3 leachates. The leachates from the first three steps always contain less than 25% of the total U. The major portion of U in these samples is associated with the U(IV)/organic matter and/or the residual phase. In samples NA12, NA14A and NA14B, U leached in step 4 makes up nearly 70% of total U. NA11 is exceptional in that more than 70% of its U content is associated with the residual phase.

Results of Na, K, S, Fe, As, and P analyses in the leachates from each extraction step are evaluated by cluster analysis with the programme PAST (Hammer et al., 2001), in order to more accurately characterise phases and U forms dissolved in each extraction step. The results, shown in Fig. 6, reveal that in both samples, P, As and U are assigned into one group. This is in close agreement with the results from μ-XRF and μ-XAFS measurements shown below. Fe and S are not correlated with U, i.e. there is no evidence for U dependence on Fe and S, although high contents of those two elements are observed in the sediment. As a large amount of K is leached in step 2, alumosilicates or carbonate complexes are likely more responsible for U distribution than are carbonate minerals.

The results from the SE study correlate with U(IV)/U(VI)-separation results, where the major part of U was identified to be associated with the U(IV) phase. In order to confirm that U in steps 4 and 5 is really in the tetravalent state, analyses of AR in the different SE leachates from sample NA13 were performed. The analyses were limited to the leachates from steps 1, 2, 4 and 5, since the U content in the third step is too low, <3% of total U. The results are shown in Fig. 7. The AR in steps 1 and 2 are quite similar, with values of approx. 1.75. Upon comparing this value with results from U(IV)/U(VI)-separation we conclude that U extracted in these first two steps is U(VI). In contrast, the $^{234}U/^{238}U$-AR in leachates from

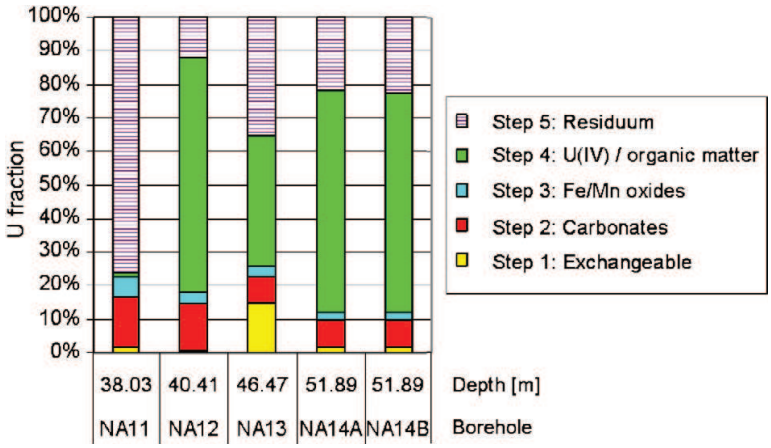

Fig. 5. Uranium content in the five fractions of the different samples from the clay/lignite horizon (borehole depth of each sample is indicated).

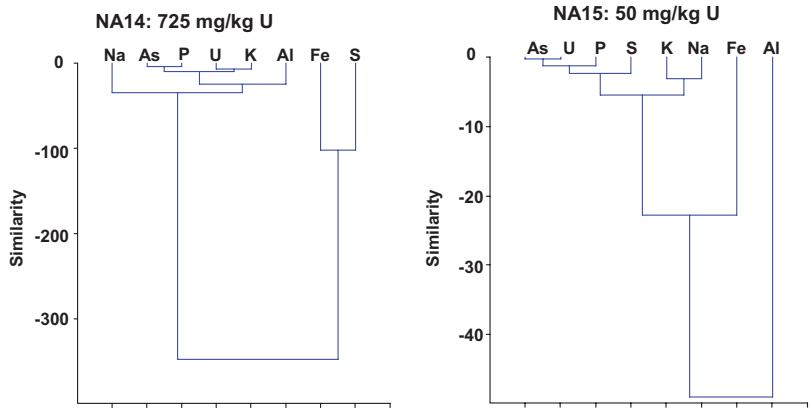

Fig. 6. Cluster analyses for extended SE results of samples from the boreholes NA14 and NA15.

steps 4 and 5 are around 0.5 to 0.6, which matches well the AR values observed in the U(IV) and U(res) fractions from U(IV)/U(VI)-separation. This correspondence confirms that U extracted in steps 4 and 5 is U(IV).

The amount of U(VI) determined by the two methods differs. From U(IV)/U(VI)-separation, 44% of U(VI) was obtained, whereas U extracted by steps 1 and 2 consists of only 22.5% U(VI). One possible explanation for this discrepancy is that part of the U(IV) was oxidised during the U(IV)/U(VI)-separation. We expect such an oxidation to affect a AR decrease in the U(VI) phase by dilution with U(IV) originally having a lower AR. The lower 1.2 AR value observed in the separation, compared to values of 1.75 and 1.76 from SE steps 1 and 2, might be an indication that partial oxidation of U(IV) to U(VI) actually occurred. In order to confirm this supposition, a systematic study on the U redox states during U dissolution is under way.

3.3. Microscopic methods

No U(VI)-bearing mineral phase was observed in the sediment by means of any of the applied microscopic methods. The U-bearing minerals identified by ASEM, in combination with electron microprobe, are monazite, zircon, xenotime, uraninite and ningyoite. Monazite–(Ce) (nominally $CePO_4$) is the most frequent actinide-bearing mineral in all samples. Most monazite occurs as angular grains up to 25 μm in diameter. The grains are often fractured and regions along fractures appear darker in BSE images than the unfractured portions of grains (Fig. 8). The angular shape of the monazite grains, including shards, suggests that the grains are broken fragments of larger crystals.

Xenotime–(Y), containing Th and U in concentrations (in wt.%) $0.06 < ThO_2 < 1.18$ and $0.89 < UO_2 < 3.93$, occurs in all sediment sections in minor amounts. It forms overgrowths on zircon or independent grains usually less than 20 μm in size. The REE contents and patterns of xenotime from the sediment are indistinguishable from that in the underlying granite of the same borehole.

The similar composition of xenotime, monazite and zircon in the clay/lignite horizon and in the granite, as well as the angular shape of a large number of mineral grains, indicate that they are primary minerals of detritic origin. The determined U/Th-ratios indicate that less than 10% of the U in the enriched clay/lignite horizon is associated with primary minerals monazite, xenotime and zircon. The bulk of the uranium must, therefore, be associated with secondary U-minerals.

Ningyoite and uraninite have been identified as secondary minerals in samples NA4, NA5 and NA6 characterised by a high

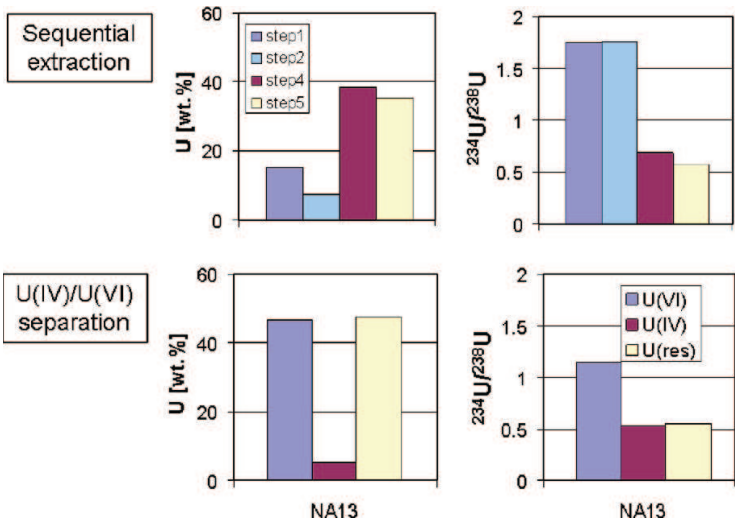

Fig. 7. Uranium content and $^{234}U/^{238}U$-activity ratios in SE leachates from steps 1, 2, 4 and 5 (top), compared to U(IV), U(VI) and U(res) fractions (bottom) in sample NA13.

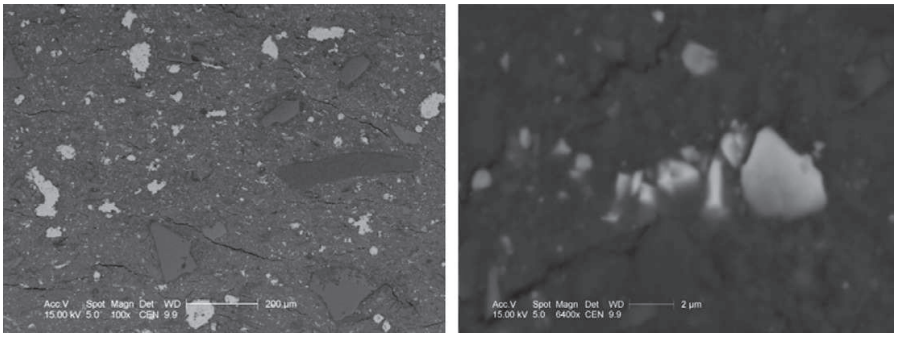

Fig. 8. Image of monazite grains in the sample from 36 m of borehole NA6.

U content. To ascertain whether uraninite is really of secondary nature, two single, idiomorphic grains ($8 \times 8\,\mu m$ in size) from the clay/lignite horizon in NA6 were probed by electron microprobe. These grains exhibit a near-endmember composition and containing only traces of Si, Ti, and Al. Whether these three elements form part of the mineral structure or represent analytical artefacts from adjacent phases is impossible to resolve. The most important chemical feature of the uraninite in sample NA6 is that Th, Pb and (Y+REE) are present in amounts below their detection limits. This is distinctly different from the composition of the uraninite in the deeper, non-kaolinised granite, which contains several oxide weight percentages of Th and Pb, Y-contents (0.1–0.3 wt.%) and yields a Th–U–total Pb age of 315.1 ± 2.8 Ma (2σ STDW), in accordance with the age of other Erzgebirge granites of similar composition. These compositional differences are an unequivocal indication that the clay/lignite horizon uraninite is of secondary nature.

3.4. μ-XRF and μ-XAFS

Confocal μ-XANES results show uranium to be present in the tetravalent state and μ-EXAFS indicates the existence of a tetravalent uranium phosphate/sulphate phase (Denecke et al., 2005). The analyses of a number of tomographic cross-sections of elemental distributions recorded over different sample areas show a strong positive correlation between U and As. From μ-XANES measurements at the As K-edge at numerous sample positions, the presence of As(0) and As(V) was established. Furthermore, analysis of tomographic cross-sections of Fe, As(0), As(V), and U distributions reveal a correlation between As(V) and U and a linear correlation between As(0) and Fe. U and Fe are not correlated (Denecke et al., 2007). The linear correlation between As(0) and Fe shows that both components must be incorporated into the same mineral, implying the presence of arsenopyrite in the sample. This is confirmed by the observed similarity between As K XANES for arsenopyrite and that observed in As(0)-rich portions of the sediment. Further indication of the presence of arsenopyrite is seen in elemental distribution maps recorded with a high lateral resolution, where an As-rich boundary layer or rim surrounding framboidal Fe nodules is observed. Uranium occurs in immediate vicinity of these As-rich boundary layers.

From these results, a hypothesis for one of the driving mechanisms for uranium-enrichment by secondary uranium(IV) minerals in the sediment is elaborated. The arsenopyrite in the sediment reduced the mobile, groundwater-dissolved U(VI) to less-soluble U(IV), thereby immobilising the uranium in the sediment. As a

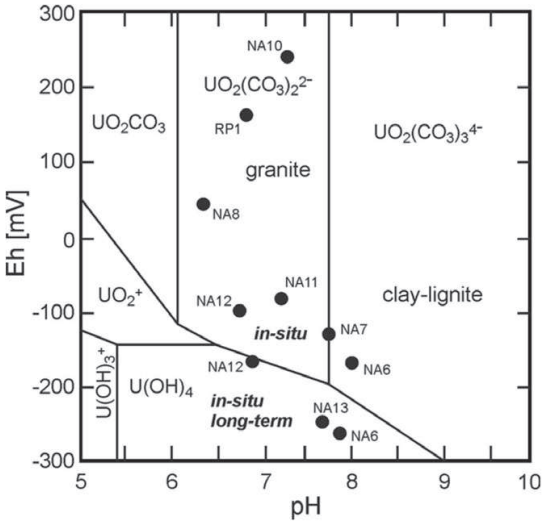

Fig. 9. pH–Eh-phase diagram of aqueous uranium species. The dots represent groundwater measurements and illustrate the differences in the geochemical environment between granite and the clay/lignite horizon.

consequence, As(V) was formed. Uranium, therefore, is associated with As(V). These findings are consistent with that from extended SE analysis described above.

4. Geochemical conditions in the clay/lignite horizon

The Ruprechtov groundwaters are generally low mineralised, with ionic strengths in the range of 2×10^{-3} and 2×10^{-2} mol/l. Groundwaters from the clay/lignite horizon are of the Ca–HCO_3-type, whereas groundwaters from the granite are from the Ca–SO_4-type. The geochemical conditions in the clay/lignite horizon are further characterised by low Eh-values and pH-values between 7 and 8 (Fig. 9), whereas the granite waters are more oxidising, with pH-values slightly below 7. These conditions are reflected by low U concentrations in the range of approx. 5×10^{-10}–5×10^{-9} mol/l in the water from clay/lignite horizons and concentrations up to 5×10^{-8} mol/l in the granite water. Geochemical calculations with PHREEQC show that U concentrations in the clay/lignite horizon are likely controlled by amorphous uraninite (Noseck and Brasser, 2006).

Laboratory data suggest that indigenous sulphur-reducing bacteria, extracted from samples taken at the site, helped maintain the redox potential at a level promoting reduction of U(VI) to U(IV) (Abdelous et al., submitted for publication). It seems that the bacteria have most likely played a role during formation of sulphide minerals, such as pyrite, which are frequently observed in the clay/lignite layers at the site. The reduction of sulphates to sulphides resulted in the formation of pyrite. Fig. 10 is an image of framboidal pyrite, whose shape suggests mineral growth by activity of microbes.

5. Integration of results: uranium enrichment scenario

Integration of all available information from our multi-method analyses, combined with current knowledge of the geological development of the site (Noseck and Brasser, 2006) results in the following scenario for U enrichment at the Ruprechtov site. Detrital input of U-bearing minerals (monazite, zircon, xenotime) predate the kaolinisation of the granite and is older than 30 Ma. During the Lower Oligocene and Miocene (30–16 Ma), the major volcanic activity occurred and deposited tuffaceous material in the basins. The alteration of granite to kaolin, i.e. by reaction of CO_2 with feldspars, and the argillisation of the tuffaceous material took place during this period. Microbial activity in the clay/lignite horizon led to the reduction of dissolved sulphate by sulphate-reducing bacteria, thereby leading to the formation of pyrite nodules. Sorption of As and subsequent formation of arsenopyrite occurred on the surface of the pyrite nodules. In this period, CO_2-rich water likely initiated U release from accessory minerals in the granite by formation of soluble uranyl-carbonate complexes. Uranium transported into the clay/lignite horizon accumulated there by reduction of U(VI) to U(IV). One important reaction, which could be traced back until today, was the reduction of U(VI) by thin arsenopyrite layers on pyrite nodules formed by microbial sulphate reduction. Probably, microbial degradation of organic matter in the clay/lignite horizon caused phosphate release into the groundwater. This process is likely still active today (Noseck et al., in preparation). The increased phosphate concentrations caused the precipitation of U as secondary phosphate minerals, e.g., ningyoite. Secondary uraninite might have formed at later stages of the geological history at conditions of lowered U concentrations, where saturation of ningyoite was no longer maintained.

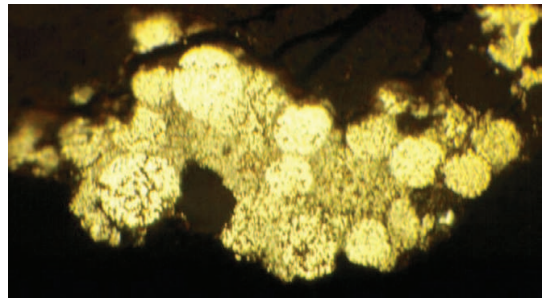

Fig. 10. Microphotograph of framboidal pyrite in the clay/lignite horizon.

The U series disequilibria results show that transport and immobilisation of U in the clay/lignite layers continued following the major input of U during the Tertiary. This, more recently enriched U seems to occur partially in the U(VI) state. However, we have not yet been able to identify the form of this U. We assume that it occurs adsorbed on clay or organic material.

The potential impact of these processes on AR in the sediment and groundwater in the clay/lignite horizon is illustrated in Fig. 11. We assume that at the time of major U input during the late Tertiary (>10 Ma), the AR in the infiltrating groundwater was unity, as it is today. Inflowing U(VI) was reduced at that time in the clay/lignite horizon and precipitated as secondary mineral phases. Therefore, the immobile U(IV) phase formed had the same ratio of unity.

Due to α-recoil related processes over a time frame of several million years, selective leaching of ^{234}U decreases the AR in the stable secondary U(IV) phase. The preferred mobilisation of ^{234}U for ^{238}U also leads to an AR increase in the pore-water and in the groundwater-bearing layers, with low flow velocity in the clay/lignite horizon. The AR in the pore-water and groundwater-bearing layers is also affected by slow inflow of water from the infiltration area, containing U with AR around 1. Typical AR values in the clay/lignite horizon are in the range between 1.5 and 4. Similar values are found in the more accessible U fractions in the immobile phase,

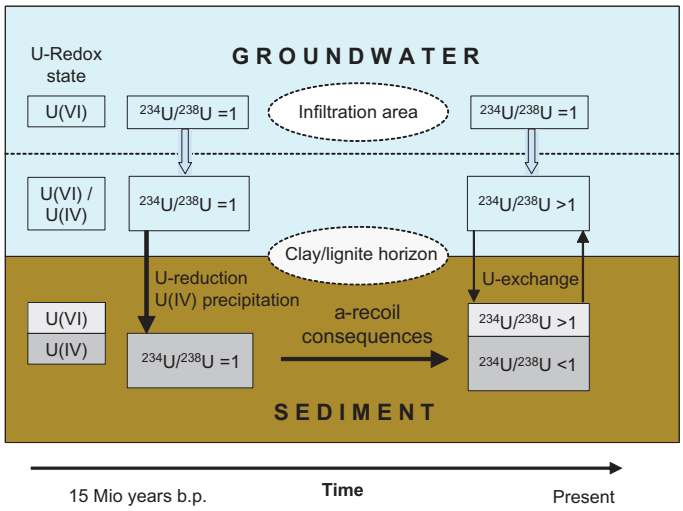

Fig. 11. A model for the development of the $^{234}U/^{238}U$ AR in the groundwater-sediment-U system in the clay/lignite horizon. The uranium redox state in each component is shown in the boxes on the left. ARs (boxes) in dissolved and immobile phases in the clay/lignite horizon are affected by inflow of water from the infiltration area (open arrows), mobilisation/immobilisation processes and consequences of α-recoil processes (closed arrows) during the very long time frames (see text).

which have been more recently accumulated in the clay/lignite horizon.

6. Conclusions and outlook

The paper shows the great potential of combining macroscopic and microscopic methods to provide insight into the U enrichment processes at the Ruprechtov site, and at similar sites elsewhere. Microscopic methods aided in identifying important mineral phases and their origin, i.e. primary minerals of detrital origin or secondary minerals. Detailed X-ray spectroscopic investigations with a micro-focussed beam identified U as a tetravalent phosphate or sulphate mineral phase, in good agreement with ASEM and electron-microprobe results. Furthermore, the spatial distribution of elements and element correlations, i.e. Fe with As(0) and U with As(V), have revealed one important immobilisation mechanism of U(VI) by reduction to U(IV) on arsenopyrite layers formed on pyrite surfaces.

The results from microscopic methods are supported by cluster analysis of sequential extraction results, demonstrating the correlation of U with As and P. Furthermore, U(IV)/U(VI)-separation and SE, coupled with analysis of AR in each phase, identified that the major part of U occurs in the tetravalent state, in agreement with results from spectroscopic methods. It was established that the U(IV) phase remained stable over geological times under the reducing conditions in the clay/lignite horizon. Additionally, an easier accessible fraction of U(VI) was identified in the clay/lignite horizon, which was formed more recently.

To separate U(IV) and U(VI), a wet chemical method was applied for the first time to the samples from Ruprechtov site. The results are very promising, but the quantification of U(IV) and U(VI) phases using the separation method needs to be assessed, to ascertain if possible redox disturbances are caused by the U dissolution. A systematic study aimed to compare U(IV)/U(VI)-separation and SE methods with homogenised samples is under way. In addition, the effect that Fe has on the redox state of U during the sample dissolution will be investigated.

Acknowledgements

This work was financed by the German Federal Ministry of Economics and Technology (BMWi) under contract no. 02 E9995, by RAWRA and Czech Ministry of Trade and Industry (Pokrok 1H-PK25), and by the European Commission within the integrated project FUNMIG.

References

Abdelous, A., Grambow, B., Andres, Y., Noseck, U., submitted for publication. Uranium in argillaceous sediments: sorption/desorption processes and microbial effects. Environ. Sci. Technol.

Denecke, M.A., Havlová, V., 2006. Element correlations observed in Ruprechtov Tertiary sediments: micro-focus fluorescence mapping and sequential extraction. In: Proceedings of the Second Annual FUNMIG Workshop, Stockholm, Sweden, 21.11–23.11.2006.

Denecke, M.A., Janssens, K., Proost, K., Rothe, J., Noseck, U., 2005. Confocal micro-XRF and micro-XAFS studies of uranium speciation in a Tertiary sediment from a waste disposal natural analogue site. Environ. Sci. Technol. 39 (7), 2049–2058.

Denecke, M.A., Somogyi, A., Janssens, K., Simon, R., Dardenne, K., Noseck, U., 2007. Microanalysis (micro-XRF, micro-XANES and micro-XRD) of a Tertiary sediment using synchrotron radiation. Microsc. Microanal. 13 (3), 165–172.

Ervanne, H., Suksi, J., 1996. Comparison of ion-exchange and coprecipitation methods in determining uranium oxidation states in solid phases. Radiochemistry 38, 324–327.

Förster, H.-J., 1998a. The chemical composition of REE–Y–Th–U-rich accessory minerals from peraluminous granites of the Erzgebirge–Fichtelgebirge region, Germany. Part I: The monazite–(Ce) – brabantite solid solution series. Am. Miner. 83 (3–4), 259–272.

Förster, H.-J., 1998b. The chemical composition of REE–Y–Th–U-rich accessory minerals from peraluminous granites of the Erzgebirge–Fichtelgebirge region, Germany. Part II: Xenotime. Am. Miner. 83 (11–12), 1302–1315.

Hammer, Ø., Harper, D.A.T., Ryan, P.D., 2001. PAST: paleontological statistics software package for education and data analysis. Palaeontologia Electron. 4. <http://palaeo-electronica.org/2001_1/past/issue1_01.htm>.

Havlová, V., Laciok, A., 2006. Geochemical study of uranium mobility in Tertiary argillaceous system at Ruprechtov site, Czech Republic. Czech J. Phys. 56 (Suppl. D8).

Noseck, U., Brasser, Th., 2006. Application of transport models on radionuclide migration in natural rock formations – Ruprechtov site. Gesellschaft für Anlagen-und Reaktorsicherheit (GRS) mbH, GRS-218, Braunschweig.

Noseck, U., Brasser, Th., Raijlich, P., Laciok, A., Hercik, M., 2004. Mobility of uranium in Tertiary argillaceous sediments – a natural analogue study. Radiochim. Acta 92, 797–803.

Noseck, U., Rozanski, K., Dulinski, M., Laciok, A., Brasser, Th., Hercik, M., Havlova, V., Buckau, G., in preparation. Characterisation of hydrogeology and carbon chemistry by use of natural isotopes – Ruprechtov site, Czech Republic. Appl. Geochem.

Percival, J.B., 1990. Clay mineralogy, geochemistry and partitioning of uranium within the alternative halo of Cigar Lake uranium deposit, Saskatchewan, Canada. Carleton University, Ottawa, Ph.D. Thesis.

Suksi, J., Rasilainen, K., Pitkänen, P., 2006. Variations in the $^{234}U/^{238}U$ activity ratio in groundwater – a key to characterise flow system. Phys. Chem. Earth 31 (10–14), 556–571.

Tessier, A., Campbell, P.G.C., Bosson, M., 1979. Sequential extraction procedure for the speciation of particulate trace metals. Anal. Chem. 51, 844–851.

Thiel, K., Vorwerk, R., Saager, R., Stupp, H.D., 1983. ^{235}U fission tracks and ^{238}U-series disequilibria as a means to study recent mobilisation of uranium in Archaean pyritic conglomerates. Earth Planet Sci. Lett. 65, 249–262.

[VI.]
NOSECK, U., ROZANSKI, K., DULINSKI, M., HAVLOVA, V., SRACEK, O., BRASSER, TH., HERCIK, M., BUCKAU, G. (2009):

Carbon chemistry and groundwater dynamics at natural analogue site Ruprechtov, Czech Republic: Insights from environmental isotopes. Applied Geochemistry, Volume 24, Issue 9, 1765-1776.

Applied Geochemistry 24 (2009) 1765–1776

Contents lists available at ScienceDirect

Applied Geochemistry

journal homepage: www.elsevier.com/locate/apgeochem

Carbon chemistry and groundwater dynamics at natural analogue site Ruprechtov, Czech Republic: Insights from environmental isotopes

Ulrich Noseck [a,*], Kazimierz Rozanski [b], Marek Dulinski [b], Václava Havlová [c], Ondra Sracek [d], Thomas Brasser [a], Mirek Hercik [c], Gunnar Buckau [e]

[a] Gesellschaft für Anlagen- und Reaktorsicherheit (GRS) mbH, Theodor-Heuss-Str. 4, 38122 Braunschweig, Germany
[b] AGH – University of Science and Technology, Faculty of Physics and Applied Computer Sciences, Al Mickiewicza 30, 30-059 Kraków, Poland
[c] Nuclear Research Institute Řež plc (NRI), 250 68 Řež, Czech Republic
[d] Ochrana podzemních vod (OPV s.r.o.; Protection of Ground Water Ltd), Bělohorská 31, 169 00 Praha 6, Czech Republic
[e] Forschungszentrum Karlsruhe, Institut für Nukleare Entsorgung, P.O. Box 3640, 76021 Karlsruhe, Germany

ARTICLE INFO

Article history:
Received 16 September 2008
Accepted 12 May 2009
Available online 24 May 2009

Editorial handling by Dr. R. Fuge

ABSTRACT

Hydrological, geochemical and environmental isotope data from groundwater wells at Ruprechtov natural analogue site were evaluated to characterize the flow pattern and C chemistry in the system. The results show that water flow in the Tertiary sediments is restricted to 1–2 m thick zones in the so-called clay/lignite horizon with two different infiltration areas in the outcropping granites in the western and south-western part of the investigated area. Generally the flow system is separated from the underlying granite by a kaolin layer up to several tens of metres thick. Differences in stable isotope signatures in the northern part of the site indicate very local connections of both flow systems via fault zones. The observed increase of $\delta^{13}C$ values and decrease of ^{14}C activities in dissolved inorganic C during evolution of the groundwater from the infiltration area to the clay/lignite horizon was modelled using simple open- and closed-system models as well as an inverse geochemical model (NETPATH), which included changes in other geochemical parameters. The results from both types of models provided some insights into timescales of groundwater flow, but mainly revealed that additional sources of C are active in the system. These are very likely biodegradation of dissolved and sedimentary organic C (DOC and SOC) as well as the influx of endogenous CO_2. The occurrence of microbial degradation of SOC in the clay/lignite layers is indicated by the increase of biogenic DIC, DOC, and phosphate concentrations. The impact of microbial SO_4 reduction on this process is confirmed by an increase of $\delta^{34}S$ values in dissolved SO_4^{2-} from the infiltration area to the clay/lignite horizon with an enrichment factor of 11‰. The very low DOC concentrations of 1–5 mg C/L in the clay/lignite horizon with an organic matter content up to 50% C is probably caused by very low availability of organic matter to the processes of degradation and DOC release, demonstrated by extraction experiments with SOC.

1. Introduction

Natural analogue studies contribute to the safety aspect for radioactive waste repositories in deep geological formations. They provide a better understanding of mobilisation and immobilisation processes of naturally occurring radionuclides in complex geological systems over extended periods of time. The Ruprechtov site, located in the north-western part of the Czech Republic, has been investigated from this perspective. It represents an analogue for potential migration processes in similarly structured overburden of salt domes, which are foreseen as potential host rocks for radioactive waste repositories such as the Gorleben site in Germany. The occurrence of layers with a high content of organic material at the Ruprechtov site is of special interest, because in the overburden of the Gorleben site lignite-rich horizons act as a source for humic colloids, which might facilitate radionuclide transport (Buckau et al., 2000a).

A prerequisite for better understanding of radionuclide migration at the site identified as a natural analogue is a thorough characterisation of the hydrogeological conditions, including time scales of groundwater flow in the area. Therefore, during recent years a comprehensive drilling programme has been implemented at the Ruprechtov site (Noseck and Brasser, 2006). The characterisation of the groundwater flow regime at the site was based on determination of the hydraulic properties of the sedimentary layers, water-level measurements, analyses of major and trace elements as well as environmental isotope concentrations in groundwater. Furthermore, isotopic data were used to obtain a better insight into the complex C chemistry at the site. This sets

* Corresponding author. Tel.: +49 531 8012247; fax: +49 531 8012200.
E-mail address: ulrich.noseck@grs.de (U. Noseck).

0883-2927/$ - see front matter © 2009 Elsevier Ltd. All rights reserved.
doi:10.1016/j.apgeochem.2009.05.007

up the basis for understanding the features and processes responsible for generation of dissolved organic matter, e.g. humic colloids.

A flow pattern for the Ruprechtov aquifer system has already been described by Noseck et al. (2004). The present contribution is a continuation of this work. For current evaluation of the system more drilling data and a substantially larger set of isotope data were available.

2. Geology of the study area

The Tertiary Sokolov basin, where the Ruprechtov site is located, was filled with tuffitic material by major volcanic activity during the Oligocene and Miocene. These tuffs are now argillized and denominated as pyroclastic sediments. At the Ruprechtov site, the basin is surrounded and underlain by Carboniferous granitic rocks, which have been intensively kaolinized in their upper part. Kaolin layers reach thicknesses of several tens of meters and in general represent low-permeability aquitards in the system. It is supposed that the kaolinisation process occurred mainly during the Miocene, after coverage with tuffitic material (Noseck and Brasser, 2006). The basal Staré-Sedlo Formation (or equivalent rocks) fills depressions on the basement top and is overlain by the so-called volcano-detritic formation, which is mainly composed of volcanogenic series and intercalated lignite seams. The argillized lignite seams consist of up to 50% organic matter and are associated with sandy material in many boreholes. Therefore, this layer is denoted as the clay/lignite–sand horizon. Uranium enrichment is observed within the lower part of and slightly below the lignite seams. A simplified geological cross-section is shown in Fig. 1.

An important feature of the kaolin/pyroclastics-interface is its strong morphology and substantial differences in kaolin thickness. The interface reveals a complex structure with elevations and depressions, where the greatest kaolin thicknesses form elevated regions and lowest thicknesses of only a few meters coincide with depressions. The occurrence of fault zones in this area is known from a previous geological survey and their positions correlate with the morphological depressions (Noseck and Brasser, 2006). Therefore, areas with very low kaolin thickness might represent a connection of different groundwater systems in the granite and Tertiary sediments.

3. Materials and methods

3.1. Hydrogeology

Altogether 12 wells were drilled and lined in the study area in order to sample and characterize groundwater flow. Seven additional boreholes, which were drilled within the framework of kaolin exploration at the site, became available for this study. These additional boreholes are equipped with relatively long screens which may lead to the mixing of water originating from different water-bearing horizons. The location of sampled boreholes is shown in Fig. 2.

Hydraulic conductivities have been determined by laboratory experiments performed on selected drill cores and by on-site pumping tests. Laboratory experiments have been performed according to DIN 18130, T1 (1998) with constant pressure head. Deionized water was used as fluid. For interpretation of on-site pumping tests the methods of Theis and Cooper-Jacob have been applied (Todd, 1980).

3.2. Water chemistry

Samples were obtained with a bladder pump and then filtered through 0.45 μm filters and for most analyses acidified with ultrapure HCl in the field. Concentrations of major and trace ele-

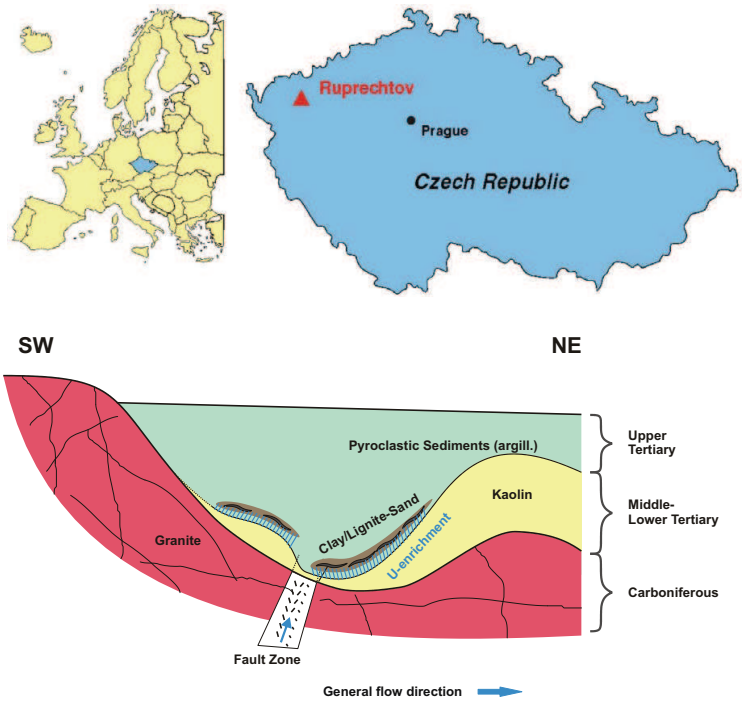

Fig. 1. Location of the Ruprechtov site in the Czech Republic (top) and simplified geological cross section of the Tertiary basin at Ruprechtov site (bottom).

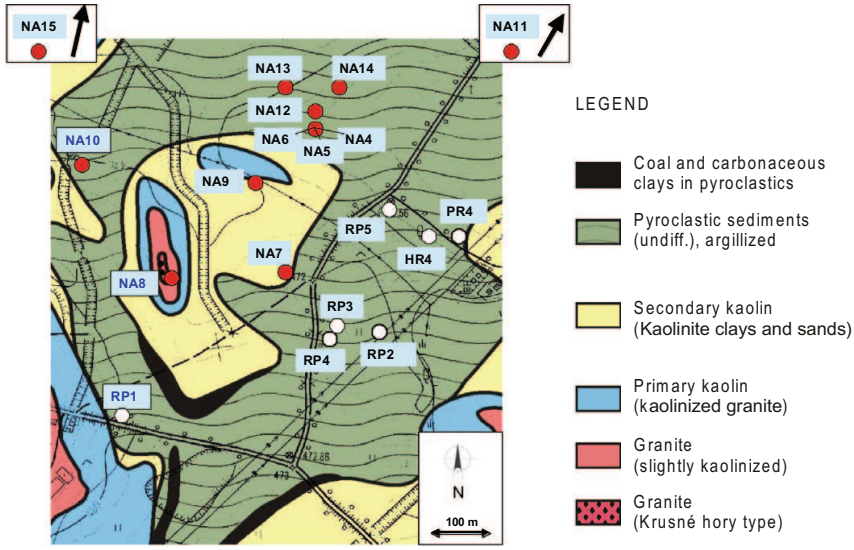

Fig. 2. The location of boreholes at Ruprechtov site, shown on the background of the geologic map. Dark dots indicate research boreholes drilled in the framework of this study. White dots indicate boreholes which were drilled for other purposes and made available for this study. Figure is based on topographic map, which also shows e.g. roads and drainage channels.

ments were determined using an X-series ICP-MS with quartz controlled 27 MHz ICP generator and high performance quadrupole mass analyzer. Silicon concentration was determined with an IRIS Intrepid XUV ICP-OES. The respective analytical uncertainties (one standard deviation) are in the order of 0.5% for major elements and <5% for trace elements and silicon. Chloride was determined by argentometric titration, alkalinity was determined by titration with HCl using the Gran plot to determine end-point, and SO_4^{2-} was determined by ion chromatography. DIC was measured by conversion to CO_2 with H_3PO_4 followed by infrared detection with a TOC/TN 1200 analyser. For DOC analyses the sample was firstly acidified with H_3PO_4 to pH 2 in order to degas DIC. Then DOC was converted to CO_2 by combustion with O_2 and determined using infrared detection with the TOC/TN 1200 analyser. Phosphate and NO_3^- concentrations were determined by photometry. For CH_4 determination groundwater was sampled using special vials in order to prevent air intrusion. After gas–water equilibration in the vial under laboratory conditions CH_4 was determined using gas chromatography with a Thermo-Finnigan TRACE GC 2000 with FID and ECD detection and a Supelco capillary chromatography column Carboxen 1006 Plot 30 m × 0.53 mm.

Table 1
Physical and chemical parameters of groundwater samples collected in the Ruprechtov aquifer system during sampling campaign in May 2004. All concentrations are expressed in mg/L. Eh-values are expressed in mV.

	NA4	NA5	NA6	NA7	NA8	NA9	NA10	NA11	NA12	NA13	NA14	NA15	RP1	RP2	RP5
T (°C)	9.60	9.00	9.80	9.10	9.00	7.30	8.40	9.80	9.10	9.90	9.20	9.40	9.70	9.60	9.10
pH1	n.a.	n.a.	8.00[a]	8.00[a]	6.20[a]	7.19[a]	7.40	6.89	6.65	7.65	6.85	7.29	6.81[a]	7.72[a]	7.00[a]
pH2	6.78	7.05	7.80[a]	7.05[a]	6.45[a]	6.83[a]	6.95	7.04	6.68	7.41	7.00	7.09	6.75[a]	7.35[a]	6.89[a]
pH3	6.75	7.04	7.57	7.49	6.15	6.97	6.67	7.11	6.73	7.66	6.94	6.71	6.40	7.70	6.93
Eh1	n.a.	n.a.	−280[b]	−35[a]	48[a]	324[a]	240	−91	−160[b]	−252[b]	−59	58	149[a]	−3.8[a]	133[a]
Eh2	6	−10	−115[a]	−107[a]	143[a]	355[a]	485	65	15	25	120	245	363[a]	25[a]	160[a]
Al	0.20	0.26	0.22	0.33	0.10	0.15	n.a.	n.a.	n.a.	n.a.	n.a.	n.a.	0.14	0.21	0.25
Ca	51.00	68.90	48.00	86.85	26.24	28.03	40.40	65.60	44.70	54.60	48.70	31.60	31.00	47.10	43.70
Fe	1.87	0.99	0.73	0.13	1.32	0.91	0.37	5.45	2.27	0.83	0.10	0.31	0.34	2.89	1.16
K	13.10	12.30	12.05	6.50	1.40	2.70	8.40	18.90	9.70	16.50	14.60	10.80	2.90	10.30	11.20
Mg	23.60	29.35	18.60	17.90	4.00	5.30	8.40	28.90	19.80	21.70	20.80	12.50	8.80	23.80	21.40
Na	23.30	45.25	37.20	16.40	10.90	14.10	15.50	91.20	20.10	35.80	39.50	25.30	13.40	41.80	19.20
Si	10.30	7.80	7.40	4.40	15.05	18.70	13.00	7.70	15.90	8.00	12.60	11.60	16.80	3.30	9.90
Cl	3.90	8.80	3.60	6.60	4.30	0.60	5.90	10.40	4.30	10.10	13.60	4.00	20.70	26.40	5.54
SO_4	19.80	31.50	49.50	28.20	59.10	11.80	40.80	178.60	22.90	22.90	30.80	40.10	19.80	55.00	14.80
PO_4[b]	0.19	0.47	0.2	0.72	0.3	0.08	0.16	0.30	0.04	0.14	0.21	0.10	0.35	0.11	0.15
CO_2	40.71	43.60	6.70	9.60	31.70	8.60	24.50	40.60	63.00	10.50	32.80	13.80	44.40	1.00	20.50
NO_3	0.80	0.40	1.20	1.10	1.70	1.10	7.20	1.40	0.30	1.00	2.30	3.50	3.20	2.50	2.20
HCO_3	330.50	469.30	291.80	332.10	44.20	163.50	159.40	379.00	269.20	349.00	316.60	186.70	117.00	277.00	279.00
CH_4	0.634	0.097	0.072	0.007	n.a.	n.a.	0.003	0.011	0.028	0.04	0.022	0.004	n.a.	n.a.	n.a.

pH1: measured in situ; pH2: measured on-site; pH3: measured in laboratory (T = 20 °C); Eh1: measured in situ, Eh2: measured on-site.
[a] Sampling campaign from May 2003.
[b] Long-term value.

Field parameters (pH, Eh and temperature) were measured by an in situ probe directly in the sampled boreholes, and in the laboratory. The chemical analyses were performed at Gesellschaft für Anlagen- und Reaktorsicherheit (GRS) mbH and at the Technical University Braunschweig. The results are reported in Table 1.

3.3. Environmental isotopes

Environmental isotope analyses of different types of groundwater samples were performed to characterize in more detail the flow regime and C chemistry of the Ruprechtov aquifer system. Stable isotope ratios ($^2H/^1H$ and $^{18}O/^{16}O$) were determined in near-surface waters to identify typical local infiltration waters. Additionally, ^3H concentrations in water, $^{14}C/^{12}C$ and $^{13}C/^{12}C$ isotope ratios in DIC and DOC pools, as well as $^{34}S/^{32}S$ isotope ratios in dissolved SO_4^{2-}, were determined in groundwater samples from several wells.

The isotope ratios $^2H/^1H$, $^{18}O/^{16}O$, $^{13}C/^{12}C$ and $^{34}S/^{32}S$ are reported as per mil. deviations (δ^2H and $\delta^{18}O$, $\delta^{13}C$ and $\delta^{34}S$) from the respective isotope ratio of the internationally accepted standards (VSMOW, VPDB, VCDT), as given below for the $^{18}O/^{16}O$ ratio:

$$\delta^{18}O = \left[\frac{(^{18}O/^{16}O)_{sample}}{(^{18}O/^{16}O)_{standard}} - 1\right] \cdot 1000$$

The respective analytical uncertainties (one standard deviation) are in the order of 0.1‰ for $\delta^{18}O$ and $\delta^{13}C$, 0.2‰ for $\delta^{34}S$ in the case of NA6/NA7 and 0.3‰ in the case of all other wells and 1.0‰ for δ^2H. The concentration of ^3H is reported in Tritium Units (TU). One TU corresponds to the ratio $^3H/^1H = 10^{-18}$. The analytical uncertainty of the reported ^3H concentrations is in the order of 0.5 TU. The ^{14}C concentration is reported in percent modern carbon (pmc) and the quoted analytical uncertainty is in the order of 0.5 pmc and 0.3 pmc, for radiocarbon content in DIC and DOC, respectively.

The ^3H and stable isotope composition of water, as well as ^{14}C content and $\delta^{13}C$ values of the DIC pool were determined at the Isotope Laboratory at AGH University of Science and Technology, Krakow, Poland. Deuterium and ^{18}O content of water samples were determined using the established techniques: Zn reduction for δ^2H and CO_2-equilibration for $\delta^{18}O$ (Coleman et al., 1982; Epstein and Mayeda, 1953). Tritium content in water samples was measured using electrolytic enrichment and liquid scintillation spectrometry, whereas the radiocarbon content of the DIC pool was determined using benzene synthesis combined with liquid scintillation spectrometry.

For determination of $^{14}C/^{12}C$ ratios in DOC 2L groundwater samples were filtered with a 0.45 μm silver filter, evaporated to 50 mL at 0.1 bar and acidified to pH 2 to remove DIC. The samples were then freeze-dried, combusted at 900 °C in a quartz capsule with CuO and Ag wool and afterwards reduced to graphite with H_2 and Fe catalyser at 600 °C. Analysis of ^{14}C and ^{12}C was done by accelerator mass spectrometry. Results were converted to percent modern carbon (pmc) units.

The analyses of $^{34}S/^{32}S$-ratios in dissolved SO_4 were performed following the technique of Coleman and Moore (1978), in which SO_2 gas is released by combustion with excess Cu_2O and silica, at 1125 °C. Liberated gases were then analysed on a VG Isotech SIRA II mass spectrometer.

The analyses of $\delta^{13}C$ in SIC followed the methodology of McCrea (1950). Degassed samples were decomposed in 100% H_3PO_4 in vacuum at 25 °C. Liberated gases were analysed using a Finnigan Mat 251 mass spectrometer working in a continuous flow regime. The $\delta^{13}C$ content in DOC was determined from the evaporated residuum, after carbonates and bicarbonates had been removed, that was acidified with 100% H_3PO_4. Liberated gases were analysed using a Finnigan Mat 251 mass spectrometer.

The results of the isotope analyses are summarized in Table 2. Table 2 also contains information on the depth of the screened horizon in the sampled boreholes as well as on the lithology and hydraulic conductivity of the water-bearing layers. For NA4, NA5 and NA6 boreholes, analyses from three consecutive sampling campaigns were available.

4. Results and discussion

4.1. Hydrology

Laboratory experiments on selected drill cores as well as on-site determination of hydraulic conductivities (pumping tests) revealed that only distinct water-bearing layers exist with k-values of 10^{-5} m/s–10^{-8} m/s and thicknesses of about 1–2 m only, mainly in the vicinity of the clay/lignite–sand layer. In contrast, the pyroclastic sediments and the underlying kaolin have a lower hydraulic conductivity, with typical k-values of 10^{-10} m/s–10^{-11} m/s. The k-values for the different wells are shown in Table 2. As indicated above, fracture zones and areas with very low thickness of underlying kaolin might represent hydraulic connections between clay/lignite–sand layers and granite.

4.2. Hydrogeochemistry

The chemical conditions of the site are characterized by low mineralized waters with ionic strengths in the range from 0.003 mol/L to 0.02 mol/L. The pH values vary in the range 6.2–8 and the Eh-values from 435 mV to −280 mV. More oxidising conditions with lower pH-values are found in the near-surface granite waters of the infiltration area. In the clay/lignite horizon conditions are more reducing with Eh-values as low as −280 mV. The Eh-values measured directly by in situ probe are significantly lower than those measured on-site in pumped water (cf. Table 1). The latter method is more susceptible to disturbances by contact with atmosphere, which is probably responsible for the observed differences in Eh-values.

Groundwater from nearly all boreholes of the clay/lignite horizon is of Ca–HCO_3-type. The exceptionally high Na and SO_4 concentrations in NA11 are probably an artefact of contamination by drilling fluid. The waters from the infiltration area in granite (NA8, NA10 and RP1) as well as water from borehole NA12 with significantly lower alkalinity and Ca concentration are defined as Ca–SO_4-type water. All DOC values are in a range between 1 and 5 mg/L. In a number of boreholes from the clay/lignite horizon CH_4 concentrations of over 0.01 mg/L (up to 0.7 mg/L) were detected.

In order to identify the most important factors controlling the groundwater geochemistry a principal component analysis (PCA) was performed using the program PAST (Hammer et al., 2001).

The results show that most information is covered by two components: Principal Component 1 (PC1) accounts for 80.6% and Principal Component 2 (PC2) accounts for 15.3% of the variability in the data set. PC1 is well defined and has a highly positive loading for HCO_3, positive loadings for Ca, Na, and Mg and a highly negative loading for the redox potential, i.e. samples with low Eh are covered by this component. It represents a geochemically evolved reducing groundwater, similar to the water from the clay/lignite horizon with increased concentrations of cations and with high concentration of HCO_3^-. PC2 is not that well defined and has a positive loading for Si, highly negative value for HCO_3 and negative values for Na, and Mg. This component represents immature

Table 2
Depth of screened horizons, lithological units and environmental isotope data for boreholes in the Ruprechtov aquifer system sampled between 2003 and 2006. The table shows also DIC, DOC and SO_4^{2-} concentrations in the analysed groundwater samples.

Well no.	Screen horizon (m)	Lithology	k (m/s)	$\delta^{18}O$ (‰)	$\delta^{2}H$ (‰)	Tritium (TU)	^{14}C DIC (pmc)	DOC (pmc)	$\delta^{13}C$ DIC (‰)	DOC (‰)	$\delta^{34}S$ SO_4^{2-} (‰)	DIC (mg/L)	DOC (mg/L)	SO_4^{2-} (mg/L)
NA4	34.5–36.5	clay/lignite, U	1.52×10^{-06}	−9.78	−68.0	<0.5	3.2	40.0	−11.0	−26.6	24.63	74.2	4.22	19.8
NA5	19.3–21.3	U	5.47×10^{-08}	−8.98	−61.9	<0.5	5.3	n.a.	−10.9	−25	n.a.	90.8	n.a.	31.5
NA6	33.4–37.4	clay/lignite, U	5.62×10^{-07}	−9.27	−64.6	0.6	13.1	n.a.	−12.4	−26.8	23.5	60	3.27	49.5
NA7/1	15.5–19.5	kaolin	1.88×10^{-07}	−8.96	−61.5	<0.5	n.a.	n.a.	n.a.	n.a.	n.a.	61.7	3.88	28.2
NA7/2	10.5–11	clay/lignite, U	4.40×10^{-05}	−9.00	−61.1	<0.5	39.4	n.a.	−16.1	−27.3	20.4	60.8	n.a.	12.3
NA8	8.5–24	granite	2.00×10^{-06}	−9.22	−62.9	1.1	71.9	64.6	−21.9	−27.8	−8.5	14.5	3.01	59.1
NA9	4.4–10	kaolin	3.26×10^{-06}	−8.95	−60.8	<0.5	72.1	n.a.	−20.5	−27.1	n.a.	37.1	n.a.	11.8
NA10	19.5–27.5	granite	2.86×10^{-08}	−8.89	−61.5	1.6	54.6	n.a.	−16.2	−26.4	0.2	33.8	1.99	40.8
NA11	33.2–39	clay/lignite, U	6.50×10^{-06}	−9.00	−65.5	1.5	7.8	n.a.	−9.6	n.a.	n.a.	82.4	n.a.	178.6
NA12	36.5–39.3	clay/lignite, U	3.80×10^{-07}	−8.87	−61.9	<0.5	26.5	70.0	−16.0	−25.6	20.11	67	3.69	22.9
NA13	42.2–48	clay/lignite, U	2.30×10^{-09}	−9.24	−65.9	1.5	n.a.	44.3	n.a.	−27.2	n.a.	68.8	2.32	22.9
NA14	67.6–77.6	granite	2.75×10^{-08}	−9.33	−64.9	0.6	9.8	n.a.	−12.8	n.a.	16.43	69.1	n.a.	30.8
NA15	28.8–31.6	granite	1.19×10^{-07}	−9.88	−70.9	<0.5	11.8	n.a.	−13.7	n.a.	n.a.	39.4	n.a.	40.1
RP1	5–18	granite	3.37×10^{-07}	−9.52	−66.9	<0.5	21.0	n.a.	−16.8	n.a.	3.48	33.4	1.36	19.8
RP2	25–43	clay/lignite, U	2.78×10^{-06}	−9.81	−69.0	1.1	16.8	n.a.	−13.2	−26.6	n.a.	52.4	1.83	55.0
RP3	25–48	clay/lignite, U	2.25×10^{-05}	−9.60	−68.2	1.0	13.3	n.a.	−15.3	−26.6	n.a.	59.7	n.a.	24.6
RP5	30–58	clay/lignite, U	5.08×10^{-08}	−9.75	−68.4	<0.5	6.4	n.a.	−11.7	n.a.	n.a.	58.1	n.a.	14.8
HR4	46.5–95	granite	n.a.	−9.31	−64.3	1.2	29.9	n.a.	−14.5	−26.2	n.a.	n.a.	n.a.	n.a.
PR4	5–32	clay/lignite, U	n.a.	−9.00	−63.7	9.7	n.a.	n.a.	n.a.	n.a.	n.a.	n.a.	n.a.	n.a.

Data are single values from measuring campaigns in 2003, 2004 and 2006, respectively. Exceptions are $\delta^{18}O$, $\delta^{2}H$ and ^{3}H data for wells NA4, NA5, NA6 and RP5 and 14C values in DIC for wells NA4 and NA5, which are averages of 2 or 3 analyses, respectively.

groundwater, probably dominated by the dissolution of silicates close to recharge areas in the granitic formation.

The results of PCA are illustrated in Fig. 3 indicating a progressive geochemical evolution from the left to the right. Wells from infiltration areas NA10 through RP1, NA9 and NA8 have relatively low values of PC1. On the other hand, clay/lignite wells NA12, NA13, NA11, NA4, NA14, NA5, and especially NA6, and NA7 have high values of PC1. This is consistent with decreasing Eh-values and increasing HCO_3 concentrations in the same direction.

Groundwater in most of the analysed wells reaches saturation with respect to carbonate minerals. This is shown in Fig. 4 where calculated saturation indices for several carbonate minerals are presented. Only groundwater samples in the boreholes NA8, RP1, NA12 and NA9 are undersaturated with respect to carbonate-bearing minerals. Calculations have been performed with PHREEQC (Parkhurst and Appelo, 1999) and thermodynamic database NAPSI_290502(260802) (Hummel et al., 2002).

4.3. Isotopes of water and flow pattern

Tritium is absent in the majority of the analysed boreholes, indicating the pre-bomb age of groundwater. Some traces of ^{3}H were found in NA8, NA10, NA11, NA13, RP2, RP3 and HR4. The highest concentration of ^{3}H (9.7 TU), comparable with the current concentration of ^{3}H in local precipitation, was found in borehole PR-4.

Deuterium and ^{18}O contents in the analysed wells are shown in Fig. 5. It is apparent that stable isotope composition of the analysed water samples varies in a rather broad range: $\delta^{18}O$ changes from approximately −9.8‰ to −8.8‰. In general, the data points cluster around the world meteoric water line (WMWL). The range of $\delta^{2}H$ and $\delta^{18}O$ values in recent local infiltration waters have been determined on the basis of isotope analyses of representative water samples in the study area (Noseck et al., 2002). This range is marked on Fig. 5 by the bold, grey line. A number of data points in Fig. 5 reveal more negative $\delta^{2}H$ and $\delta^{18}O$ values when compared to local, recent infiltration waters, suggesting the influence of the altitude and/or the climatic effect.

Spatial distribution of $\delta^{2}H$ and $\delta^{18}O$ values is shown in Fig. 6. In general, the analysed waters can be divided into two groups, isotopically heavier groundwater in the NW region of the study area (marked with a white frame) and isotopically light groundwater in the SE region (marked with a grey frame). The waters in the NW region can be further subdivided into a group with $\delta^{18}O$ values

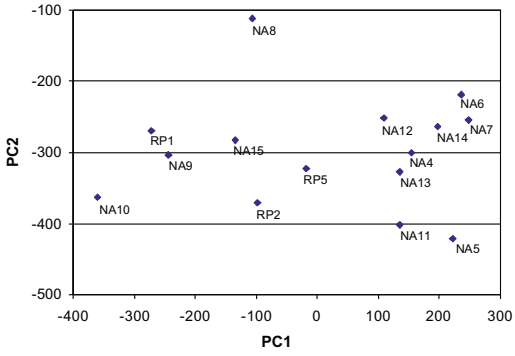

Fig. 3. Results of Principal Component Analysis: plot of PC1 vs. PC2 (see discussion in the text).

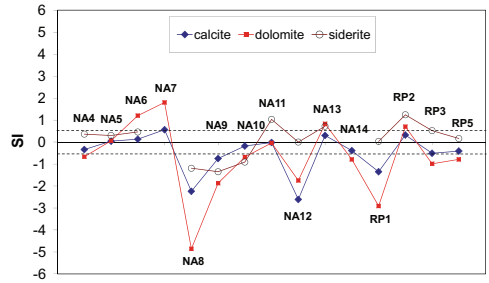

Fig. 4. Saturation indices (SI) for carbonate-bearing minerals in selected groundwater samples from Ruprechtov site. Horizontal lines indicate SI ranges where equilibrium is assumed.

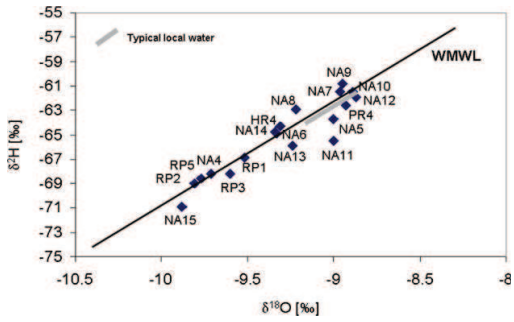

Fig. 5. Stable isotope composition of the analysed groundwater samples in the Ruprechtov aquifer system. Bold grey line denotes isotope signature of local, recent infiltration waters.

between −8.8‰ and −9.0‰ and a group with $\delta^{18}O$ values between −9.2‰ and −9.4‰.

The distribution of hydraulic heads measured in April 2004 is shown in Fig. 7. The data indicate a hydraulic gradient from SW to NE. The boreholes sampling water from granite are marked in a white frame, all other values are given in a light grey frame. Three western wells (NA8, NA10 and RP1) represent groundwater from near-surface granite. They contain measurable amounts of ^3H but differ significantly in stable isotope composition. Whereas NA10 and NA8 reflect signatures of recent local waters (cf. Fig. 5), water from RP1 is isotopically lighter. The most probable explanation of the differences in stable isotope composition among those wells is that water from RP1 originates from an infiltration area which is elevated by about 200–300 m when compared to the other two wells.

Several boreholes in the south-eastern region of the study area (RP2, RP3 and RP5) reveal similar stable isotope signatures as RP1 borehole. This suggests hydraulic connection between RP1 and the SE region of the study area. PR4 and HR4 located in the eastern part of the study area are older drillings which are not well documented. The elevated $\delta^{18}O$ values measured in those wells might be caused by admixture of surface water. This is very likely, particularly for PR4, where the filter horizon covers the depth interval from 5 m to 32 m. A strong indication for such admixture of surface water is provided by elevated ^3H content in those wells (9.7 TU and 1.2 TU in PR4 and HR4, respectively).

Water samples originating from near-surface horizons (boreholes NA9, NA7 and NA5) reveal stable isotope ratios similar to NA10, indicating hydraulic connections to the infiltration area in the NW of the study area.

Boreholes located in the northern part of the study area reveal a relatively large range of δ^2H and $\delta^{18}O$ values. NA12 shows similar values to NA10, suggesting hydraulic connection to the western infiltration area. A cluster of three wells (NA4, NA5 and NA6) shows isotopically depleted water in the deeper horizon (NA4 and NA6, screened from ca. 33 m to 37 m), suggesting an elevated recharge area, whereas NA5 screened between 19 m and 21 m, falls into the range of recent local infiltration (cf. Fig. 5). Other boreholes in this region (NA13 and NA14) seem to represent mixtures of isotopically depleted water and local infiltration water. NA13 shows some traces of ^3H, which is rather unexpected for the deep horizon sampled by this well.

The water in the deeper granite (NA14) may represent a mixture of water originating in the north-western infiltration area and water infiltrated in the south-western area. Additionally, there seems to be a hydraulic connection between the north-western infiltration area and the water-bearing horizons in the northern area of the Tertiary (NA12, NA13 and NA6). Since those wells are located in a region of low kaolin thickness, where fault zones occur, local connections between water-bearing horizons in the Tertiary and underlying granite are likely. Therefore, groundwater in this region might represent a mixture of underlying granite water and infiltration water from the north-western infiltration area.

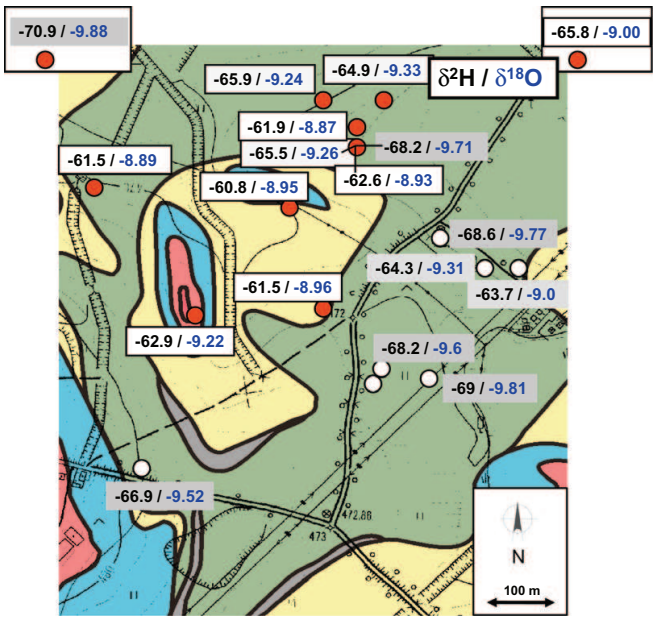

Fig. 6. Spatial distribution of δ^2H and $\delta^{18}O$ values in groundwater samples representing the Ruprechtov aquifer system.

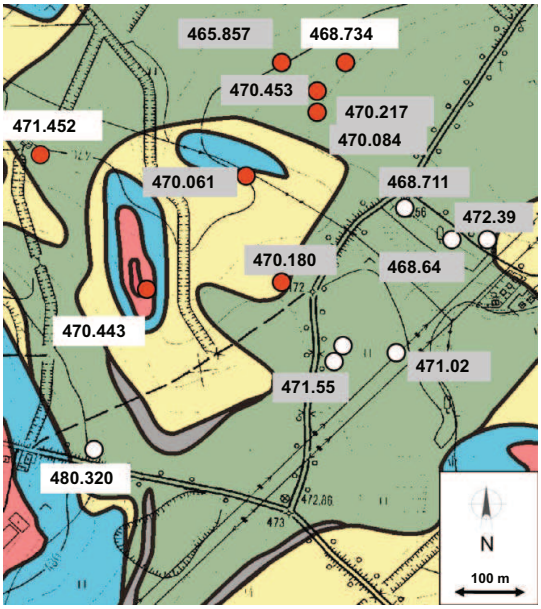

Fig. 7. Hydraulic heads in the Ruprechtov aquifer system based on measurement in April 2004.

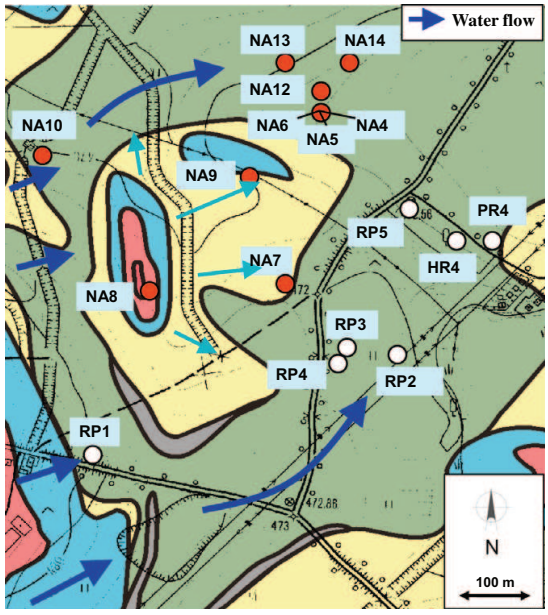

Fig. 8. Conceptual model of groundwater flow pattern in the studied Ruprechtov aquifer system.

Boreholes NA15 and NA11 are more than 1 km away from the study area. Due to the complex, heterogeneous geological structure, including fault zones and the irregular morphology of the Tertiary basement, it is difficult to judge if and how those wells are hydraulically connected with the area under consideration.

The different lines of evidence discussed above provided the basis for the conceptual model of groundwater flow pattern in the studied Ruprechtov aquifer system. The model is shown in Fig. 8. The general direction of groundwater flow is from SW to NE, with a local infiltration area in the outcrops of granite.

4.4. Carbon isotopes

Carbon isotopes were determined in the Ruprechtov aquifer system in order to obtain additional information on the time scales of groundwater flow and to characterize water mixing processes as well as chemical reactions within the C system. The isotope measurements comprised both DIC and DOC pools in groundwater.

Radiocarbon activity and $\delta^{13}C$ values of DIC have been determined for 16 boreholes. $\delta^{13}C$ values of the DOC pool were obtained for 12 wells while ^{14}C activity in DOC was determined only in 4 wells. It is apparent from Table 2 that ^{14}C activities and $\delta^{13}C$ values of DIC cover a wide range of values, from 72.1 to 3.2 pmc and from $-21.9‰$ to $-10.4‰$, respectively. The ^{14}C activity found in the DOC pool ranges from ca. 40 to 70 pmc, while $\delta^{13}C_{DOC}$ values change only slightly, between ca. $-25.0‰$ and $-27.8‰$.

The radiocarbon content of the analysed groundwater samples has been plotted in Fig. 9 as a function of respective $\delta^{13}C$ values. A broad, inverse relationship between radiocarbon content of the DIC pool and its $\delta^{13}C$ values is apparent, with high concentrations of radiocarbon associated with the most negative $\delta^{13}C$ values. While the ^{14}C activities and $\delta^{13}C$ values observed in NA8 and NA9 (ca. 72 pmc and $-21‰$) are expected for fresh infiltration water from the recharge zone devoid of carbonates, C isotope composition of DIC in NA10 and RP1 boreholes located on major direc-

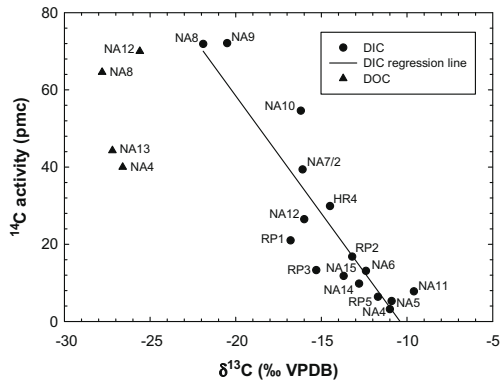

Fig. 9. Radiocarbon activity [pmc] versus $\delta^{13}C$ values of DIC and DOC pool in the sampled boreholes of the Ruprechtov aquifer system.

tions of groundwater flow (cf. Fig. 8) indicates that those waters have already evolved chemically and isotopically (cf. discussion below). Although measured ^{14}C activities in the DIC pool (cf. Table 2) can be converted to uncorrected groundwater "ages" (Noseck and Brasser, 2006), it is obvious that C isotope values should be interpreted in the context of geochemical evolution of the DIC pool, taking into account possible addition and/or removal of C isotopes from the system via precipitation/dissolution reactions. As expected, the observed ^{14}C activities of the DOC pool are located to the right-hand side of the regression line in Fig. 9 and can be converted to ages of organic matter sources.

The following processes influencing ^{14}C activities and $\delta^{13}C$ values in DIC should be considered in the context of the present study: (i) dissolution of sedimentary inorganic C (SIC), (ii)

microbial degradation of dissolved and/or sedimentary organic C (DOC and SOC, respectively) and (iii) input of endogenous CO_2.

Sedimentary inorganic C from the Tertiary formation is free of radiocarbon and its $\delta^{13}C$ values are expected to be about 0‰. This is confirmed by analyses of $\delta^{13}C$ in siderite from boreholes RP5 and NA5 showing values of 1.8‰ and 2.6‰, respectively. Dissolution of SIC leads to reduced activities of ^{14}C and gradual increase of $\delta^{13}C$ values of the DIC pool. The $\delta^{13}C$ value of the SOC pool is expected to be around −25‰ to −27‰. This is underpinned by analyses of two samples from Tertiary SOC in core material from RP2 showing values of −26.6‰ and −24.9‰, respectively (Noseck and Brasser, 2006). Although SOC in the Tertiary is obviously free of radiocarbon, the dissolved organic C originating in the soil zone may contain significant amounts of ^{14}C, depending on the age of organic matter from which the dissolved fractions (HA, FA, hydrophilic acids) were derived. The endogenous CO_2 is free of radiocarbon and, according to the literature, its $\delta^{13}C$ values vary from −6‰ to −3‰. In the Eger rift region, approximately 30 km SW of the study area, Weise et al. (2001) found $\delta^{13}C$ values of endogenous CO_2 to be around −2.7‰.

The evolution of the C isotope composition of the DIC pool in the infiltrating water recharging the given groundwater system can be addressed using two contrasting conceptual models (e.g. Deines et al., 1974; Clark and Fritz, 1997): (i) the open-system model assuming that the pore water in the unsaturated zone is in continuous contact with an infinite reservoir of soil CO_2 of constant parameters (partial pressure, C isotope composition) during the process of dissolution of the mineral carbonate phase, (ii) the closed-system model where the infiltrating water first equilibrates with the soil CO_2 reservoir and then moves to the region where dissolution of mineral phase(s) takes place, without contact with the CO_2 reservoir. Both models lead to very different C isotope composition of the DIC pool, particularly with respect to the radiocarbon content, and to the different size of the DIC pool in the infiltrating water.

These two simple models have been used as a first, semi-quantitative step in the interpretation of C isotope data gathered in the framework of this study. They also provide a general conceptual framework in which the C isotope data can be linked to the size of the DIC pool. The ^{14}C activities and $\delta^{13}C$ values measured in the sampled boreholes were plotted as a function of the size of the DIC reservoir (Fig. 10a and b), superimposed on that are different trend lines predicted by the simple models mentioned above.

The trajectories marked in Fig. 10 by black lines (solid and dashed) indicate the initial evolution of the C isotope composition of the DIC pool. First, soil CO_2 of prescribed characteristics (partial pressure 0.01 atm, ^{14}C activity equal to 100 pmc, $\delta^{13}C$ equal to −24‰) dissolves gradually in the infiltrating water until saturation with respect to $CaCO_3$ (^{14}C activity equal to 0 pmc, $\delta^{13}C$ value equal to 2‰) is reached. The saturation points are marked by stars. From those points on, the solution was allowed to evolve further under closed-system conditions (grey solid and dashed lines) by adding new C in the form of CO_2, devoid of ^{14}C. Two different $\delta^{13}C$ values of this additional C were considered: −27‰ and −16‰. The first value corresponds to CO_2 derived from decomposition of SOC, the second one representing a 1:1 mixture of biogenic CO_2 ($\delta^{13}C$ of −27‰) and endogenous CO_2 with a $\delta^{13}C$ value of around −3‰.

As seen in Fig. 10a, the ^{14}C data cluster around the closed-system trend lines with two-step addition of C to the solution. Some data points are located either to the right-hand side (NA8, NA9, NA10 and NA12) or below (NA15, RP5, NA5 and NA4) the trend line. The ^{13}C data (Fig. 10b) provide an additional constraint on the process of adding additional C to the system. The majority of data points are located between the trend lines representing two different $\delta^{13}C$ values of gaseous CO_2 entering the solution: −27‰ and −16‰. While $\delta^{13}C$ values observed in well RP2 reflects the dominating contribution of CO_2 from decomposition of organic matter, for borehole NA11 they suggest that both sources of CO_2 are represented in approximately equal proportions.

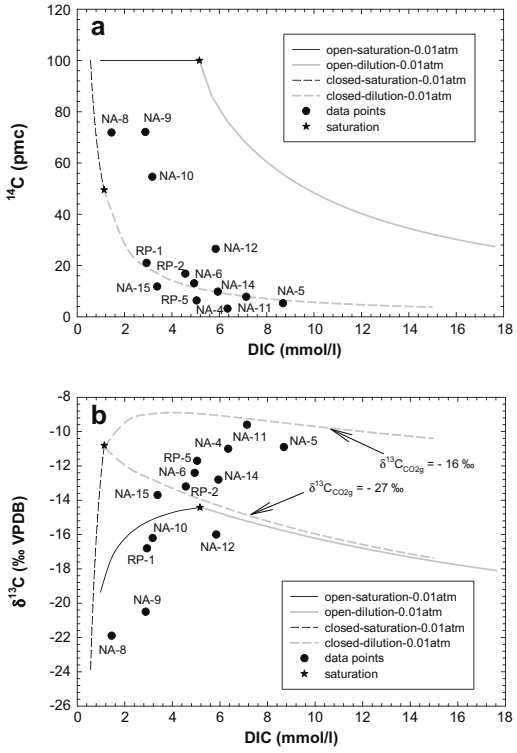

Fig. 10. Carbon isotope evolution of the DIC reservoir under open- and closed-system conditions. Stars indicate saturation of the solution with respect to $CaCO_3$. Subsequent evolution of the DIC reservoir (grey lines), resulting from input of additional C, was calculated via consecutive equilibrium stages with a solid carbonate phase (see text for details).

Groundwater in boreholes NA8, NA9, NA12 and RP1 is undersaturated with respect to carbonate minerals (cf. Fig. 4). Well NA8 characterized by the lowest mineralization is situated in granitic rocks. Well NA9 has a considerably higher HCO_3^- concentration when compared to NA8 and slightly higher concentrations of the main cations, with reduced concentrations of NO_3^- and SO_4^{2-}. Similar ^{14}C activities and $\delta^{13}C$ values in both waters suggest that oxidation of DOC in the unsaturated zone contributed additional C to the solution shifting these data points to the right-hand side of the trend lines shown in Fig. 10. Carbon isotopes from well RP1 are difficult to interpret. While the ^{14}C activity falls on the line representing the closed-system model, its $\delta^{13}C$ value indicates an open-system model. Well NA12 shows the highest carbonate content among the discussed group of wells. The measured ^{14}C activities and $\delta^{13}C$ values suggest a significant admixture of C probably originating from decomposition of organic matter depleted in ^{14}C, combined with dissolution of carbonates.

The position of data points representing wells NA15, RP5, NA5 and NA4 below the trend line in Fig. 10a could be interpreted in terms of water age. The distance between the trend line and the given data point (between ca. 1.3 and 5.9 pmc) can then be converted to radiocarbon age. The resulting ages would be in the order of 1.8–8.6 ka.

Although the discussion of C isotope data in the context of simple models presented above gives interesting insights with respect to sources of C in the solution and possible age effects, it does not provide a full description of the chemical and isotopic evolution of groundwater in the studied system as the trend lines shown in Fig. 10 represent geochemical evolution of a hypothetical solution under prescribed boundary conditions. Such a description can be accomplished only in the framework of fully fledged geochemical models.

4.4.1. Inverse modelling

Inverse modelling was carried out using the NETPATH code (Plummer et al., 1994). NETPATH is an interactive computer program allowing simulation of chemical and isotopic mass-balance reactions between two prescribed points (wells) in a given aquifer system. If sufficient isotopic data are available, Rayleigh-type calculations can be performed to predict the C isotopic composition and to derive the groundwater age at the end-point. As a result of NETPATH modelling, multiple hypotheses with respect to geochemical evolution and the resulting age of the DIC pool usually emerge. They may be further used to constrain the groundwater ages.

Two pairs of wells were selected for model calculations using the NETPATH code: NA10–NA12 and RP1–RP2. They are located along the flow lines originating in two hypothetical infiltration areas, in the SW and NW of the study area, respectively (cf. Fig. 8).

Four groups of models (N1, N2, N3 and N4) were tested using the NETPATH code. Configuration of constraints and phases used in the modelling is summarized in Table 3.

The initial C isotope composition of the phases was the same for all tested models: $\delta^{13}C$ (dolomite, calcite, siderite) = 2.0‰, $\delta^{13}C(CO_2$ gas) = −3.0‰, $\delta^{13}C(CH_2O)$ = −27.0‰. Calcite, dolomite, siderite and gaseous CO_2 were assumed to be radiocarbon-free. Two different values of radiocarbon activity in the SOC pool were assumed in the model calculations: 0 and 60 pmc.

The results of the modelling exercise are summarized in Fig. 11 which shows ^{14}C activities calculated by the NETPATH code for the end-point wells (RP2 and NA12), starting from the values observed in the initial wells (RP1 and NA10, respectively). The models which gave $\delta^{13}C$ values inconsistent with the observed ones (groups N1 and N2) were not included in Fig. 11. Each bar shown in Fig. 11 represents a group of 2–6 chemically different models fulfilling the constraints outlined in Table 3 and leading to similar ^{14}C activities in the end-point well. Models within the given group differ in proportions between individual fluxes of C (endogenous CO_2, DOC/SOC, calcite/dolomite) and minerals entering the solution or being precipitated during chemical evolution of water. They also differ with respect to the extent of Ca and Mg/Na cation exchange reactions.

Table 3
Groups of NETPATH models. '×' sign means that given constraints and phases are applied.

	Group N1	Group N2	Group N3	Group N4
Constraints:				
C, S, Ca, Mg, K, Fe and RS	×	×	×	×
Na	×	×	×	
Cl	×	×	×	
^{13}C		×	×	×
Phases:				
CH_2O (diss.), calcite (diss.), CO_2 gas (diss.), dolomite (diss.), goethite (diss.), gypsum (diss.), Mg/Na exchange, pyrite, siderite and sylvite	×	×	×	×
Halite	×	×	×	
Exchange			×	×

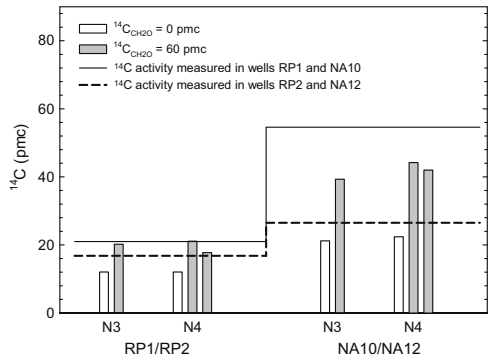

Fig. 11. Comparison of measured and modelled radiocarbon activities in wells RP2 and NA12. Geochemical modelling was performed using NETPATH code (see text for details).

No reliable models could be found within N1 and N2 groups. The calculated values of $\delta^{13}C$ for N1 and N2 groups were significantly different from those measured in wells RP2 and NA12. This disagreement suggests that Ca/Na exchange is an important process for the chemical evolution of the solution between initial and final wells.

The assumption that additional C delivered to the solution is free of radiocarbon (open bars in Fig. 11) leads to calculated ^{14}C activities in the end-point wells (RP2 and NA12) significantly lower than the measured ones, creating 'negative' ages in the range between −5.5 and −23 ka for RP2 and −2.3 and −8.6 ka for NA12.

The second set of models (heavy bars in Fig. 11) was calculated assuming that additional biogenic C added to the solution has a ^{14}C activity equal 60 pmc. The calculated radiocarbon activities in the end-point wells are generally higher than the measured ones. The differences between measured and calculated activities, when converted to groundwater ages, yield values between 0.45 and 1.9 ka for RP2 and 3.2–4.2 ka for NA12. It should be noted that 3 out of 5 models for RP2 and 4 out of 6 models for NA12 fulfil the chemical and isotope constraints (group N4 in Table 3) without assuming an additional source of C in the solution in the form of endogenic CO_2.

4.4.2. Role of microbial degradation of SOC

Further information on evolution of the DIC pool is derived from isotopic characterisation of DOC. Generally, the concentration of DOC in groundwater from the Ruprechtov site is low, with values from 1 to 5 mg C/L, with only slightly elevated values in water from the clay/lignite horizon when compared to granite. First DOC characterisation of water from the clay/lignite horizon by MALDI-TOF-MS indicated lower molecular organic matter substances with characteristics of fulvic acids (Havlova, 2006). The DOC concentrations were much lower than those observed in the overburden from the Gorleben site (concentrations up to 200 mg C/L), despite the fact that clay/lignite layers in the Ruprechtov site contain up to 50% SOC.

In Gorleben aquifers the conversion of sedimentary organic matter by microbial reduction with release of DOC and DIC plays an important role (Buckau et al., 2000a). A schematic presentation with major elements of this mineralisation process is shown in Fig. 12.

The conditions for microbial degradation of SOC by SO_4 reduction in the clay/lignite layer in the Ruprechtov aquifer system are fulfilled. The SO_4 is available in all boreholes and its concentrations vary between 10 and 60 mg/L (cf. Table 1). Also, the existence of

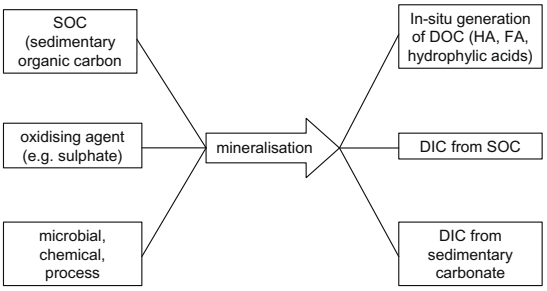

Fig. 12. Conceptual description of the mineralisation of sedimentary organic C (Buckau et al., 2000a).

SO_4-reducing bacteria in the clay/lignite layer has been demonstrated through analyses of sediments from borehole NA4 (Abdelouas et al., in press).

Mineralisation by the oxidation of SOC and subsequent formation of DOC and DIC as shown in Fig. 12 is accompanied by the reduction of electron acceptors like SO_4^{2-}, i.e. the decrease in concentrations of these species coupled with increasing DOC. Such a trend, with respect to SO_4 concentration, can be observed in groundwaters from granite and clay lignite horizons (Fig. 13). On the other hand, an increasing trend is evident for phosphates, which are released in this process. This is in agreement with observations from the Gorleben site, where phosphate concentration rises with increasing DOC concentration in groundwater. It is an indicator that SOC oxidation is microbially mediated. Microbes metabolize SOC, by reducing SO_4^{2-} and/or NO_3^- and releasing originally SOC-bound phosphates into the solution.

The $\delta^{13}C$ values of DOC are in a range between −25‰ and −27.8‰. This is in agreement with expected values around −27‰ for DOC formed by degradation of C-3 cycle plants (Clark and Fritz, 1997). In earlier analyses significantly higher $\delta^{13}C$ values in two boreholes, i.e. NA4 (−16.9‰ and −22.9‰) and NA12 (−23.7‰) have been found. The increase of $\delta^{13}C$ values, especially for NA4 within 3 a, indicates an initial contamination with organic C with a higher $\delta^{13}C$ value caused by drilling. Therefore, it is assumed that the lowest values measured most recently (August 2006) are most reliable.

The ^{14}C activity values of the DOC pool were only available for four boreholes. Wells NA4, NA12 and NA13 were chosen because they represent water from the clay/lignite horizon and NA8 is located in the infiltration area around the granite outcrop (cf. Fig. 1). The ^{14}C activity of dissolved organic C (humic and fulvic acids) under forest prior to nuclear atmospheric testing is expected to be around 50–60 pmc (Buckau et al., 2000b). If degradation of Tertiary sedimentary organic material in the clay/lignite layers is occurring, ^{14}C activity in DOC in the clay/lignite layers should be reduced. Assuming that the value of approximately 65 pmc in NA8 is typical for infiltration water (although NA8 is not the major source for water from clay/lignite layers) the lower values of 40 and 44 pmc found in the two boreholes in clay/lignite layers (NA4 and NA13) would support the hypothesis of DOC formation due to the degradation of SOC, assuming groundwater in those wells is not several thousand years old. If the observed decrease of ^{14}C activity were to be entirely due to radioactive decay of ^{14}C, the resulting apparent ages would be in the order of 3.1–3.9 ka, in broad agreement with the results of NETPATH geochemical modelling for well NA12 which is situated close to wells NA4 and NA13. However, the ^{14}C activity of DOC found in NA12 (app. 70 pmc) is even higher than that in NA8 possibly indicating some contamination of unknown origin. Unfortunately, no reliable value could be obtained for borehole NA10 from the western infiltration area.

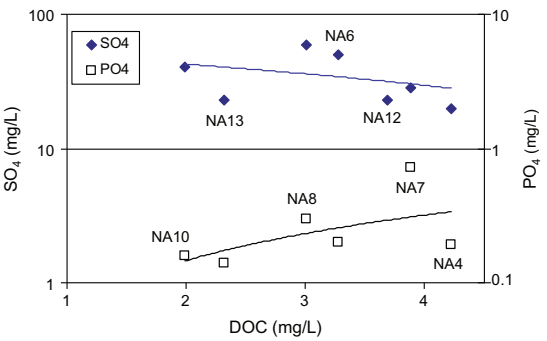

Fig. 13. Concentrations of SO_4^{2-} and PO_4^{3-} with trend lines for selected Ruprechtov wells from the western and northern area as a function of dissolved organic C concentration.

Additional insights into possible in situ degradation of SOC can be gained from S isotope analyses of dissolved SO_4^{2-}. Assuming a simple organic compound, complete SO_4 reduction can be written as

$$SO_4^{2-} + 2CH_2O = H_2S + 2HCO_3^-$$

In the presence of Fe the reaction product (H_2S) will be fixed as mono-sulphide and afterwards transformed to pyrite. Microbial SO_4 reduction is accompanied by isotope fractionation. The lighter isotope ^{32}S is preferentially metabolized by the microbes leaving residual SO_4^{2-} in the solution enriched in ^{34}S, whereas $\delta^{34}S$ values in precipitated sulphides decrease (Clark and Fritz, 1997).

The results of $\delta^{34}S$ analyses of dissolved SO_4 are shown in Fig. 14a. For wells NA10 and RP1 representing NW and SW infiltration areas (dashed circle), the $\delta^{34}S$ values are low and vary between 0.2 and 3.5‰. Water from the local infiltration area in granite around NA8 is different, with an even lower $\delta^{34}S$ value of −8.45‰. Waters from the clay–lignite horizon (solid circle) show higher $\delta^{34}S$ values, in the range between 16.4‰ and 24.6‰. Substantial $\delta^{34}S$ enrichment of dissolved SO_4 in these boreholes is a strong indication that SO_4 reduction occurs in the clay/lignite layers. Fig. 14b shows an increase of $\delta^{13}C$ in DIC with increasing $\delta^{34}S$ values. This observation supports the mechanism assumed in the conceptual model in Fig. 12, i.e. that the formation of DIC by degradation of sedimentary organic matter goes together with additional formation of DIC by dissolution of SIC (Buckau et al., 2000a).

A similar enrichment in the heavy S isotopes has been observed in numerous studies e.g. in groundwater from the "Niederrheinische Bucht", where $\delta^{34}S$-values of dissolved SO_4 of between 1‰ and 49.5‰ were observed by Schulte et al. (1997). They found $\delta^{34}S$ values systematically increasing with depth, with the highest values in deep reducing water in the vicinity of lignite layers, where SO_4 reduction occurs. With the initial SO_4 concentration in the infiltration area and the concentration after SO_4 reduction in the clay lignite horizon an enrichment factor ε can be derived from the Rayleigh equation

$$\varepsilon = \frac{\delta^{34}S_{SO4} - \delta^{34}S_{SO4.initial}}{\ln \frac{C_{SO4}}{C_{SO4.initial}}}.$$

Based on the data from all wells shown in Fig. 14 an enrichment factor of 11.4‰ was calculated as a best fit of the straight line in Fig. 14c. Compared to other investigations, this value is relatively low, but not unusual for bacterial SO_4 reduction. Enrichment fac-

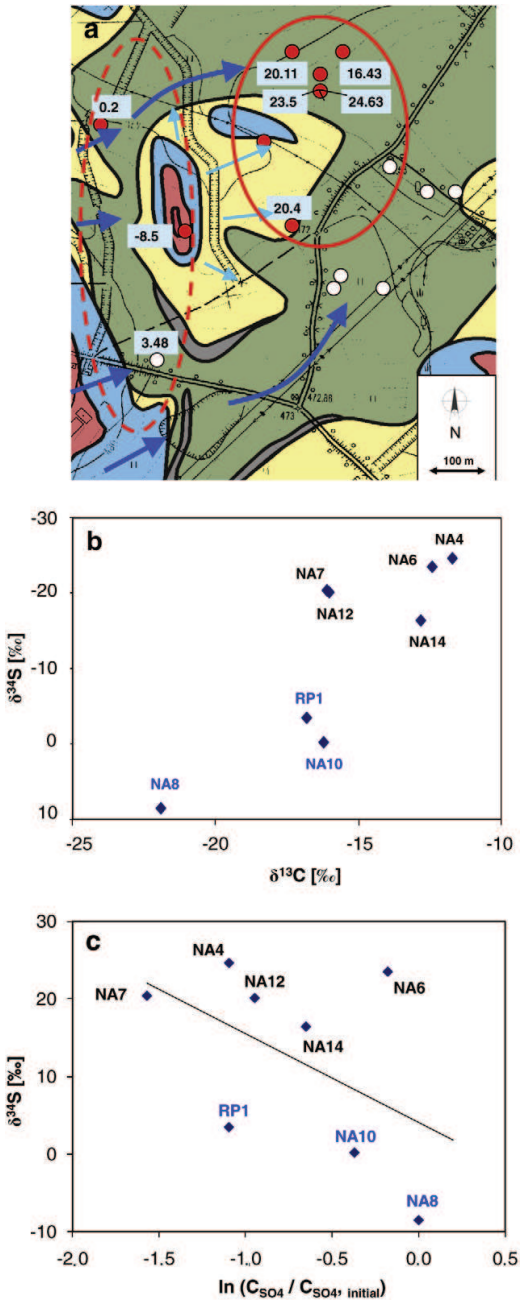

Fig. 14. (a) Distribution of $\delta^{34}S$ in different boreholes at Ruprechtov site, (b) $\delta^{34}S$ versus $\delta^{13}C$, and (c) $\delta^{34}S$ versus $\ln(C_{SO4}/C_{SO4,\ initial})$. For further explanation see the text.

tors in a similar range between 9‰ and 11‰ have been observed, e.g. in studies by Strebel et al. (1989), Spence et al. (2001), and Knöller et al. (2004).

The results of $\delta^{34}S$ analyses provide a strong indication that microbial reduction of SO_4 occurs in the clay/lignite horizon using sedimentary organic C as electron donor. However, this process only slightly increases the DOC content in the water-bearing layers in the clay lignite horizon, with concentrations up to 5 mg C/L. First analyses of SOC from the clay lignite horizon indicate that the composition of the sedimentary organic matter plays an important role. Extraction by the alkali method (dissolution and precipitation) according to IHSS scheme (Cervinka et al., 2007) indicates that the low concentration of dissolved organic matter in the Ruprechtov system is caused mainly by low availability of organic matter for degradation. Only a small fraction of SOC is extractable/releasable to the groundwater. After alkaline extraction more than 50% of the organic matter remains in the residual fraction. An additional reason for low DOC content might be the strong sorption properties of clay layers that could fix humic acids on the sediment matrix (Wang and Xing, 2005). Sorption experiments to investigate this effect in groundwater-sediment samples from the clay–lignite horizon at Ruprechtov site are under way.

5. Conclusions

Environmental isotopes were used to characterize C chemistry and dynamics of groundwater flow at the nuclear waste repository natural analogue in the Ruprechtov aquifer system in the northwestern part of the Czech Republic. The results so far reveal somewhat complex hydrogeological conditions, with infiltration areas in the outcropping granites in the western and southern part and preferential water flow in layers only a few metres thick, which do not represent a continuous aquifer, but rather distinct areas of increased permeability. In general, active water flow is confined to the Tertiary formation and the underlying granite, which are separated by a kaolin layer of variable thickness. There are strong indications for local connections of the flow systems in the underlying granite and in the Tertiary sediments in the northern part, where the kaolin thickness is very small and the existence of fault zones is confirmed.

Modelling of C isotope data with the aid of simple models (open- and closed-system) as well as inverse geochemical modelling performed with the aid of the NETPATH code highlights the need for additional sources of C in the system to properly explain the observed chemical and isotopic evolution of the DIC reservoir. The most probable sources of this additional C include the biodegradation of dissolved and sedimentary organic C as well as the influx of endogenous CO_2.

There are strong indications that microbial reduction of SO_4 contributes to the formation of DOC and biogenic DIC in the clay/lignite layers. These are, in particular, the increase of $\delta^{34}S$ in dissolved SO_4^{2-} and an increase of biogenic DIC and phosphate with increasing DIC concentration along the potential flow path of groundwater in the system.

Environmental isotope data, combined with the chemical composition of water and geochemical modelling also allowed some insights into timescales of groundwater flow. They helped to identify potential infiltration areas and major directions of groundwater flow. The presence of ^3H in some wells (e.g. NA8, NA10) points to the contribution of recent infiltration occurring after the 1950s. The modelling of chemical and isotopic evolution of the DIC pool with the NETHPATH code also yielded some information on apparent groundwater ages in the system. For the most probable scenario of this evolution, assuming that the additional C added to the solution is devoid of radiocarbon, the inverse modelling yields negative radiocarbon ages of the DIC pool suggesting a short transition time for groundwater. In the second scenario (^{14}C activity of the additional C equal to 60 pmc), the resulting age differences between investigated pairs of wells are between 0.45 and 1.9 ka for RP1/RP2 and 3.2–4.2 ka for NA10/NA12, pointing to groundwaters ages in similar ranges. This scenario, although being

rather unlikely, indicates that when some ^{14}C is present in the additional C being added to the solution, originating for instance from the decomposition of dissolved organic C of soil origin, the calculated age differences between the modelled pairs of wells will grow. The overall current evidence suggests, however, that groundwater in the Ruprechtov aquifer system is most probably not older than ca. 1 ka.

Acknowledgements

This work was financed by the German Federal Ministry of Economics and Labour (BMWA) under Contract nos 02 E 9551 and 02 E 9995, by RAWRA and the Czech Ministry of Trade and Industry (Pokrok 1H-PK25) and by the European Commission within the integrated project FUNMIG. The contribution of AGH was partly supported by statutory funds of the AGH University of Science and Technology (Project no. 11.11.220.01). Comprehensive rewiews by N. Plummer and P. Swart significantly improved the manuscript.

References

Abdelouas, A., Grambow, B., Andres, Y., Noseck, U., in press. Uranium in argillaceous sediments: sorption/desorption processes and microbial effects. Environ. Sci. Technol.

Buckau, G., Artinger, R., Geyer, S., Wolf, M., Fritz, P., Kim, J.I., 2000a. Groundwater in situ generation of aquatic humic and fulvic acids and the mineralization of sedimentary organic carbon. Appl. Geochem. 15, 819–832.

Buckau, G., Artinger, R., Geyer, S., Wolf, M., Fritz, P., Kim, J.I., 2000b. ^{14}C dating of Gorleben groundwater. Appl. Geochem. 15, 583–597.

Cervinka, R., Havlova, V., Noseck, U., Brasser, Th., Stamberg, K., 2007. Characterisation of organic matter and natural humic substances extracted from real clay environment. Proc. 3rd Annual Workshop Proc. 6TH EC FP – FUNMIG IP, Edinburgh, 26–29 November 2007.

Clark, I.D., Fritz, P., 1997. Environmental Isotopes in Hydrology. Lewis Publishers, Boca Raton, New York.

Coleman, M.L., Moore, M.P., 1978. Direct reduction of sulfates to sulfur dioxide for isotopic analysis. Anal. Chem. 50, 1594–1595.

Coleman, M.L., Shepherd, T.J., Durham, J.J., Rouse, J.E., Moore, G.R., 1982. Reduction of water with zinc for hydrogen isotope analysis. Anal. Chem. 54, 993–995.

Deines, P., Harmon, R.S., Langmuir, D., 1974. Stable carbon isotope ratios and the existence of a gas phase in the evolution of carbonate ground waters. Geochim. Cosmochim. Acta 38, 1147–1164.

DIN 18130 (en), 1998. Soil-investigation and Testing. Determination of the Coefficient of Water Permeability – Part 1: Laboratory Tests (DIN 18130-1:1998-05). Beuth-Verlag, Berlin-Wien-Zürich.

Epstein, S., Mayeda, T., 1953. Variation of ^{18}O content of waters from natural sources. Geochim. Cosmochim. Acta 4, 213–218.

Hammer, O., Harper, D.A.T., Ryan, P.D., 2001. Past: paleontological statistics software package for educational and data analysis. Paleontol. Electron. 4, 9–178.

Havlova, V., 2006. Pers. Comm. October 2006.

Hummel,W., Berner, U., Curti, E., Thoenen, T., Pearson, F.J., 2002. Nagra/PSI Chemical Thermodynamic Data Base Version 01/01 (Nagra/PSI TDB 01/01) NAPSI_290502.DAT. Last Modified 26-August-2002.

Knöller, K., Fauville, A., Mayer, B., Strauch, G., Friese, K., Veizer, J., 2004. Sulfur cycling in an acid mining lake and its vicinity in Lusatia. Germany. Chem. Geol. 204, 303–323.

McCrea, J.M., 1950. On the isotopic chemistry of carbonates and a paleotemperature scale. J. Chem. Phys. 18, 849–857.

Noseck, U., Brasser, Th., 2006. Radionuclide transport and retention in natural rock formations – Ruprechtov site. Gesellschaft für Anlagen- und Reaktorsicherheit, GRS-218, Köln.

Noseck, U., Brasser, Th., Pohl, W., 2002. Tertiäre Sedimente als Barriere für die U-Th-Migration im Fernfeld von Endlagern. Gesellschaft für Anlagen- und Reaktorsicherheit, GRS-176, Köln.

Noseck, U., Brasser, Th., Raijlich, P., Hercik, M., Laciok, A., 2004. Mobility of uranium in tertiary argillaceous sediments – a natural analogue study. Radiochim. Acta 92, 797–801.

Parkhurst D.L., Appelo C.A.J., 1999. User's guide to PHREEQC – a computer program for speciation, batch-reaction, one-dimensional transport, and inverse geochemical calculations. Version 2. US Geol. Surv., Water-Resour. Invest. Rep. 99-4259.

Plummer L.N., Prestemon E.C., Parkhurst D.L., 1994. An interactive code (NETPATH) for modelling NET geochemical reactions along a flow PATH. Version 2.0. US Geol. Surv., Water-Resour. Invest. Rep. 94-4169.

Schulte, U., Strauß, H., Bergmann, A., Obermann, P., 1997. Isotopenverhältnisse der schwefel und kohlenstoffspezies aus sedimenten und tiefen grundwässern der niederrheinischen bucht. Grundwasser 3, 103–110.

Spence, M.J., Bottrell, S.H., Thornton, S.F., Lerner, D., 2001. Isotopic modelling of the significance of bacterial sulphate reduction for phenol attenuation in a contaminated aquifer. J. Contam. Hydrol. 53, 285–304.

Strebel, O., Böttcher, J., Fritz, P., 1989. Use of isotope fractionation of sulfate–sulfur and sulfate–oxygen to assess bacterial desulfurication in a sandy aquifer. J. Hydrol. 121, 155–172.

Todd, D.K., 1980. Groundwater Hydrology. John Wiley & Sons, New York.

Wang, K., Xing, B., 2005. Structural and sorption characteristics of adsorbed humic acid on clay minerals. J. Environ. Qual. 34, 342–346.

Weise, S.M., Bräuer, K., Kämpf, H., Strauch, G., Koch, U., 2001. Transport of mantle volatiles through the crust traced by seismically released fluids: a natural experiment in the earthquake swarm area Vogtland/NW Bohemia, Central Europe. Tectonophys 336, 137–150.